Economic optimisation of energy use and storage, and its influence on power networks

Karolis Petruskevicius

Department of Mathematics

January 21, 2021

Contents

List of Figures

List of Tables

Nomenclature

Nomenclature

$\bar{D}(t)$	Average national power demand at time t.
χ	Maximum power imbalance during an iteration of optimal price search
Δt	Discrete time step period.
ϵ	Charging and discharging losses of energy storage facility.
η_{max}^{lower}	Lower limit of the power plant efficiency distribution.
η_{max}^{upper}	Upper limit of the power plant efficiency distribution.
Γ	Instantaneous rate of the power plant profit.
$\hat{T}(t)$	A single point temperature measurement of the outdoor temperature.
ι	Rate of power plant fuel input at which the power plant would be synchronised to the grid.
λ	Power plant fuel cost.
λ_{coal}	Fuel input cost for coal.
λ_{gas}	Fuel input cost for gas.

$_t$ Set of all admissible control policies for energy storage facilities.

$\mathbb{H}_t$ Set of all admissible control policies for a domestic heater.

$\mathcal{D}(\pi^{wholesale})$ A set of demands that comprise M number of demand agents $\{H_1, H_2, ..., H_M\}$.

$\mathcal{S}(\pi^{wholesale})$ A set of system supply values at different times that comprises G number of agents that can dispatch energy to the grid, and each choose to supply $\{W_1, W_2, ..., W_G\}$ at time t.

ν Power plant fuel input at which the power plant has been in the de-synchronisation state for a period of half the MZT

Ω Set of all possible wholesale electricity price policies.

ϕ Adjustment prices for optimal price search algorithm

$\pi(t)^{distribution}$ Power distribution cost at time t.

$\pi^{domestic}$ Price of electricity as received by the domestic user. The domestic price includes network and other charges in addition to wholesale prices $\pi^{wholesale}$.

$\pi^{gas}(t)$ Domestic cost of gas at time step t.

π^{real} Observed market index price of wholesale electricity.

$\pi^{wholesale,*}$ Optimal wholesale electricity price policy.

$\pi^{wholesale,q}$ Wholesale electricity price policy at iteration q.

$\pi^{wholesale}$ Policy of wholesale electricity prices.

$\pi^{wholesale}(t)$ Wholesale electricity price at time step t.

ψ^{fcOM} Ratio between fixed costs for operation and maintenance and the fuel cost at maximum power output.

ψ^{fc} Ratio of fixed costs of synchronising the power plant, and the fuel cost at maximum power output.

ρ Discounting rate to adjust for the time value of money.

$\varepsilon(W)$ The efficiency of the power plant given the current power output W.

ε_{max} Maximum efficiency achievable by the power plant.

ε_{min} Lowest efficiency achievable by the power plant.

$\varrho(W)$ Percentage power output of the power plant relative to full load.

ς Rate of fuel cost at maximum power plant generating capacity.

$\widetilde{D}(t)$ Relative average national demand at time t.

ζ Allowed imbalance between supply and demand

$\{\mathcal{Q}(\tau, c), \mathcal{U}(\tau, c), \tau\}$ A path satisfying both $\frac{dQ}{d\tau}$ and the discrete dynamics of U which arrives at the discrete point $\{Q_j, U\}$ at time $\tau = \tau_{n+1}$, assuming that the control c is held constant over the time interval τ_{n+1} - τ_n.

$\{\mathcal{Q}(\tau_n, c; Q_j, \tau_{n+1}), \mathcal{U}(\tau_n, c; U(\tau_{n+1}))\}$ The departure point of the numerical solution of the PDE at τ_n.

a_{11} Heat transfer coefficient from indoor temperature to outdoor temperature.

a_{12} Heat transfer coefficient from the heater to internal temperature.

$AC(U)$ The running costs of the power plant, per unit time given the current fuel input and state of the power plant.

$c \in {}_t$ Optimal control policy for energy storage facility.

C Charge level of an energy storage facility.

c The control variable of the energy storage facility discharging (-1), charging (1), idle (0).

$c \in \mathbb{R}$ Control variable of the power plant.

C^{max} The maximum capacity of the energy storage facility at which it can charge and discharge to the grid.

c_{max} The maximum increase in the fuel input over the time step that meets the ramp up conditions.

c_{min} The maximum decrease in the fuel input over the time step that meets the ramp down conditions.

$d(\pi, t)$ Aggregate national demand at time t.

$D(t, \pi^{wholesale})$ Total system demand of all houses at time t given price policy $\pi^{wholesale}$

D^{dsr} The maximum capacity of industrial and commercial DSR.

$d^{\text{dsr}}(\pi^{wholesale})$ Amount of DSR available given wholesale electricity price $\pi^{\text{wholesale}}$.

$d^{b\_charge}(\pi, t)$ Aggregate of all grid batteries when charging at time t.

$d^{baseload}(t)$ Aggregate base load demand at time t.

$d^{dsr}(\pi, t)$ Aggregate DSR turn up at time t.

$d^{ev}(t)$ Aggregate EV load at time t.

$d^{hp}(\pi, t)$ Aggregate HP load at time t.

$d^{interconnector}(t)$ Aggregate interconnector flows at time t.

$H \in \mathbb{H}_t$ Optimal control policy of instantaneous energy consumed by the heater in the building.

H Rate of domestic heater power input.

$H(t)$ Rate of domestic heater power input at time t.

H_{max} Maximum rate of power for the domestic heater.

H_{min} Minimum rate of power for the domestic heater.

I A single point of internal temperature of the building.

$I(t)$ Single point internal air temperature measurement at time t.

$I^*(t)$ The time-dependent desired temperature of the user at time t

J The discounted integral of the profits over the time horizon from t to T.

MEL_g Individual agents' maximum export limit.

p User cost and temperature discomfort trade-off coefficient.

Q Rate of fuel input to a power plant.

q Iteration number in finding optimal price

$Q(t)$ Rate of fuel input to power plant at time t.

q^{max} Maximum number of iterations imposed on the optimal price search algorithm

Q_{max} Maximum rate of fuel input of the power plant.

$R(\pi^{wholesale})$ The aggregate absolute energy imbalance

$s^{b\_discharge}(\pi, t)$ Aggregate battery discharging into the grid at time t.

$s^{biomass}(t)$ Aggregate biomass power plant supply at time t.

$s^{ccgt}(\pi, t)$ Aggregate CCGT power plant supply at time t.

$s^{curtailed}$ Wind power curtailment.

$s^{curtailment}(\pi, t)$ Aggregate wind curtailment due to negative prices at time t.

$s^{hydro}(t)$ Aggregate hydro power plant supply at time t.

$s^{interconnector}(t)$ Aggregate interconnector power supply when importing at time t.

$s^{ocgt}(\pi, t)$ Aggregate OCGT power plant supply at time t.

$s^{other}(t)$ Aggregate power supply from other sources at time t.

$s^{solar}(t)$ Aggregate solar power supply at time t.

S^{wind} Total capacity of wind power production.

$s^{wind}(t)$ Aggregate wind power supply at time t.

$s^{wind}(t)$ Wind power availability at time t.

T Terminal time of the simulation.

t Time identifier.

$U \in \mathcal{U}$ Operating state of the power plant.

$U(t)$ Indicator function to identify whether the user requires temperature set points.

V Solution to optimal control PDE.

$V(I, t)$ Value function for domestic heater user.

$V^u_{j,n}$ The approximation of the solution of the power plant at time τ_n, fuel input Q_j and state $U = u$.

W Rate of power production by a power plant

$W(t)$ Aggregate national supply at time t.

$W(t, \pi^{wholesale})$ Total system supply of all generators at time t given price policy $\pi^{wholesale}$

$W(t; \pi^{wholesale})$ The total supply of all energy supply agents given a price policy $\pi^{wholesale}$ and is chosen for the entire period $0 \leq t \leq T$.

$W_g(t; \pi^{wholesale})$ Individual agent output, where g denotes an individual generating agent and t denotes time given a pricing policy $\pi^{wholesale}$ over the period

W_{max} Maximum rate of power output of the power plant.

MEL Maximum Export Limit. Maximum level at which the BMU may be exporting power in to the National Electricity Transmission System at the Grid Entry Point or Grid Supply Point.

NDZ Notice to Deviate from Zero. Notification time required for a BMU to start exporting energy.

RDEE* Run Down Elbow Export, where * indicates levels 1,2,3. Level measured in power output at which specific Run Down Rates are valid. BMU can provide up to three levels.

RDRE* Run Down Rate Export, where * indicates levels 1,2,3. Limit on the rate of decrease in output for an exporting BMU. BMU can provide up to three rates for different output levels.

RUEE* Run Up Elbow Export, where * indicates levels 1,2,3. Level measured in power output at which specific Run Up Rates are valid. BMU can provide up to three levels.

RURE* Run Up Rate Export, where * indicates levels 1,2,3. Limit on the rate of increase in output for an exporting BMU. BMU can provide up to three rates for different output levels.

SEL Stable Export Limit. Minimum level at which the BMU can, under stable conditions (load at which the power plant can be safely operated), export to the National Electricity Transmission System at the Grid Entry Point or Grid Supply Point.

Disclosures

The author of this thesis is developing algorithms that can generate optimal control strategies for the HPs of domestic customers in Great Britain (GB) whose electricity is supplied on the Octopus Energy agile tariff. More information about the company can be found on the companys' website (www.homelyenergy.com). Company has recently been acquired by Evergreen Energy that has a sister company Evergreen Smart Power providing domestic Demand Side Response (DSR) services in Great Britain. More information can be found on companys' website (www.evergreenenergy.co.uk).

Acknowledgements

My sincere gratitude goes to my supervisors Dr. Paul Johnson, Prof. Peter Duck and Prof. Sydney Howell. I thank you for your patience with me throughout this journey and all of your input, insightful comments and guidance. Without your support and encouragement in testing and trying new concepts, I would not be where I am in life. I had never imagined when I started this program that by the end of it, I would have created a successful business that is making what we have studied a reality. I could not have asked for a better supervisory team.

Further, I would like to thank Dr. Alessandra Parisio and Dr. William Bodel for their insightful conversations, questions and comments on the thesis. I am thankful to my office colleagues Dr. Jose Eduardo Martinez Sosa, Dr. Angeliki Loukatou and Zubair Amit Arfan for all the "maths" talks that we've had throughout the years and for bearing with me.

I am also thankful to my whole family; for all of your support through all these years, for believing in me and providing me with the opportunities to excel (Ačiū visiems) and also my friend Rebecca who has been there throughout this journey, supported me and put up with me.

The author of the thesis acknowledges financial support from EPSRC (EP/L016141/1) through the Power Networks Centre for Doctoral Training and Salford University for supporting us with access to smart meters' lab for our real world trial.

Abstract

The electrification of heating and electric vehicles, under present fixed electricity tariffs, is expected to increase the total and peak demand of electricity. One way to provide for these peaks will be for the power plants to be run part loaded during off-peak times, less efficiently, to increase their power production during peaks. Power network reinforcement and new generation capacity will also likely be required to support the additional electricity demand. Demand Side Response, utilising real-time pricing (RTP), is one possible alternative solution. Monetary incentives can encourage users to re-time their power consumption to off-peak periods allowing utilisation of more efficient power plants. In our proposed system, electric heaters in domestic houses autonomously respond to day-ahead RTP (DA-RTP) electricity prices and weather forecasts, thus reducing electricity demand during peaks and user costs while maintaining comfort.

We evaluate the benefits of such a system by simulating an electricity market using Agent-Based Modelling. Agents (houses, power plants, energy storage facilities) are all individually optimised using dynamic optimisation. Power plants and energy storage facilities maximise their profits given forward wholesale electricity prices, subject to operational constraints. We use balancing mechanism (BM) dynamic data and

part-load efficiency curves to model the power plants' operating characteristics. The building heating controller minimises users' costs subject to DA-RTP electricity prices and flexibility in the users' indoor temperature. We use internal and external temperatures from 823 houses in England to estimate representative thermal building models and heating patterns.

Our results show that a DA-RTP pricing structure of domestic electricity could drive up to 24% savings in HP user energy costs, up to 6.7% reduction in average peak electricity demands, better utilisation of more efficient power plants, and lower grid carbon emissions when compared to a fixed pricing structure. All the above grid benefits are achieved while preserving our defined user comfort and, in some cases, improving it.

Chapter 1

Introduction

In line with the Climate Change Act 2008, Great Britain (GB) has set targets to reduce carbon emissions by at least 100% of 1990 levels by 2050 [1]. To achieve this, GB is expected to see an increase in renewable energy generation and electrification of domestic heating, moving away from gas boilers to electric heating. The following topics emerge from the current research in the possible 2050 energy pathways, as outlined by the literature review in [2]:

- De-carbonisation of the whole electricity system will be required, although significant uncertainty remains on how GB will be producing its electricity in the future.
- Electrification of space heating and significant Heat Pump (HP) uptake. The current domestic annual heat demand in GB is 425 TWh, of which only 37.8 TWh is currently supplied by electricity.

- Peak electricity demand for heat alone could reach 65 GW, exceeding today's average peak electricity demand of around 42 GW.

HPs are regarded as the most popular solution for electrification of heating by the government, energy researchers, and the System Operator (SO), which is National Grid (NG) in GB [3]. Presently, an estimated 180,000 homes have HPs installed in GB [3]. The SO reports annually on the state and future of the energy developments in GB as part of their Future Energy Scenarios (FES) report [3]. In the 2019 version of the FES [3], SO predicted significant growth in HP technology uptake, expecting 0.5 M to 3.7 M HPs to be installed by 2030, reaching 3.3 M to 18.5 M by 2050 [3]. To achieve these HP penetration targets, the government is supporting households in GB through financial incentives such as Renewable Heating Incentive (RHI) [4] and recently green home grants [5]. Policy changes have also helped make progress in supporting renewable technologies with recent government legislation supporting the ban on gas boiler installations in new build properties from 2025.

With the electrification of heating and transport, the GB market will see an increased need for flexible resources (electricity loads with consumption that can be shifted within the day) to achieve electricity system balance. Balancing supply and demand, i.e, making sure that electricity supply and demand are equal at every point in time, has traditionally been achieved by ensuring sufficient generation to meet the forecasted demand while considering a margin for forecasting errors and power plant outages. This system balancing usually requires selected power plants to be run part-loaded, less efficiently, to provide for power imbalances between supply and demand. In addition to the electrification of vehicles and domestic heating, the GB market is also expecting to see a change in power generation composition. Variable power generation from renewable sources, such as wind and solar, already provide a growing share of electricity

and are expected to increase further in future years, alongside new nuclear power stations [6]. GB is expecting to phase out coal power plants by 2025; currently, there is 8.28 GW of available coal plant capacity compared to the total capacity of the system of 108.4 GW. Some of this lost capacity must be provided by alternative sources such as renewables or newly built power plants.

Renewable power generation is an essential part of helping GB achieve its carbon reduction targets. However, renewable power generation is often intermittent, as the wind might not be blowing, and the sun might not be shining when electricity is required. To provide for periods of power deficits arising from the shut-down of coal power plants and periods when renewable power is not available, the GB network will need to find ways to store energy in large quantities or better manage electricity consumption throughout the day. An alternative would be to build more conventional gas power plants, although more fossil fuel plants would invalidate the efforts to move towards a decarbonised electricity system.

Contributions list of this thesis is as follows:

- Introduction of the inter temporal market price search algorithm that uses Agent-Based Modelling (ABM) concepts to find equilibrium wholesale market prices where individual in-depth agent optimization can be parallelized.
- Geneneralization of the power plant modelling introduced in [7] and inclusion of operational power plant constraints such as minimum zero time, stable exporting limits, notice to deviate from zero and ramp rates.
- Introduction of the simplified building optimisation model introduced in [8] and the inferrence of optimal temperature schedules of the users in England and their

building thermal characteristics.

- Evaluation of autonomous heating controllers in supporting the UK grid development across FES scenarios.

In this chapter, we motivate the study and discuss the background of the concepts discussed in the thesis. We introduce the current state of the energy market and expected changes for the future. We provide brief introductions to Demand Side Response (DSR), GB electricity market trading arrangements,and ABM next.

1.1 Demand Side Response

DSR can complement or provide an alternative to installing large-scale batteries to store energy produced from renewable sources. Better electricity management can be achieved by incentivising users to use electricity during the times when it is abundantly available. DSR is defined by the US Department of Energy (DoE) as [9]:

"Changes in electric usage by end-use customers from their normal consumption patterns in response to changes in the price of electricity over time, or to incentive payments designed to induce lower electricity use at times of high wholesale market prices or when system reliability is jeopardised."

DSR differs from demand reduction, as it aims to change the timing of the demand rather than reduce energy demand overall [6] and as a result DSR requires flexible

loads to achieve electricity consumption shifting. Flexible loads do not need to be turned on at specific times of the day and are split into two categories [6]:

- Thermal inertia - space and water heating, refrigeration, and air conditioning. It takes time for the buildings' internal temperature to change even if the heater is turned off, this is discussed in detail later in the thesis.
- Time shiftable loads - appliances that are not required to be turned on at a specific time. Examples include washing machines, dishwashers, and tumble dryers. In [10] authors optimised the behaviour of wet appliances with respect to carbon and have shown that on average, a household with only grid supply can reduce the carbon footprint of a wet appliance by 23.9% by optimally scheduling its start time and by 74.7% when house is equipped with PV as well as grid supply.

DSR programs can be grouped into categories. Different groupings are provided across the literature. Here we provide a brief overview of the groupings discussed in [11, 12, 6, 13]:

- Incentive-based control - customers are offered economic incentives to deliver a reduction in demand. Incentive-based control programs are further divided into:
  - Direct Load Control (DLC) - customers sign up to programs based on economic incentives and allow power companies to control their demand. Examples include Heating, Ventilation, and Air-Conditioning (HVAC), water heaters, pool pumps. DLC is mainly concerned with peak load management [14], and DLC is seen as the technology capable of providing fast

time-scale, predictable control opportunities, especially for the provision of ancillary services such as regulation and contingency reserves as discussed in [15].

  - Interruptible load - user loads can be interrupted during system contingencies for an economic incentive.
  - Load as a capacity resource - users pre-commit load reduction levels when system contingencies occur.
  - Critical Peak Rebate (CPR) - users get a pre-determined rebate for reducing their use of electricity during peak times.

- Price Based Control (PBC) - different prices are charged to the consumer for using electricity at different times to disincentivise consumers using electricity during peak times and system contingencies. PBC is further divided into the following groups:

  - Real-Time Pricing (RTP) - retail prices of electricity track wholesale prices. Economists believe that this is the most efficient DSR mechanism for competitive markets [16]. Prices can be communicated to the user in the following ways:

    * Day-Ahead Real-Time Pricing (DA-RTP) - provides a 24-hour schedule a day in advance.
    * Real-Time Real-Time Pricing (RT-RTP) - notifies prices to users in real-time. If the response is automated, RTP can create short-term responses for system balancing. RTP is considered capable of providing the required interaction between distributed energy resources (DER), small-scale energy generation units connected at the distribution level, and DSR [17].

- Time-of-Use (TOU) - electricity prices are set for different periods for the whole contract length (e.g. Economy 7, Economy 10) [18].
- Variable Peak Pricing (VPP) - a TOU tariff but with a varying time of peak pricing daily.
- Dynamic time-of-use - prices of electricity are allowed to vary between different fixed prices, but the timing of these is not fixed.
- Critical Peak Pricing (CPP) - power companies are entitled to call critical events during the period of high wholesale market prices and system emergency conditions. In the CPP scenario, the prices of electricity are increased during the emergency conditions by a known amount. The number of emergency events with higher prices are usually limited in the year and are limited in duration during each event.
- Time-of-Use Critical Peak Pricing (TOU-CPP) - time-of-use pricing combined with critical peak pricing.

In this thesis, we focus on electricity pricing, which tracks the wholesale electricity markets and is identified above as DA-RTP.

1.1.1 Enabling technologies

Smart meter roll-out in the GB has increased the potential for smaller consumers such as domestic users and small commercial entities to respond to wholesale prices of electricity [6] as domestic electricity suppliers can now monitor their customer electricity usage in each half-hourly period. Other enabling technologies helping DSR market for the small consumers include:

- In-home displays that allow domestic users to monitor the real-time electricity price
- Direct load control or programmable communicating thermostats and smart appliances, such as smart plugs and conventional timers [6].

This increase in energy management systems available to domestic users provides an avenue for a RTP tariff uptake [13] moving domestic electricity consumers closer to becoming active participants, i.e. buyers and sellers of electricity, in wholesale electricity markets.

The benefits of RTP tariffs and HPs that are able to react to price signals include the reduced need to build power plants [6, 13, 16, 17], more efficient use of renewable energy and electricity networks helping GB reduce carbon emissions [19, 11, 6, 13, 16] as well as reduced costs for end-users [13, 16]. Later in this thesis, we attempt to assess the benefits of RTP tariffs in the domestic sector. We quantify the increase in renewable power use, CO_2 emissions, heating bill savings for the domestic users, and network and power plant reinforcement.

1.1.2 Flexibility services

In addition to managing the electricity demand through RTP tariffs, there is also the potential for the SO to manage the balancing of the system by providing incentives for domestic and commercial electricity users to turn their electricity consumption up or down. The SO is the body responsible for making sure the supply and demand of the electricity in the system is in balance. When unexpected changes in the production or

consumption of power occur on the grid, the SO can utilise flexible resources to balance the system, by asking flexible resources to reduce or increase power consumption (choosing whichever is the lowest cost solution). It is expected that a large increase in flexible resources will be required by Distribution Network Operator (DNO)s in the future when a large number of high electricity consumption assets such as HPs and electric vehicles are installed on the network.

Electric heating systems, such as HPs, or air-conditioning devices are ideal for providing flexibility services as buildings have inherent thermal inertia. Thermal inertia means that it takes time for the internal temperature to change even after the heating or cooling equipment is turned off. Turning heating or cooling equipment off for a half-hour would not significantly affect the user comfort but could provide the necessary shifting of electricity consumption away from the peaks. However, suppose we were to consider setting up HPs as a provider of response services. In that case, the cumulative consumption of these has to be high enough to meet minimum requirements imposed by the flexibility service user that could be the DNO or the SO. Domestic HPs usually have an electricity consumption of around 1.5 kW to 4 kW. Currently, the SO requires minimum cumulative consumption of at least 1 MW to act as a demand reduction provider; this would be equivalent to 666 HPs. This limit is expected to be slightly lower for DNOs, in some cases, even 100 kW could be accepted (66 HPs) as reported in [20].

DSR trials, such as "NEDO" [21] in the Greater Manchester area, was used to investigate the potential of using HPs to sell flexibility services to the SO. They have shown that HPs can be turned off for several hours (1-4 hours, depending on the building) without significantly impacting the comfort of the users. For further details a domestic DSR review is provided in [22]. [15] provides real-world experiences on using DSR

for spinning reserve (capacity that is available by increasing the power output of the power plants that are already generating power). International experiences of DSR programs can be found in [13, 6, 16]. We can summarise the findings from [13, 6, 16, 21, 15, 18] who conducted trials with DSR as follows:

- Policy is crucial for the evolvement of DSR.
- Revenue streams or cost-saving opportunities need to be present in the market to provide incentives for DSR providers.
- DSR programs are becoming increasingly popular, even for small-scale users.
- Consumer engagement is affected by opt-in (customers need to actively sign-up to provide DSR) or opt-out (customers are signed up to DSR by default but can withdraw from the scheme) and automation.
- Motivations for enrolment onto DSR programs include financial and environmental benefits.
- Trust, risk, and complexity are key factors affecting consumer engagement.
- Routines within a household affect their enrolment.

1.1.3 DSR market barriers

There are still significant barriers in place that hinder the mass uptake of DSR. These barriers include the high cost of hardware [23], issues surrounding advanced metering infrastructure such as latency, bandwidth, data ownership [15]. Information and Communications Technology (ICT) developments and reduction in flexibility enabling

hardware costs could provide a better environment for the future rise of DSR deployments.

Historically, the inclusion of DSR in balancing services has also been problematic due to regulatory barriers. Recently, regulatory developments regarding DSR use as noted in the Energy Efficiency Directive [24] have called to remove incentives in transmission and distribution tariffs that hinder the uptake of DSR. The primary catalyst for these changes has been attributed to renewable generation and DSR being seen as a critical technology to shift energy consumption to periods of high renewable energy production [13].

Customer engagement with DSR programs has also been discussed [13, 16] as a barrier for wider uptake of DSR schemes. The high cost of customer acquisition, for companies looking to aggregate domestic users loads, and the lack of effective building automation systems [23] has made it problematic for users to participate in DSR programs. Some users have also felt DSR programs to be too intrusive in their nature [25]. Customers seemed not to like the exposure to real-time prices due to price volatility [16] and the energy bill risks attached to it. There has been a debate on possible remuneration contracts for users, to make these programs more attractive [26, 27].

1.1.4 Transactive Energy

A further extension of DSR is Transactive Energy (TE). In 2017, the author attended the TE conference in Portland to gain a better understanding of state of the art ideas in grid management. The TE concept envisages a system where individual suppliers and users of energy interact with each other through market mechanisms to achieve

a supply and demand balance in a real-time, autonomous and decentralised manner [12]. Such a system involves information exchange between all the participating units in the system: demand response resources, intermittent renewable generation, storage devices, grid monitoring, and control devices [11].

TE highlights the following as discussed in [12]:

- Distributed intelligent devices are controlled in real-time, smaller time-scales than regular hourly control, which reduces the need for the SO to call on grid assets for balancing as system balance is achieved through the use of real-time prices.
- Devices are controlled based on economic incentives rather than centralised commands. Well functioning markets should theoretically achieve the maximisation of the social welfare for all market participants.
- Devices are managed under human supervision, but not directly by the users. This control mechanism means that users still supply the operation preferences for the appliances that can be controlled, but the optimisation algorithms within the appliances will derive the final physical control.
- Provides both market and control functionality.
- Both supply-side resources and demand-side resources are coordinated through economic incentives.

In future energy systems, electric vehicles and HPs will contribute large loads on distribution networks. The use of economic incentives, as part of the TE concept, would allow system operators to actively manage distribution and transmission networks

without the need for a central authority to coordinate system balancing. Further details of TE ideas and methods are provided in [11, 12].

1.2 Electricity Prices

A new quantitative framework for assessing the impact of HP uptake in GB on the price of electricity is provided in this thesis. To find domestic electricity prices in future HP scenarios, we will be modelling the interactions of electricity users and producers and will estimate future predicted wholesale electricity prices, together with network and other costs. The wholesale electricity price is the price of electricity as sold by the power plants to commercial customers or electricity suppliers. Domestic consumers in GB, in the majority of cases, purchase their electricity requirements from retailers (e.g. EDF, nPower, Octopus Energy and others); we will refer to these as electricity suppliers. This is in contrast to entities which generate electricity, which will be referred to as generators or power plants.

Wholesale electricity prices currently contribute around 33.5% of domestic electricity bills, as shown in figure 1.1. A second major component in the mix of the costs are network costs that contribute another 25.46% of the costs. Environmental and social obligation costs follow at 17.45% with operating costs being 17.15%. Other direct costs contribute 1.26%, VAT adding 4.76% leaving the supplier pre-tax margin at 0.4%. All costs are discussed in more detail next.

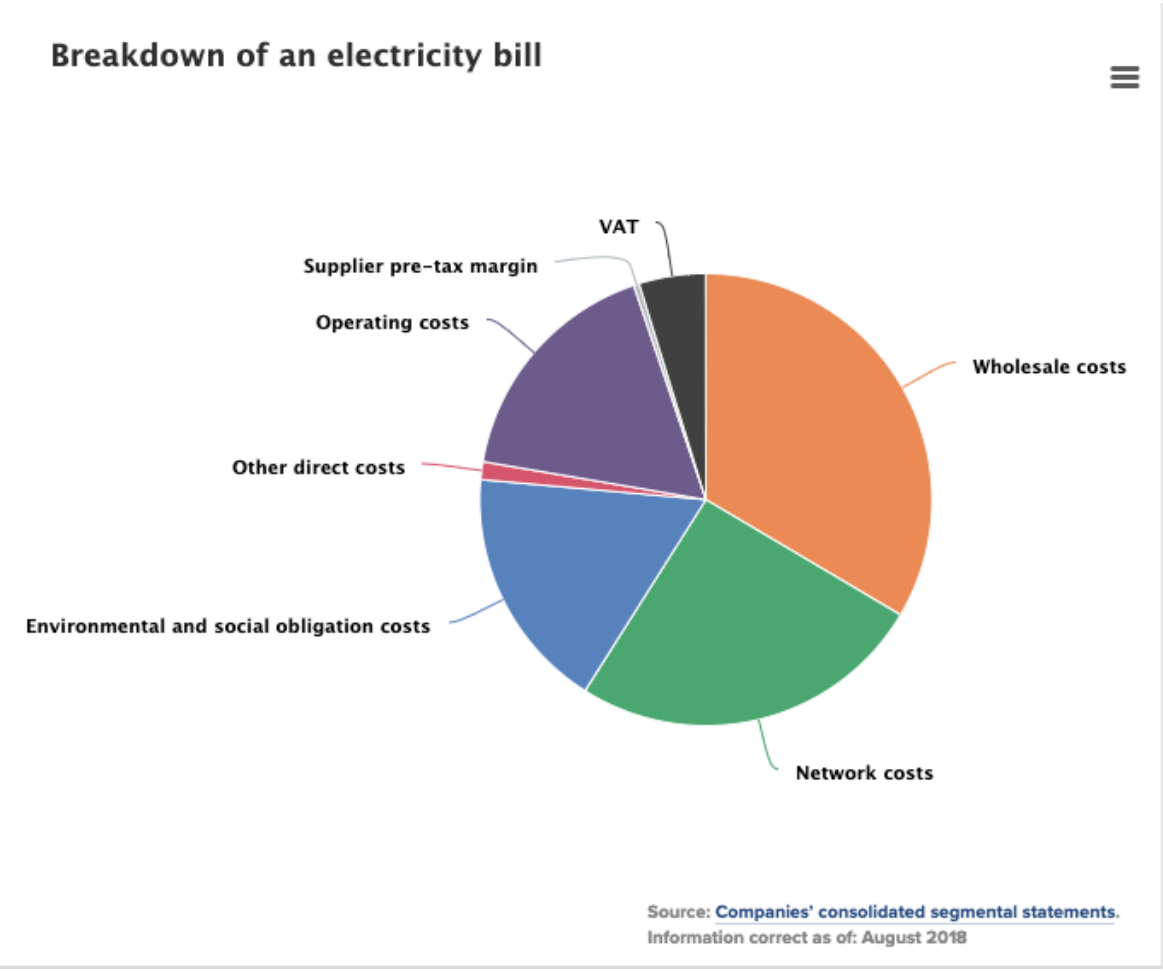

Figure 1.1: Breakdown of an electricity bill as of August, 2018. Picture source [28].

1.2.1 Wholesale Electricity Price

The wholesale electricity market in GB is competitive. Suppliers are allowed to purchase their electricity needs from power plants of their choice and vice versa. In GB electricity is traded (bought and sold) in half-hour chunks called "Settlement Periods". Energy suppliers, those using or delivering electricity to their customers, can purchase electricity from producers at any point up to an hour before the settlement period in which the electricity is delivered. This point is called gate closure, and electricity cannot be traded during the hour before delivery.

Long-term contracts are usually signed between companies to cover the baseload of electricity. The baseload of electricity could be regarded as the minimum load for the electricity supplier that their customers will consume. Additional power purchases, above the baseload, are further refined by electricity suppliers closer to the delivery period. These purchases are made in day-ahead markets, where electricity is bought and sold for half-hourly and hourly periods, from one day in advance up to an hour before the electricity delivery period.

1.2.2 Distribution Use of System Charges (DUoS)

Figure 1.1 indicates that network costs are the second biggest contributor to electricity bills. Network costs include both the distribution and transmission network charges. Distribution Use of System (DUoS) aim to recover the costs of installation and maintenance of a distribution network. DUoS charges against the user depend on the location of the user, the time at which the electricity is used, and the line loss

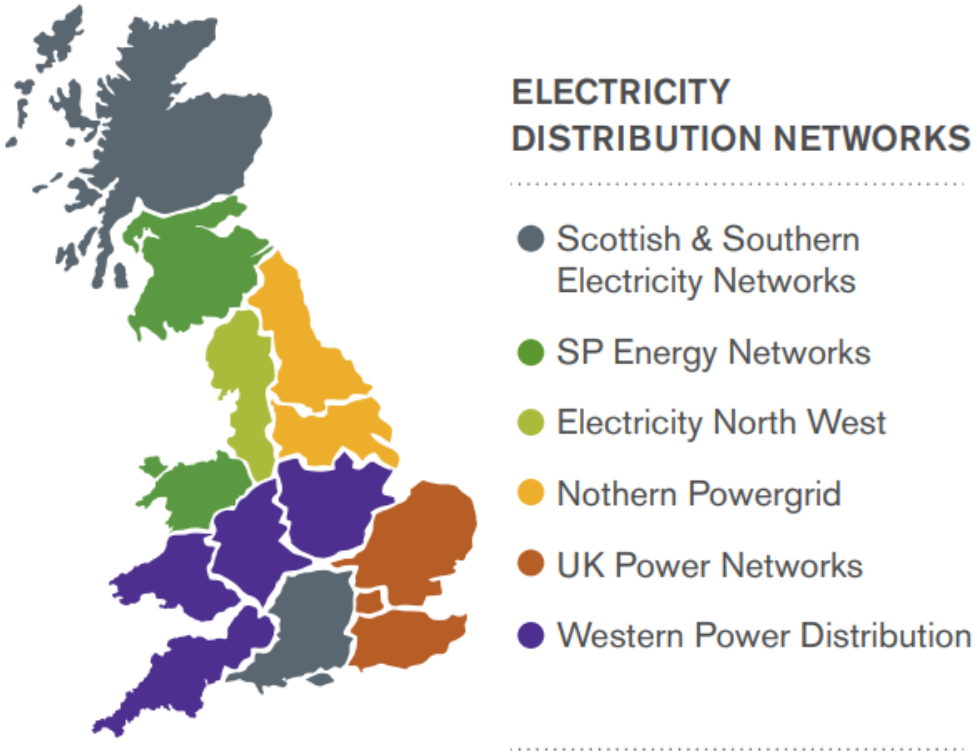

Figure 1.2: Map of the electricity DNOs [29]

factor as explained next. In GB, the electricity distribution network has 14 operators, owned by six ownership groups; a map of these regions is provided in figure 1.2.

Specific charges for each area are specified on the network operators page in the use of system charging statement document, an example of which for Electricity North West can be found in [30]. We also provide an example of one of these documents in figure 1.3. As we can see, DUoS charges are separated into red, amber, and green periods. These are different charges for specific times of the day to account for the different levels of stress that the DNO expects on the network. For half-hourly settled domestic customers (those that opt in to be Half-Hourly (HH) settled), specific charges

Annex 1 - Schedule of Charges for use of the Distribution System by LV and HV Designated Properties

Electricity North West - Effective from 1 April 2017 - Final LV and HV charges

Time Bands for Half Hourly Metered Properties

Time periods	Red Time Band	Amber Time Band	Green Time Band
Monday to Friday (Including Bank Holidays) All Year	16:00 to 19:00	09:00 to 16:00 19:00 to 20:30	00.00 - 09.00 20.30 - 24.00
Saturday and Sunday All Year		16:00 to 19:00	00.00 - 16.00 19.00 - 24.00
Notes	All the above times are in UK Clock time		

Time Bands for Half Hourly Unmetered Properties

	Black Time Band	Yellow Time Band	Green Time Band
Monday to Friday (Including Bank Holidays) March to October Inclusive		09.00 - 20.30	00.00 - 09.00 20.30 - 24.00
Monday to Friday (Including Bank Holidays) November to February Inclusive	16:00 to 19:00	09:00 - 16.00 19.00 - 20.30	00.00 - 09.00 20.30 - 24.00
Saturday and Sunday All year		16:00 to 19:00	00.00 - 16.00 19.00 - 24.00
Notes	All the above times are in UK Clock time		

Tariff name	Open LLFCs	PCs	Unit charge 1 (NHH) or red/black charge (HH) p/kWh	Unit charge 2 (NHH) or amber/yellow charge (HH) p/kWh	Green charge(HH) p/kWh	Fixed charge p/MPAN/day	Capacity charge p/kVA/day	Reactive power charge p/kVArh	Exceeded capacity charge p/kVA/day	Closed LLFCs
Domestic Unrestricted	011, 041, 441, 511		2.181			3.13				
Domestic Two Rate	031, 051, 061, 451, 531		2.595	0.194		3.13				
Domestic Off Peak (related MPAN)	081, 581		0.249							
Small Non Domestic Unrestricted	131, 191, 631		2.089			3.13				
Small Non Domestic Two Rate	161, 171, 661		2.143	0.162		3.13				
Small Non Domestic Off Peak (related MPAN)	091, 591		0.180							
LV Medium Non-Domestic	241, 431, 481, 751		1.766	0.123		10.58				
LV Sub Medium Non-Domestic	242, 432, 482, 752		1.455	0.097		39.99				
HV Medium Non-Domestic			1.257	0.067		163.21				
LV Network Domestic	821		13.094	1.349	0.174	3.13				

Figure 1.3: Distribution Network Operators across the GB provide information on the DUoS charges in the Use of System Charges document. This is an example view of system charging statement from Electricity North West for the year 2018 [30].

are attributed as per the "Low-Voltage (LV) Network Domestic" tariff. For Non Half-Hourly (NHH) settled customers, a constant charge is specified that is irrespective of the time at which the electricity is consumed and is as per the "Domestic Unrestricted" tariff. In addition to the per-unit charges of electricity, users also have to pay a daily fixed charge regardless of the charging tariff.

Using the information provided in figure 1.3, we can calculate the DUoS charges for a domestic customer as follows:

- NHH settled customers:

  - Per kWh charge - customers are charged 2.161 p/kWh for the power consumed irrespective of the hour at which this consumption has taken place.
  - Fixed charge - the customer is charged 3.13 p per day irrespective if there is any power consumption during this particular day.

- HH settled customers
  - Per kWh charge - Distribution system charges are specified for different times of the day. If a customer uses power between 16:00-19:00, he will be charged 13.094 p/kWh. If the consumption takes place between 00:00-09:00 and 20:30-24:00 the charge will only be 0.174 p/kWh.
  - Fixed charge - same as for NHH metered customers.

In figure 1.4, we present a breakdown of the time-dependent "LV Network Domestic" DUoS charges for different regions. From the figure, we can see that these rates vary significantly across different regions, although in all regions there is a peak between 16:00 until 19:00. This is the period when domestic users tend to come back home and consume large amounts of power.

1.2.3 Transmission Network Use of System Charges (TNUoS)

In addition to DUoS charges, electricity suppliers and commercial users have to pay transmission charges that aim to recover the costs of installing and maintaining transmission systems in England, Wales, Scotland, and Offshore. Transmission Network Use of System (TNUoS) charges are further passed onto the domestic users and reflected in their domestic energy bill. Table 1.1 shows TNUoS charges for different regions in GB for NHH settled users.

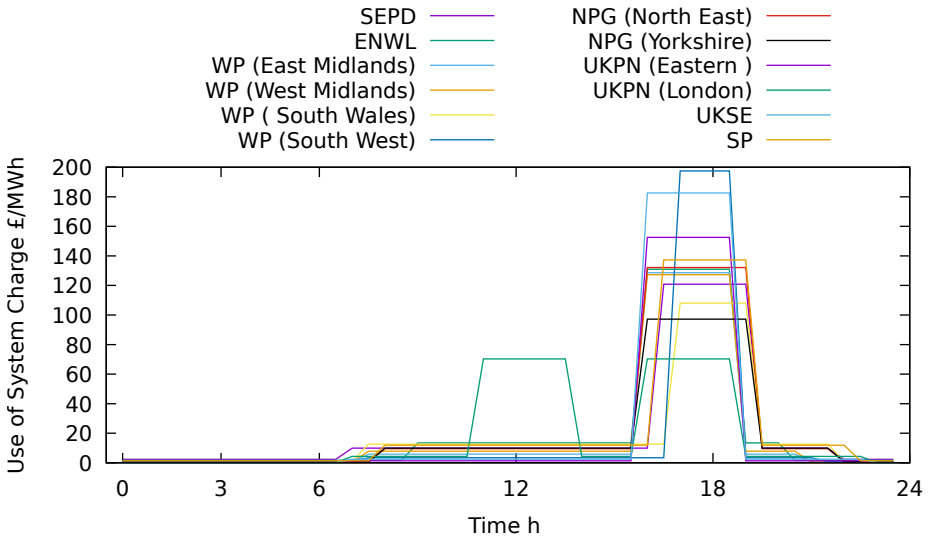

Figure 1.4: DUoS charges for different regions in England. All regions have an increase in the DUoS charges in the evening when power consumption is the highest on the system. London also has a peak around noon.

Region	TNUoS charge £/MWh
Northern Scotland	6.215608
Southern Scotland	4.262747
Northern	5.943493
North West	5.878185
Yorkshire	5.978783
N Wales and Mersey	6.607274
East Midlands	6.248796
Midlands	6.426317
Eastern	7.095134
South Wales	5.77537
South East 5	7.47522
London	5.487378
Southern	7.04792
South Western	7.464813

Table 1.1: TNUoS charges £/MWh for different regions in GB.

In addition to consumption charges, electricity generators (i.e. power plants) are required to pay additional transmission charges to the SO. Power producer charges are based on their Transmission Entry Capacity (TEC), that is the maximum production capacity of power plants and their geographical location. In our wholesale market simulations, transmission system charges attributed to the power plants are assumed to be included inside the calibrated model cost functions, so do not need to be explicitly modelled. Transmission charges as charged to the power plants would not depend on the time of day and therefore should not significantly impact the optimal operation of the power plants.

TNUoS charging structure in GB has recently changed to a fixed charge for all users. As the TNUoS charge does not represent a large part of the domestic user bills and is not time-dependent, therefore not influencing the timing of the power consumption, in our market simulations, it will be assumed that it is captured in the "other costs" part of the charges against the domestic user.

1.2.4 Balancing System Use of System Charges (BSUoS)

During the settlement period (the half-hourly period when electricity is used and produced), a party that sold electricity is obliged to deliver their contracted volumes and electricity users need to consume their contracted volumes. As electricity generally cannot be stored economically in large quantities, the power generated minus losses (heat losses when transporting) must equal system demand. If demand and supply are not in balance, the frequency of the system can deviate from the target 50Hz (which is the required frequency), and the system can become unstable [31]. In the case where demand and supply do not match, the SO must correct these imbalances.

The SO will match supply and demand by giving instructions to selected electricity users or/and producers to change their contracted volumes (amount of power they initially expected to produce or consume). After each half-hour of power delivery, the metering of supply and demand will take place, and those that have deviated from their contracted volumes will be charged an imbalance price. Imbalance prices are calculated by the SO and are defined as the price of electricity £/MWh that Balancing Mechanism (BM) participants will have to pay/receive for the shortage/surplus of electricity from their contracted volumes. Those who consumed more electricity than they contracted will need to buy the shortfall at the imbalance prices. Those who produced less electricity than they contracted will need to buy the shortfall at imbalance prices. A more comprehensive explanation of market arrangements in GB is provided in [32]. In our modelling, we assume there are no imbalances. The modelling tool relies on matching the future predictions of demand and supply and we do not assume any randomness in our modelling, meaning the demand and supply in all half hours will always be matched.

In addition to managing imbalances caused by demand forecasting errors and other deviations from contracted volumes, the SO is responsible for making sure that power in the transmission network is transported subject to transmission network constraints. Transmission network constraints are physical constraints of the network where power cannot be transported between two parts of the network because the network infrastructure is not able to carry the volumes required. An example of such instance could be the delivery of power from the north of Scotland, where renewable power is abundantly available, to the South of England. If the network capacity during renewable energy production periods is insufficient, the power would need to be sourced closer to the South of England from less efficient power plants. However, network constraints are not explicitly modelled in this thesis.

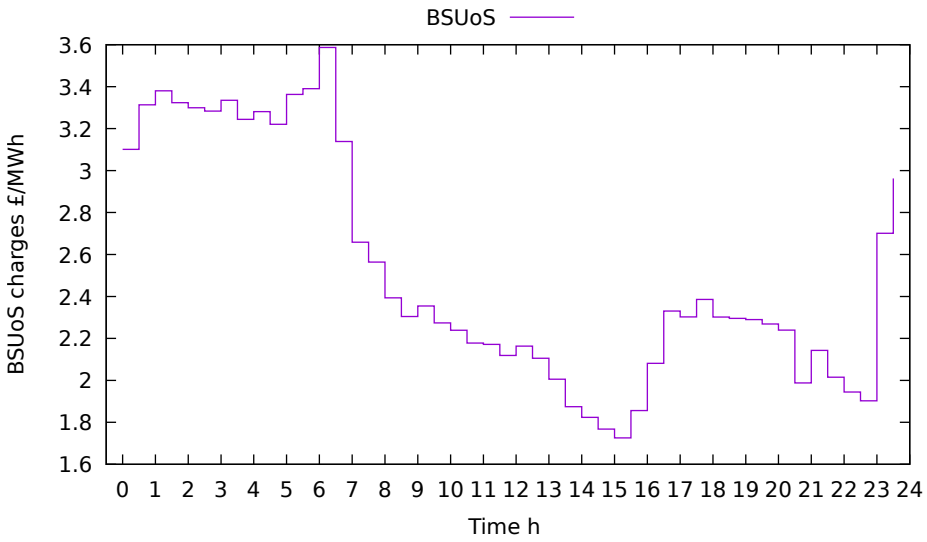

Figure 1.5: BSUoS charges calculated using the half hourly national grid data for the year 2017. We have calculated these by taking an average of all the BSUoS for particular half-hours. [33]

Balancing System Use of System (BSUoS) charges allow the SO to recover costs incurred in the process of balancing the electricity system. BSUoS charges are distinct from the imbalance prices discussed previously. BSUoS prices are not known a priori and are charged after the power consumption and production has taken place. An average of balancing costs over the year of 2017 for each half-hourly period is provided in figure 1.5. Higher charges overnight are observed and could be present due to higher availability of renewable power overnight and lower demand. As the network can be restricted, the SO would need to interfere in the dispatch of power across the country.

As BSUoS charges are not a significant contributor towards electricity bills (0.3 p/kWh), we choose not to model these charges in our wholesale market simulations explicitly.

1.2.5 Agile Octopus

Octopus Energy is the first electricity supplier in GB to offer wholesale market tracking rates referred to previously as DA-RTP. The "Agile Octopus" tariff is important for our model and simulations as it provides the first step in GB to connect domestic customer demand with the supply of power, by rewarding customers who shift their consumption away from electricity consumption peaks and to periods of high renewable power generation, reducing the stress on the grid and allowing customers to reduce their bills. In this thesis, we show how tariffs like these can help GB achieve its carbon emissions targets whilst also allowing customers the possibility to save money on their energy bills.

The Agile Octopus tariff is published every day at 4 pm local time for the next 24 hours where prices of electricity are separated into 48 half-hours. This is different from traditional Economy 7 and Economy 10 tariffs as the electricity tariff changes every day and is directly linked to the wholesale electricity tariff [34]. Some countries around the world already have RTP tariffs for domestic users. An overview of what is currently offered in terms of RTP tariffs around Europe can be found in [18]. The availability of RTP tariffs allows technologies such as thermostat controllers attached to HPs to create optimal strategies that minimise the cost of heating for domestic users.

In figure 1.6, we provide a comparison of an average DA-RTP tariff in each half-hour, as provided by Octopus Energy (Agile Octopus - [34]) and the component stacked cost of delivering electricity to domestic customers including all the costs discussed previously. We show the agile rate closely tracks total cost of electricity. We can also see a significant increase in price during the period of 16:00-19:00, which corresponds

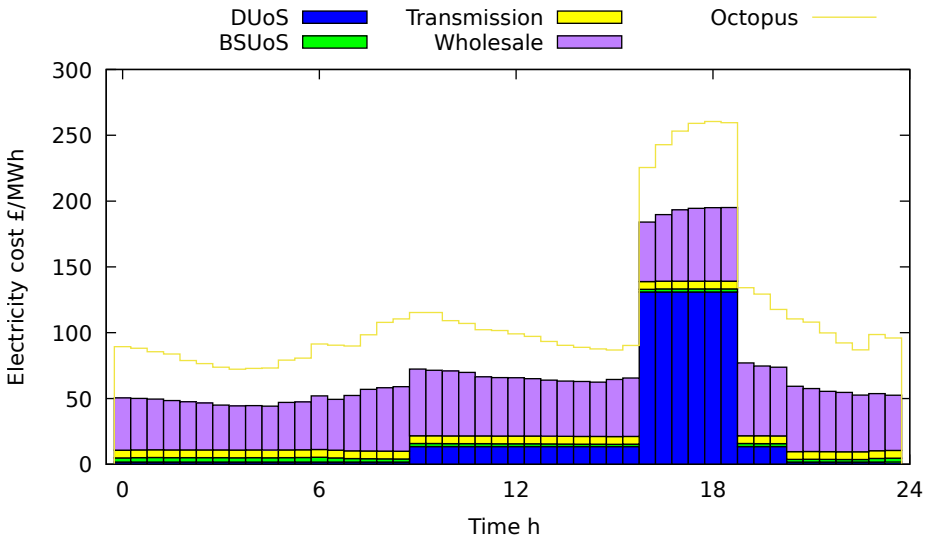

Figure 1.6: Average Octopus Energy Agile tariff comparison to the component stacked domestic user electricity cost. Averages were calculated using historical rates of octopus rate across all regions as can be accessed on [34] for the year 2018. Other costs were also calculated for the same period averaging across all regions. BSUoS and transmission charges can be found at [33], DUoS charges were taken from all DNOs across the GB, Wholesale prices were calculated using the Market Price Index data from National grid [32].

to the high DUoS charge period.

1.3 Agent-based Modelling

To achieve our goal of modelling wholesale electricity prices in future energy scenarios, we chose to use Agent-based Computational Economics (ACE) techniques. ACE is a sub-branch of ABM and is concerned with computational modelling of economic processes (including whole economies) as open-ended systems of interacting agents [35].

In ACE, each agent is specified as a separate entity, that can be regarded as an encapsulated software entity [35], with specific initial conditions. In our model, this will be each power plant and energy storage facility in supply mode on the supply side and each autonomous electric heater and energy storage facility in charging mode on the demand side. The interactions between states and entities in ACE do not need to be explicitly specified; this greatly improves the computational efficiency as the optimisation of each entity can be parallelised [35]. Its ability to include a large number of entities makes ABM particularly well suited to analyse new paradigms in the field of smart grids, such as demand response, distributed generation, distribution grid modelling, and efficient market integration [36].

Agents in ACE make their decisions based upon the external variables arising from the interaction of all system agents. In our case, the external variable is the price of electricity in each half-hour period that is affected by the interaction of the agents, namely power plants, energy storage facilities and house heaters. Each agent, house or power plant, is formulated as a separate optimal control problem and these are solved using Partial-Differential-Equation (PDE)-based approaches. An important point to note here is that the agents only interact through the wholesale price of electricity. A Walrasian auction process [37] is used to find market equilibrium prices that balance supply and demand of the system.

PDE-based approaches have been previously used to value power plants and electric dams in deregulated electricity markets [7] and find optimal control policies for building heating under stochastic weather [8] and DA-RTP prices of electricity, and solving storage problems [38, 39]. A PDE formulation of the problem enables high levels of computational speed and accuracy while incorporating dynamics and operational characteristics of the system [7]. A drawback of PDE-based approaches is the inability

to handle high dimensionality if it were to arise in the problems.

1.4 Thesis aims

This thesis presents a new framework for analysing electricity markets in GB with an increased uptake of electric HPs. The proposed system assumes HPs are installed with intelligent smart thermostats that autonomously respond to DA-RTP electricity prices and weather forecasts, thus reducing electricity demand during peaks whilst maintaining user comfort. We quantify whether a collection of HPs acting independently to central price signals, can collectively reduce consumption during price peaks and increase consumption during low price periods to help achieve system balances at a lower cost. The system benefits of using DA-RTP tariffs are compared to an equivalent system with fixed tariffs, where electricity prices for domestic customers are not varying throughout the day. Real-world data (provided in FES document) for power plant generation capacity and domestic heating consumption in 2030 is used to estimate the future electricity prices in different HP uptake scenarios.

In Chapter 2, a new framework is introduced using ACE that can simulate participants in the GB electricity market. On the demand-side, we include agents that consume electricity for domestic heating or electricity storage and can respond to RTP electricity prices. On the supply side, we include a variety of agents to represent the range of power plants seen in the GB market. The agents representing power plants devise optimal operation strategies based on future electricity prices and thermal characteristics of these power plants.

In Chapter 3, we introduce our model for a generic power plant agent. Here we follow the model devised in [7], but we make some important modifications so that the outputs are more aligned for use in our agent-based simulation. First, we remove the stochastic elements to reduce computation times, and then we add a variety of constraints on the dynamics of the power plant to make them behave more like they would in the real world. These include minimum zero time, stable exporting limits, notice to deviate from zero and ramp rates. We also generalise the model so that it can represent any power plant provided we know the efficiency of the power plant at part-loads. This model allows us to utilise information on power plant characteristics made available as part of the BM reporting service to match the behaviour of a real power plant with an agent in our market simulation. We conclude the chapter by providing information on the processing of data of power plants supplied by the SO [32].

In Chapter 4, details of the optimisation of heating in domestic buildings are provided. We follow the approach of [8] to derive a PDE that can be solved to give the optimal operational strategy of a fully autonomous heating device for domestic use. The resulting optimisation algorithm considers users' comfort levels, outside temperature forecasts and RTP tariffs. It should be noted that a business (Homely Energy) has been set up by the author to provide autonomous heating controllers (thermostats) to domestic users, which can be integrated with DA-RTP electricity tariffs. During product development, experiments have been conducted to show the potentials for savings to be made when heating is controlled autonomously (using a smart thermostat). In Chapter 4, we provide results from the trial that show at least 20% cost savings, which can be achieved when using the controller with DA-RTP tariffs. As the main aim of this thesis is to investigate the impact of electric heating on energy networks and prices, we needed to estimate the behaviour of a sample of real buildings

in GB across the electricity network. The last part of Chapter 4 provides the details of this real-world building thermal parameter estimation. Our analysis is focused on the power networks and power generation in GB. The building data, as discussed in Chapter 4, is collected for England only, but we must scale this data to the level of GB to provide analysis on the impact of HPs across the whole GB region.

In Chapter 5, we provide electricity market simulation results of the GB market for a variety of different power generation mixes and HP uptake scenarios as outlined in different scenarios of FES [3] . We show that a significant reduction of peak demand (5% to 10%) can be achieved by allowing domestic users to receive DA-RTP tariffs and operate their HPs accordingly when compared to fixed tariffs. Evidence of cost savings for the consumers is also seen (10% to 30%), along with an increase in the utilisation of the more efficient power plants and renewable power produced. An analysis is also provided on the current state of the insulation in buildings across GB and the potential benefits of insulation improvements for the power networks and a more efficient use of renewable resources.

We conclude the thesis in Chapter 6 where we discuss the limitation of the modelling, learnings and policy suggestions as well as an outline for future work.

Chapter 2

Market Mechanism

Electricity markets have been changing around the world, becoming more decentralised and liberalised in an attempt to make energy systems more efficient. De-carbonization of energy systems has also taken a central stage on the agenda of many countries around the world. This has started to lead energy systems towards one where a significant amount of power is produced from renewable energy sources. To cater for highly stochastic (unpredictable) power production, more flexibility will be required in the system. Currently, the majority of the power trading takes place through over the counter contracts weeks/months in advance. Moving forward, we will need to see an increase of trading in the day-ahead auctions to provide the liquidity required to balance highly varying power production with demand.

In this chapter, we present a model for finding an optimal set of wholesale electricity prices in which both energy generators, energy storage facilities and houses with flexible heating will participate. ABM techniques are used to model the interactions of the

operators of generators and consumers with market prices. Similar to [40, 41], we model our market as a set of agents that are maximising their utilities subject to a set of prices. The role of the market operator is to adjust prices to ensure the system is in balance (supply is equal to demand).

Our work differs from the techniques employed by [40] and [41] in the use of dynamic optimisation to find optimal control of the agents. We also build a model which takes account of inter-temporal decision making by the agents. In this way, a set of prices is devised for a time horizon in the future rather than just a single point in time.

Future extensions of the model introduced in this chapter could include peer-to-peer markets as discussed in [42], where agents are optimised to consume as much power as possible that is generated within the property or elsewhere in the local grid. In their modelling, optimisation models are used to reduce the distance between power producers and consumers, which reduces the grid use and congestion, in turn leading to a more efficient grid. Our modelling could add another dimension to the model in [42] where the local and wider grid electricity prices are determined through the interaction of the agents across the grid, therefore making the grid electricity price and surplus export rate endogenous. We believe this is important as the feed-in tariff used to compensate for PV output in [42] is no longer available. As a replacement for the feed-in tariff, export tariffs are starting to emerge in the market, such as Outgoing Octopus [43], where electricity suppliers offer daily pricing for electricity exports for domestic users that reflect the grid's supply and demand balance.

2.1 Competitive Market Simulation - Literature Review

ACE methods provide us with the tools to incorporate the complex interactions between agents (market participants) in the electricity market. Wholesale market dynamics have been studied in detail using ACE approaches review of which can be found in [44]. However, in the majority of these studies, the demand side has been taken as inflexible or assumed to have a predetermined elasticity of demand (responsiveness to prices). Lately, the agent-based models have been extended to incorporate the interactions between DSR agents and wholesale electricity prices. Agent-based representations of scheduling DSR are more flexible than pool-based schemes [40]. In this section, we provide a quick comparison of available ACE models and our model.

BID3 [45] is an internal tool used by Pöyry consultants as well as the SO, energy companies and regulators. This software uses an economic dispatch model to simulate the hourly generation of all power stations on the system, including renewable sources. Typically, modelling can also take into account DSR, such as that provided by electric vehicles and heating, but the DSR unit dynamics are generic. This is in contrast with our model, where the dynamics of each demand-side agent are modelled in detail, with agents responding to electricity prices using individual optimisation algorithms. We believe this provides a better understanding of how true market participants will interact with electricity prices and helps us evaluate potential system issues, such as sudden shifts in demand due to choppy price signals that are discussed in detail in Chapter 5.

Optimisation of the system in BID3 is achieved through linear or mixed-integer programming and the objective is to minimise system costs subject to the many system constraints that are programmed in. The supply-side modelling takes into account several considerations such as ramp rates, minimum on/off times, minimum stable generation and start-up costs. This is similar to our model. The BID3 model is also capable of modelling the electricity market whilst incorporating the capacity market considerations. We do not model the capacity market in this thesis to reduce the computational complexity of the problem. An overview brochure of the BID3 system is provided in [46] and further details are provided in [45].

The focus of [47] is to investigate market power, optimal bidding strategies of the market participants, and the level of clearing prices when Time of Use (ToU) demand response was employed in day-ahead markets. In their study, they considered reinforcement learning for their agents to submit their offers for the day-ahead market. Agents in their model can adapt their bidding strategies using the Roth-Erev learning algorithm. A multi-period linear programming method is used for solving the market-clearing price.

Similar to our modelling [47] study looks to evaluate the benefits of the electricity retailer participation in the day-ahead markets. However, their modelling has a limited number of agents and the parameters of these agents are generic. Their study is focused more on the bidding strategies for the day ahead markets rather than the clearing mechanism for that particular day ahead market. We believe that by including the real-world agent parameters, our modelling can provide a more in-depth understanding of the agent interaction with the markets.

Our model differs from [47] in that we do not require the market participants to

provide bids and offers for the day-ahead markets. Economic theory suggests that well functioning forward and spot markets should achieve maximum utility for all participants in the market. If agents can optimise their behaviour over longer time periods utilising their known dynamic models, they should be able to capture their fuel and start-up costs better.

Simulation of electricity market using demand elasticity functions has been performed in [16]. Each generator agent in their model submits their marginal cost of electricity production to the SO. The SO is then able to use an algorithm to maximise the social welfare of the system, minimising the cost of electricity production. Electricity prices can then be updated using the elasticities of the demand side. We believe that our modelling where demand agents are explicitly modelled allows us to better account for the inter-temporal demand dependencies across agents.

[48] solved a "Unit commitment and DSR commitment" problem that integrates both generator supply curves and commercial DSR supply curves. The objective function included the fuel cost of generation units, the start-up costs (hot or cold), shut-down costs, and the cost of enabled DSR. The objective of the algorithm is to minimise the cost of operating the system. Results show that 1% to 18% savings are available in the system when DSR is considered. The level of savings depends on the willingness of the demand side to participate. Our generator modelling also considers the generator costs discussed in their study; we also further refine the potential savings given different energy generation scenarios in the future.

Commercial building participation in price-based DSR programs has seen much more interest due to the size of the controllable loads in commercial properties. Even though our study focuses more on domestic user participation in DSR, we have also reviewed

some studies on commercial buildings such as [49]. In [49], prices are simulated as a day-ahead auction using bid-based DC optimal power flow. This is in contrast with our model, where we capture the participation of the agents in a continuous price exchange. Two cases are investigated: a small number of DSR commercial participants and a high number of commercial participants. These results show the DSR participation can reduce commercial building energy costs, system peaks and price volatility. In our modelling, we only consider the simplified version of commercial building participation through a simplified Industrial and Commercial DSR (I&C DSR) function of price. Results from the [49] can also support our results in that given the large number of domestic users participating in the market; domestic users should be able to capture similar savings to those achieved by commercial agents.

The use of thermal storage in DSR has been previously considered in [26]. Their study evaluates the potential of thermal energy storage and thermal inertia in demand response optimisation in the context of the day-ahead market. A dwelling's thermal demand is met by Electro-Thermal Technologies (ETT) that could be generating Combined Heat and Power (CHP) or consuming HP electricity. Stochastic programming is used. The approach considers uncertainty in outdoor temperature, DHW (domestic heat water) load, base electricity load, occupancy, and imbalance prices. The optimisation is on the retailer side where it tries to minimise its cost over a day, given the day-ahead market purchases, imbalance costs, gas purchases and payments to dwelling occupants for violation of contracted thermal comfort.

Even though in our modelling in Chapter 5 we consider all agents to be independently interacting with the market, it is unlikely that domestic users would participate in the wholesale markets themselves as opposed to accessing RTP prices through the retailer. Modelling of the optimal bidding strategies for the retailers discussed in [26]

could, therefore, be improved by including the individual agent modelling discussed in this thesis. Other authors have also investigated optimization models maximizing retailers profit such as [50] where they have proposed a genetic algorithm based distributed pricing framework to determine optimal electricity prices for different types of customers in terms of their energy monitoring equipment. This study is different from ours as we specifically focus on dynamic modelling of the agents and account for heating profiles and heat loss coefficients inferred from real world sensor data.

Similar to our wholesale market modelling, [51] propose a day-ahead pool market mechanism where they combine a solution of centralised mechanisms with the decentralised demand participation structure of dynamic pricing schemes based on Lagrangian Relaxation [52]. Schemes connecting wholesale and retail markets lead to more efficient and competitive markets. This method contains individual surplus maximising agents and a global price updating algorithm. A market objective is a form of social welfare maximisation. Participants are assumed to behave competitively, acting as price-takers and revealing their actual economic and technical characteristics to the market. The problem is converted from social welfare maximisation to an equivalent generation cost minimisation with limitations on the demand side agents. Our modelling differs in the use of dynamic pricing modelling for the individual agents and the iterative method in finding the equilibrium prices as discussed in this chapter.

Similar to the modelling discussed in this chapter, [40] present a design and evaluation of a market-clearing scheme for trading DSR in a deregulated power system using Walrasian auctions. In their modelling, DSR participants update their DSR quantity bids in response to prices adjusted by the market operator. This auction is repeated iteratively until market equilibrium is obtained at the point where the market outcome is proven to be Pareto optimal, as defined in [40]. We utilise a similar framework in

our work for finding optimal prices. Our method extends these concepts by allowing agents to take into account their inter-temporal dynamics similar to [53].

In [53], authors have discussed the importance of taking into account the inter-temporal decision making to model wholesale electricity prices. In their work, they have inferred the price/demand elasticity from real-world historical data, in contrast to our approach where we have assumed that the control of heating is done by an autonomous rational device that minimises the user discomfort as discussed later in chapter 4. In [53], the electricity price equilibrium is found using genetic algorithms where demand/supply intervals are supplied to the system operator, who the, using the intervals provided, determines the most optimal power dispatch schedule.

We agree with the [53] in that dynamic inter-dependence of agent decisions is crucial when evaluating market DSR. We discuss the importance of inter-temporal decision making in detail in Chapter 5. A more detailed literature review of agent-based modelling and simulation of smart electricity grids and markets can also be found in [36].

We also note that in literature, behavioural changes of the demand side agents to electricity prices are usually calculated using price and cross-price elasticities infered from the historical consumption data from smart meters [53]. We have chosen the alternative approach of simulating the behaviour of individual agents observed in the market and scalling these for the population behaviour due to our particular interest in the behaviour of heat pumps and RTP tariffs. We believe that heating behaviour is unique due to its cross-price elasticity dependence on the building insulation, user temperature preferences, time of heat pump operation due to noise and outside weather conditions. We believe that due to the limited amount of heat pumps currently in the market, it would be difficult to estimate these cross-price elasticities accurately.

Using our dynamic simualtion approach discussed in 5, reduces the amount of data required to be infered for these customers to user temperature preferences, building dynamics, weather forecasts. Once this information is inferred from historical data, behavioural profiles for these houses can be scalled to estimate the impact of future heat pump uptake scenarios on wholesale electricity prices and the network as discussed in 4. The modelling framework could also allow future researchers to estimate impacts of improved efficiency of the building stock and changing weather conditions without requiring inference of cross-price elasticities.

2.2 Optimal Price Search

In this section, we introduce the optimal wholesale price search algorithm. We use this algorithm to find an optimal wholesale price policy $\pi^{wholesale,*}$ from a set of all possible wholesale price policies Ω defined as follows

$$\Omega = \{\pi^{wholesale} = \{\pi^{wholesale}(t)\}_{0 \leq t \leq T} : \pi^{wholesale}(t) \in \mathbb{R} \quad \forall t\}. \tag{2.1}$$

where t is the time period of the price and T is the terminal time of the simulation.

We assume that electricity prices are discrete and do not change during the period Δt so we can write

$$\pi^{wholesale}(t) = \begin{cases} \pi^{wholesale}(0) & \text{for } t < \Delta t \\ \pi^{wholesale}(\Delta t) & \text{for } \Delta t \leq t < 2\Delta t \\ ... \end{cases} \tag{2.2}$$

We define $\mathcal{S}(\pi^{wholesale})$ as a set of system supply values at different times that comprises G number of agents that can dispatch energy to the grid, and each choose to supply $\{W_1, W_2, ..., W_G\}$ at time t and can be written as

$$\begin{aligned} &\mathcal{S}(\pi^{wholesale}) \\ &= \left\{ W(t; \pi^{wholesale}) = \sum_{g=1}^{G} W_g(t; \pi^{wholesale}) : \quad 0 \leq W_g(t; \pi^{wholesale}) \leq K_g \right\}_{0 \leq t \leq T}, \end{aligned} \tag{2.3}$$

where $W(t; \pi^{wholesale})$ is the total supply of all energy supply agents given a price policy $\pi^{wholesale}$ and is chosen for the entire period $0 \leq t \leq T$. We can calculate the total supply by summing all of the individual agent outputs $W_g(t; \pi^{wholesale})$ where g denotes an individual generating agent and t denotes time given a pricing policy $\pi^{wholesale}$ over the period. All agent outputs $W_g(t; \pi^{wholesale})$ are bounded $0 \leq W_g(t; \pi^{wholesale}) \leq K_g$ by the agents' g maximum export limit MEL_g, $K_g = MEL_g$. We define $\mathcal{D}(\pi^{wholesale})$ as a set of demands that comprise M number of demand agents $\{H_1, H_2, ..., H_M\}$ and is given by

$$\begin{aligned} &\mathcal{D}(\pi^{wholesale}) \\ &= \left\{ D(t; \pi^{wholesale}) = \sum_{m=1}^{M} D_m(t; \pi^{wholesale}) : \forall_{1 \leq m \leq M} \quad 0 \leq D_m(t; \pi^{wholesale}) \leq Z_m \right\}_{0 \leq t \leq T}, \end{aligned} \tag{2.4}$$

where $D(t;\pi^{wholesale})$ is the total demand at time period t of all demand agents given the price policy $\pi^{wholesale}$. This is given by the sum of all individual demand agents $H_m(t,\pi^{wholesale})$ at time t. All agent demands $H_m(t;\pi^{wholesale})$ are bounded $0 \leq H_m(t;\pi^{wholesale}) \leq Z_m$ by the agent m maximum power input $H_{max,m}$, $Z_m = H_{max,m}$.

In Chapter 5, we will model heat pumps, energy storage facilities and DSR as energy demand agents. Baseload and any other demand such as Electric Vehicle (EV)s will be considered as a function of time. The sum of demands of all of these agents will therefore comprise $D(t;\pi^{wholesale})$ for each time period t.

We note that some of these agents, such as domestic heat pump users, do not participate in the wholesale electricity market directly and rather purchase their power requirements through an electricity supplier or an aggreagator. When assessing the behaviour of these agents we assume that they access market electricity prices through these intermediaries and the price thse agents receive are already adjusted for network costs and supplier margin, in a similar fashion as current Agile Octopus customers, as discussed in Chapter 1. Further details on how the domestic electricity prices are calculated for different agents are provided in chapters 4 and 5.

We aim to minimise the sum of absolute energy imbalance of the system given price policy $\pi^{wholesale}$ as

$$R(\pi^{wholesale}) = \sum_{t=0}^{T} \left| W(t,\pi^{wholesale}) - D(t,\pi^{wholesale}) \right| \Delta t, \tag{2.5}$$

where $R(\pi^{wholesale})$ is the aggregate absolute energy imbalance, and is calculated as an approximate integral of the absolute differences between total system power demand

$D(t, \pi^{wholesale})$ and total system supply $W(t, \pi^{wholesale})$ over a time period $0 \leq t \leq T$.

We attempt to minimise this total imbalance of the system $R(\pi^{wholesale})$; therefore, our objective can be written as

$$\pi^{wholesale,*} = \underset{\pi^{wholesale} \in \Omega}{\arg\min} \; R(\pi^{wholesale}), \tag{2.6}$$

where the algorithm looks for an optimal price policy $\pi^{wholesale,*}$ minimising the sum of total imbalance of the system $R(\pi^{wholesale})$. This is to reflect the intention of the power exchange, where to provide a reliable supply of electricity, the supply and demand must be balanced at any given time [53] for reliable operation of the electricity grid (i.e. $D(t, \pi^{wholesale,*}) = W(t, \pi^{wholesale,*})$). We do although understand that due to the limited number of agents in our model the power produced ($W(t, \pi^{wholesale,*})$) might slightly deviate from the power consumed ($D(t, \pi^{wholesale,*})$) in some periods. We therefore find the minimum cumulative difference across all time steps similar to single step Walrasian auction approaches discussed in [37, 54], but across multiple timesteps. This provides us sufficient accuracy for the analysis of the future energy scenario power generation and consumption as discussed later in this chapter. An iterative method is used for the price policy search, and we denote each price policy attempted by the subscript q. We store all price policies attempted in Ω.

We consider the power consumption and production in different time periods to be a substitutable good for which we try to find the general equilibrium that clears the market across all time periods. The outline of the price search algorithm is provided in figure 2.1 and discussed next. Iterations are initialised with an arbitrary price policy $\pi^{wholesale,q=0}$. Our model then uses a form of Walrasian tatonnement ("trial and error"

method, see [37, 54] for an example of this) to determine the equilibrium price schedule for the system. In this auction, the auctioneer announces prices and agents provide the auctioneer with their expected supply and demand given a price policy $\pi^{wholesale,q}$. The auctioneer accumulates these and adjusts prices if the aggregate supply does not equal aggregate demand for all time periods.

The prices found using the price search algorithm should reflect the equilibrium prices that clear the wholesale electricity market (demand equivalent to supply in all time periods) and these should be similar to those observed in a well functioning competitive market. At this point we do not propose that the power exchange should employ the method discussed in this chapter in finding the equilibrium prices to clear the power exchange. We do although suggest that the use of the price search algorithm introduced here provides useful insights into the equilibrium prices and agent behaviour, that should reflect he real world future electricity market with many pariticpating players.

2.3 Simulation parameters

Agents of the price search algorithm will be discussed in detail in Chapters 4 (buildings), 3 (power plants) and 5 (energy storage facilities and other agents). We would although like to discuss the convergence of the algorithm to near-equilibrium prices in a little more detail in this section. We will therefore present results of a generic price search algorithms and discuss only general details. We will then discuss all parameters and results of the simulation in detail in Chapter 5.

Our price search algorithm objective is to match the total supply and demand of the

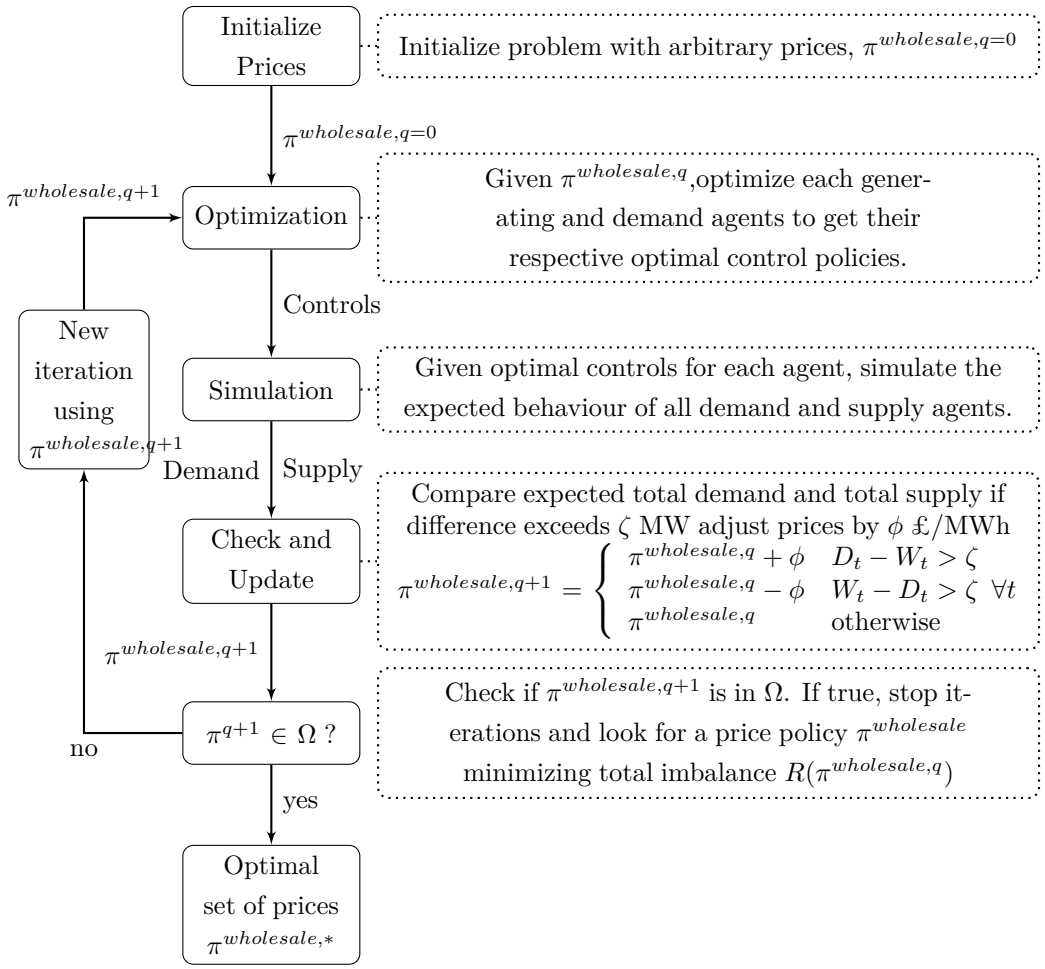

Figure 2.1: Optimal Price Search Algorithm

system in each period Δt as discussed previously. Adjustment prices ϕ were adjusted at a set number of iterations of the price search algorithm. If the iteration is denoted as q and maximum number of iterations imposed on the algorithm as $q^{max} = 1000$ (empirically tested that higher number of iterations provide little improvement on the final result), imbalance at time t as $\xi(t, \pi^{wholesale}) = \left|W(t, \pi^{wholesale}) - D(t, \pi^{wholesale})\right|$ and the maximum imbalance during the iteration at any point $0 \leq t \leq T$ as χ. ϕ was then chosen according to the rules, as shown in 2.7.

$$\phi = \begin{cases} 0.5\frac{\xi(t,\pi^{wholesale})}{\chi} & \text{for} \quad q \leq 0.3q^{max} \\ 0.1\frac{\xi(t,\pi^{wholesale})}{\chi} & \text{for} \quad q \leq 0.5q^{max} \\ 0.01\frac{\xi(t,\pi^{wholesale})}{\chi} & \text{for} \quad q \leq 0.7q^{max} \\ 0.001\frac{\xi(t,\pi^{wholesale})}{\chi} & \text{for} \quad q \leq 0.8q^{max} \\ 0.0001\frac{\xi(t,\pi^{wholesale})}{\chi} & \text{for} \quad otherwise. \end{cases} \tag{2.7}$$

Rules provided in (2.7) have been chosen heuristically as discussed next. We have observed that price adjustments ϕ can be weighted by their respective power imbalance $\frac{\xi(t,\pi^{wholesale})}{\chi}$ but these adjustments need to be small enough not to cause algorithm instability. We have observed that linear adjustments as provided in (2.7) were sufficient to allow the model to converge to near equilibrium and were not large enough to cause algorithm instability.

As part of our attempts to find the equilibrium prices faster, we have also investigated other adjustment price weighting methods. We have considered a quadratic weighting, where we used $(\frac{\xi(t,\pi^{wholesale})}{\chi})^2$ to adjust the prices as above instead of $\frac{\xi(t,\pi^{wholesale})}{\chi}$. This caused model instability and price search algorithm was unable to converge to a near-equilibrium price.

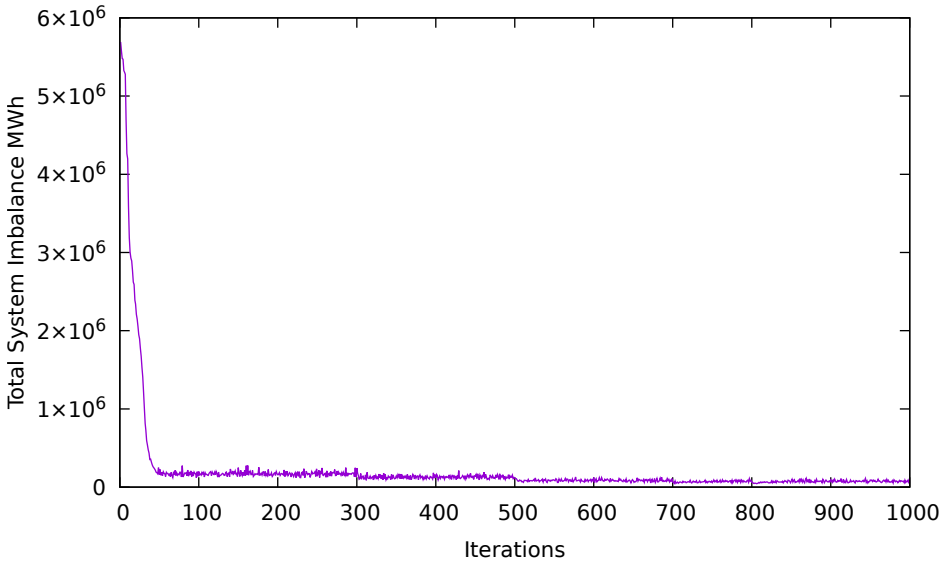

Figure 2.2: Total system imbalance of simulated system

The iteration number at which ϕ was adjusted has also been chosen heuristically. We have visually inspected the simulated total system imbalance, as shown in figure 2.2 and have determined levels at which we believe the market search algorithm has reached price equilibriums for the given ϕ values. These were then chosen as breakpoints to adjust the weighting factor for the price adjustment. We show an example plot of total system imbalance for the simulated system in figure 2.2. We can see that at the start of the breakpoint for the price adjustment the imbalance values drop quickly but once they local equilibriums are found these values do not change significantly at which point we adjust the weighing factor ($q = 300, 500, 700, 800$).

We show the convergence of the values of interest in our simulations in figure 2.3. Twenty simulations are performed with a different initial set of prices $\pi^{wholesale}(t)$ passed to the price search algorithm. In all cases, the system starts with the same initial conditions for the power generator fuel input and internal temperatures in buildings. We can see the total fuel cost and profit of the generators, as well as the average

electricity price for all users and total heating costs for all the houses in the simulation, converge to within narrow bounds as shown in figure 2.3.

There is a slight variation in the values between iterations when the near-optimal price set is found. This is due to our simulation not perfectly clearing the market, supply and demand in each time period are not precisely the same. In future work, we could increase the number of participants in the market mechanism, which should allow the market to be matched. However, increasing the number of participants will significantly increase the computational work required to reach equilibrium. For comparison purposes of the system with HPs and without HPs in Chapter 5, these slight variations of the values of interest when near-equilibrium price set is found should not significantly affect the results. As we can see, the changes in the values between the iterations are very small, so increasing the participants and hence computation times were deemed not to be necessary.

2.4 Conclusion

Dynamic decision making is critical in determining the optimal operation of energy systems. In this chapter, we have introduced a novel method of finding equilibrium wholesale electricity prices for an electricity system where agents are individually optimised and interact with wholesale electricity prices over a period of time whilst taking into account their inter-temporal constraints.

We have shown that this method of price search can allow us to evaluate the values of interest for the market such as the cost of electricity delivery and the average electricity

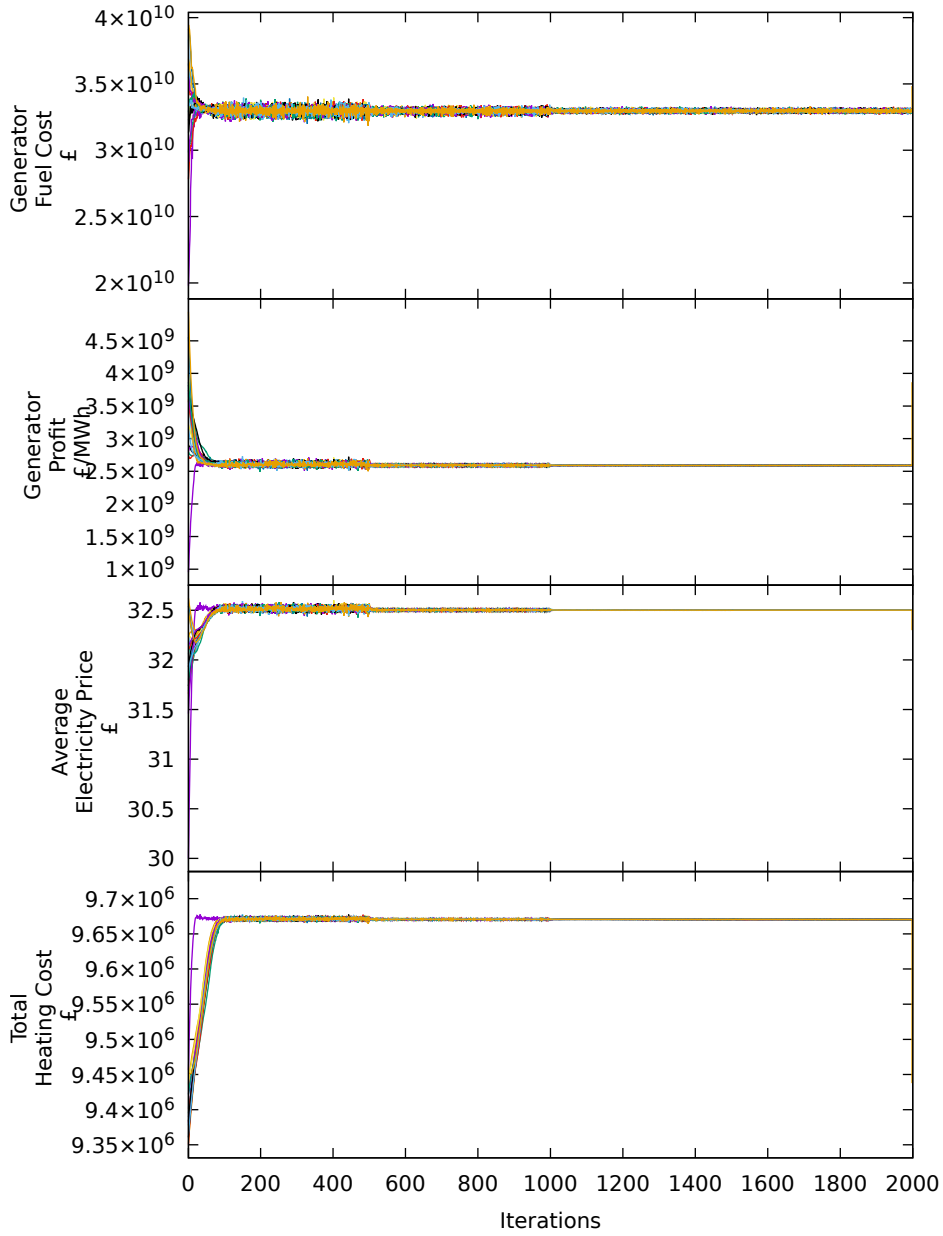

Figure 2.3: Convergence of costs of interest in market simulations against algorithm iterations.

prices as once the near-equilibrium prices of electricity are found the difference in the values of interest is minimal.

In the next chapter, we will introduce individual optimisation methods for the optimal power plant operation given a set of wholesale electricity prices, after which we will then introduce a method of domestic user heating optimisation taking into account RTP electricity prices. In Chapter 5, we will then use the market price search methods to derive wholesale electricity market prices for FES scenarios in 2030. Our models will attempt to evaluate the benefits of RTP tariffs on wholesale electricity markets when compared to fixed tariffs. Heat Pumps, energy storage and power plants will be dynamically optimised and will respond to pricing signals to match demand and supply in all periods.

Chapter 3

Power Plant Operation

In this thesis, we aim to capture the dynamics of total electricity supply and demand in GB. In order to create an accurate representation of the supply side of the electricity market, we must be able to model power plants. These models should be able to capture the properties of the operational strategies of power plants we see in the network in GB, most importantly, Open Cycle Gas Turbine (OCGT), Combined Cycle Gas Turbine (CCGT) and coal plants. These three types of power plants represent a large portion of controllable generation capacity in GB and tend to be cycled (turned on/off) depending on wholesale electricity price. This is in contrast with wind and sun power generation since the amount of wind or sun that is produced at any point cannot be controlled. Other difficult to control power sources could include nuclear power plants, which are restricted in their ability to ramp up or down given operational safety limits.

In monopolised electricity markets, the optimal operation of power generation facilities

is usually derived by the system operator solving the unit commitment problem to minimise the cost of delivering the required power to the grid [7]. Unit commitment is an optimisation problem in which the operation of a set of generators needs to be decided, taking into account electricity system constraints, individual generator operational constraints and system load requirements [7]. This global optimisation is usually performed using Mixed Integer Linear Programming (MILP) algorithms [7].

In GB, the electricity market is competitive. We, therefore, develop models to explain the optimal operation of the power plants when they are not being dispatched by a central market operator but coordinated through a competitive electricity market. Well functioning, competitive electricity markets (for an explanation of competitive electricity market structure see Section 1.2.1) work on the assumption that the decisions of different agents in the market will be made independently of each other. This means that in our model of the GB market, individual power plant optimisations can be performed independently, allowing for parallelism when computing optimal operation schedules of individual power plants and inclusion of more complex power plant dynamics in deriving these optimal schedules. Optimal operation models derived in this chapter allow us to use individual power plant information from the SO to derive individual power plant optimal operation schedules. These schedules can then be fed into our market simulation model introduced in Chapter 2 to model real-world electricity market scenarios. Our methods have been inspired by models introduced in [7]. In their work, a PDE-based method for valuation and operation of power plants has been introduced for a specific power plant.

In contrast to [7], we attempt to devise a simplified general model of power plant operation that can be solved quickly and efficiently, as well as adapt to different types of generators. We also attempt to include dynamic operating constraints such as ramp

rates, notice to deviate from zero and minimum zero times. Real-world GB data of the power plants' operational characteristics is then fed into our power plant modelling. These are provided by the power plants in GB to the NG for the BM; for the GB market structure and the role of NG refer to Section 1.2.1. We believe the inclusion of these operation characteristics allows our model to more accurately estimate different operation costs, leading to a better representation of the real-world operation of power plants.

The first part of this chapter provides a literature review of power plant operation optimisation in deregulated electricity markets. We follow on to describe how we model the costs involved in operating a power plant, outlining the power plant characteristics and expand on how information from the BM can be used to calibrate our power plant models. Then we introduce the mathematical formulation of the power plant operation model, after which we can provide a general numerical method to solve such a problem. A demonstration of the model for a bespoke power plant is then provided as evidence that the model achieves the expected behaviour for the operation of the power plant.

We conclude the chapter by providing a discussion of GB's power plant operational data cleaning and pre-processing, followed by a comparison of our simulated wholesale electricity prices against real-world GB electricity prices. Our simulated wholesale electricity prices are derived by using the published and estimated operational parameters of the power plants and attempting to operate these power plants in a way that they replicate the historical power output of these same power plants. We then compare whether the derived wholesale price of electricity for this power supply matches the wholesale prices historically observed for the respective dates.

3.1 Literature Review

Researchers from the field of mathematical finance mostly focus on the valuation of the power plants in competitive electricity markets. This is due to the increased interest in having an accurate valuation of power plants when purchases of these assets are made in competitive electricity markets. To value these power plants accurately, optimal operation of the plants needs to be considered. The valuation models, therefore, have inherent optimal power plant operation schedules. In this thesis, we are only interested in this optimal operation schedule, rather than the actual value of the power plant.

In [7], the authors derive a PDE-based model for the valuation and optimal operation of hydroelectric and thermal power generators. They assume all sellers of power in the electricity market are price takers and cannot coordinate the power generators. This greatly simplifies the unit commitment problem in that generators that are not linked physically can be modelled and optimised independently. Even though these authors derive an optimisation model for a single power production unit, these models can be used to simulate the optimal dispatch of several units in the network, as we show in this chapter. When links between the power plants do not need to be considered, the complexity of the optimal dispatch of generation assets within the system is significantly reduced and allows the inclusion of more complex generator dynamics, as compared to the dynamics considered in unit commitment problems. In particular, these authors calculate the output of the power generator in MW as a one-to-one function of the temperature of the thermal generator, which appears as a dynamic variable in the model.

Our method is similar to that introduced in [7], the main difference being that the power output will be calculated as a function of fuel input rather than temperature

and will include multiple operational states of the power plant. This allows a more general use of the model across different types of generators, including those that require long warm-up periods such as CCGT power plants. Use of fuel as the input of the modelling allows for the use of efficiency curves at different power plant load levels to account for differences between generators. Efficiency curves represent the steady-state ratio between the rate of power produced and the rate of fuel consumed. We also simplify the model introduced in [7] to exclude stochastic prices (uncertainty in the future wholesale prices). In our power plant modelling algorithm, we assume that prices of electricity that will be received by the power plant are the forward prices and are therefore known in advance. Hence, there is no uncertainty on how these will develop, which significantly reduces the computational times required for our simulations. In Chapter 5, we will present results where wholesale prices of the system become endogenous in the model and are derived through the interaction of the individual power supply and demand agents.

In [55], the authors considered real options valuation of power plants in the competitive market in the USA. In their considerations, they included start-up costs, fuel costs, and variable costs due to operation and maintenance. The focus of that paper was on the optimal operation of OCGT power plants as this allowed them to ignore power plant start-up times. The authors did suggest the inclusion of start-up times in their future work but acknowledged that this would make the problem more complex. Consideration was also included for minimum on time (time that power plants need to be operating when started before turning off). Controls included binary decisions to operate or not to operate, the frequency of control being half-hourly. They found the model's valuation over the long period for the power plants provided reasonable valuations of power plants when compared to real-world selling prices of these power plants. Power plant prices for simple gas turbines using the model of [55] were estimated to

be between 170 $/kW and 198 $/kW. The authors observed three actual power plant sales at the time that were priced at 198 $/kW, 183 $/kW and 206 $/kW. Please take note that these prices are $/kWh, and to find the actual price of the power plant one needs to multiply the capacity of the power plant (e.g. 50 MW) by this price. This paper, therefore, confirms the importance of including the start-up costs, fuel costs, variable costs due to operation and maintenance that we include in our power plant modelling. We also extend this to include start-up times that [55] considered to be essential although outside of the scope of their study.

Several papers consider the more technical aspects of power plant operation and optimisation. As mentioned previously, the more technical aspects of power plant operation are outside of the scope of this thesis but are discussed in detail in [56]. In [56], authors discuss the optimisation of a power plant from the more technical physics perspective, including the set points of controls such as mass flow rates, water levels, air temperatures. In our work, we solve a simplified problem of the power plant operation, as explained in section 3.2. Our simplified operation assumes that by estimating efficiency parameters using the observed power plant operation data and matching this to the modelled operation, we should capture most of these intricacies and reflect these in the cost of the power plant operation through these operational parameters.

In [57], the authors used MILP to solve the problem of power plant optimisation in deregulated electricity markets with the inclusion of dynamic constraints. The authors consider start-up costs in different states (cold, warm, hot), part-load efficiencies, ramp rates, the minimum downtime, and minimum operating times, as defined in section 3.2 in a similar manner to our approach. The power plant operation problem is solved using commercial software General Algebraic Modeling System (GAMS) and the solver IBM ILOG CPLEX Optimization Studio (CPLEX). The authors also discuss

the implications of increased renewable energy production in Germany on fossil fuel plant operation and profits. Simulated profits decrease significantly (ranging from 4% to 60% depending on months of the year) with the increased uptake of renewable power generation. The authors discuss that these changes in profitability can be the cause of reduced investment in fossil fuel power generation in Germany. Our research supports this argument in Chapter 5 by showing a significant drop in thermal power plant profits due to increased renewable generation. Our model differs from [57] in that it is solved using dynamic programming rather than MILP. This allows us to account for continuous dynamics and does not require us to specify distinct offline states; instead, we model the power plant behaviour as continuous with discrete time control events moving through different states of power plant operation such as offline, synchronisation and normal operation. Continuous modelling of the power plant also allows us to account for intermediary costs when moving between states.

3.2 Power plant characteristics

A fossil fuel power generating unit is an electricity-producing unit that converts heat energy to electric power. We refer to a generating unit as a single power generating unit that can be controlled for its power production. The power plant, on the other hand, can be several generating units in the same power plant facility. In our model, we can regard the generating unit as a black box that, in a steady-state when fully warmed, is supplied with fuel at rate Q MW and produces power at a rate W MW as shown in figure 3.2. We restrict the changes in the fuel input subject to ramp rate limits. We also apply part-load efficiency curves to represent the power output of W for different rates of fuel input Q.

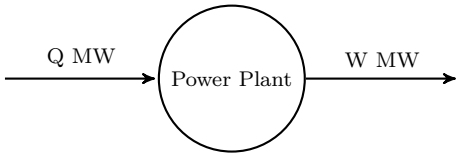

Figure 3.1: Simplified graphical depiction of the black box power plant model.

Whilst not dealing with complex internal modelling of the power plant, our models still obey simplified operational constraints as reported by NG. We expect these simplified parameters to approximate acceptably the continuous dynamics of power plants in GB. Here we provide a brief introduction of the terms used in our modelling. For a thorough explanation of power plant technical limits, please refer to [58].

For ease, we provide a quick overview of the power plant parameters that are considered for the power plant optimisation. The following informative definitions have been compiled from [58, 59];

- Maximum Export Limit (MEL) - is the maximum level in MW at which the generating unit may be exporting power into the National Electricity Transmission System at the Grid Entry Point or Grid Supply Point, as defined in [59].
- Stable Export Limit (SEL) - positive MW value representing the minimum stable export operating level. The SEL is achieved when the unit is operating within its design range, with stable combustion and stable operational NOx control measures.
- Notice to Deviate from Zero (NDZ) - prior notice required by the power plant, to start up a power plant to the point of synchronisation. The synchronisation is the point at which the generating unit is connected to the grid (i.e. starts producing power). The time it takes for the power plant to synchronise will

depend on how long the power plant has been offline (i.e. not producing power).

The ability of the power plant to change its output from synchronisation to full load is a function of the power plant design. It is dependent on the size of the plant, fuel type, initial material conditions and the ability to change (ramp) these to the final conditions. Evidence from the GB power market shows that the fastest power plants to ramp up are OCGT followed by CCGT and lastly coal power plants [58]. Nuclear power plants, on the other hand, are not even considered, as the times to increase production and decrease production are too long (up to 72 hours). The rate at which the power plant can increase its power production after they have been synchronised to the system are defined as ramp rates MW/minute. Generator operators disclose these rates to the SO to show their availability for the balancing services.

- Run-Up Rates - rates at which a particular power plant can increase its active power production within the operating range. Up to three rates can be provided. We denote these as RURE1, RURE2 and RURE3, where the Run-Up Rate Export (RURE), can be provided for each power plant with corresponding states at which it is feasible to make the next discrete jump in the rate of power that can be reliably committed to the SO. These jumps are referred to as ramp rate elbows (RUEE2 and RUEE3). A graphical depiction of the run-up rates for a BM unit (smallest entity that can be controlled within the BM) is provided in figure 3.2. We show how the power plant can increase its power production at a rate of $\frac{dW}{dt} \leq RURE1$ MW/min when power plant output is less than $0 \leq W < RUEE2$. At power output $RUEE2 \leq W < RUEE3$ the rate at which the power plant can increase power is bounded such that $\frac{dW}{dt} \leq RURE2$. For power output $W > RUEE3$ the rate of power output increase is limited by $\frac{dW}{dt} \leq RURE3$.

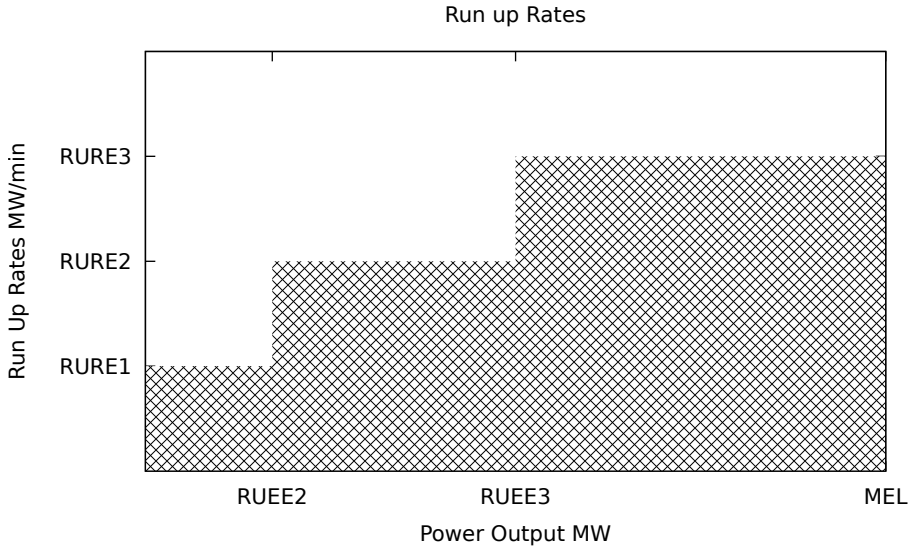

Figure 3.2: Graphical depiction of ideally simplified (for planning purposes) power plant ramp down rates.

- Run-Down Rates - rates at which a particular power plant can decrease its active power production within the operating range. Up to three rates (we denote these as RDRE1, RDRE2 and RDRE3) can be provided for each power plant with corresponding elbows (we denote these as RDEE2, RDEE3). These elbows represent the power production points at or below which power plant's committed rate of power output must be changed - downwards in the case of run-down. A graphical depiction of the run down rates is provided in figure 3.3. The bottom axis is inverted to represent the power output decreasing through the ramp rate steps $MEL \geq W \geq 0$. We show how the power plant can decrease its power production at a rate of $\frac{dW}{dt} \leq RDRE1$ MW/min when the power plant output is $MEL \leq W < RDEE2$. At power output $RDEE2 \leq W < RDEE3$ the rate at which the power plant can decrease power is bounded by $\frac{dW}{dt} \leq RDRE2$. For power output $W < RDEE3$ rate of power output decrease is limited by $\frac{dW}{dt} \leq RDRE3$.

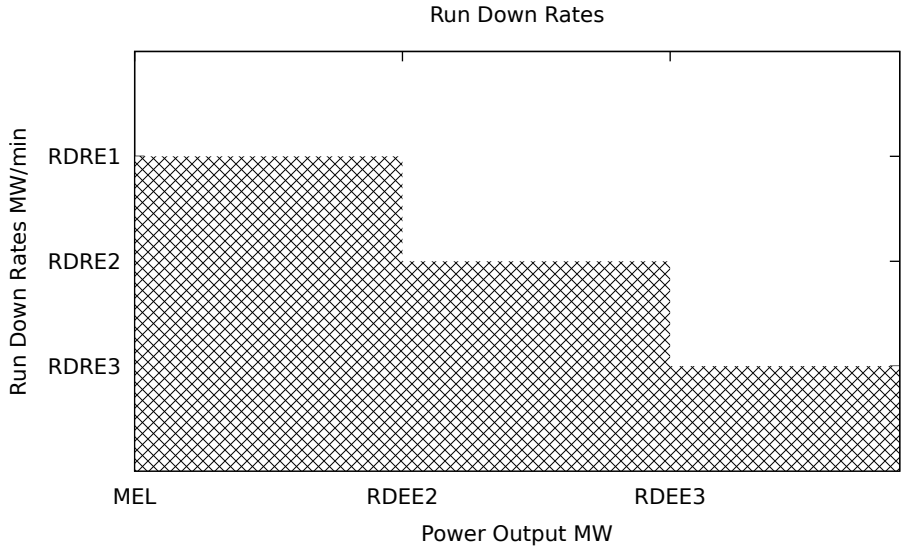

Figure 3.3: Graphical depiction of ideally simplified (for planning purposes) power plant ramp down rates.

- Power plant efficiency - power plant efficiency (i.e. $\frac{\text{power output}}{\text{fuel input}}$ %) is dependent on the load level at which the power plant is operating. Power plants are normally most efficient, i.e. the ratio between the power produced and fuel consumed is the highest when they are operating at maximum power output $W = MEL$.

When a power plant is operating below its full operating potential $W < MEL$ the steady-state efficiency of the power plant drops, therefore the ratio of power output with respect to fuel input decreases. In figure 3.4, we provide some examples of reported part-load efficiencies for gas turbines as provided in [60]. In the figure, the part-load efficiency curves can be seen continuously increasing towards the 100% load ($W = MEL$). Efficiencies provided in this figure are stable operation efficiencies and therefore might not represent true efficiencies of power plants moving through these part-load levels.

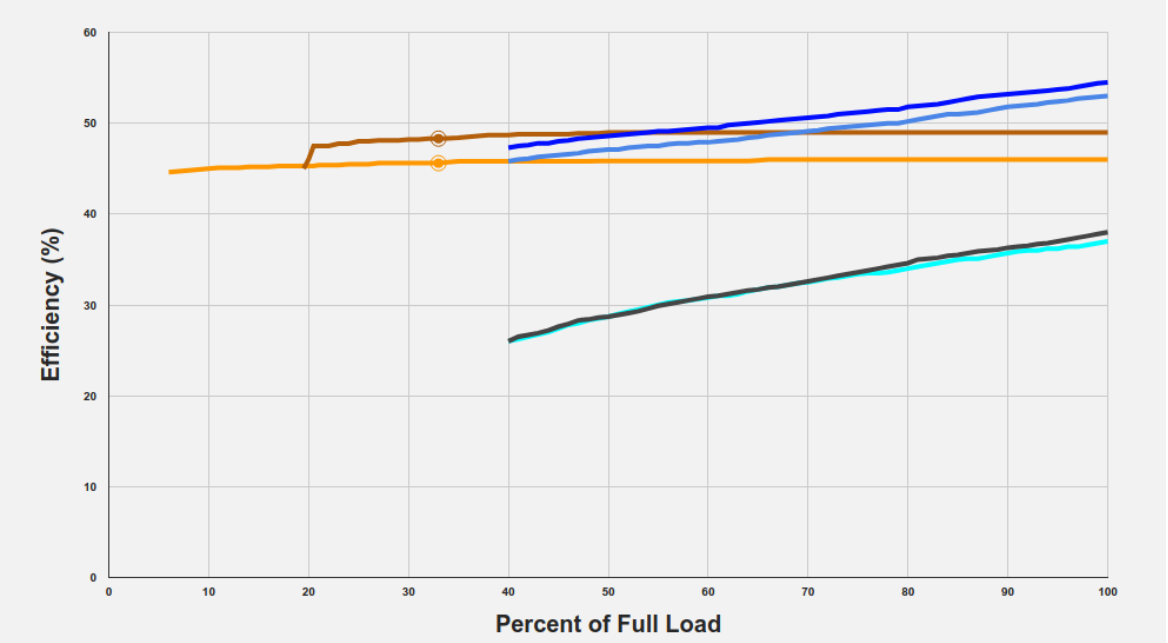

Figure 3.4: Examples of six different power plant part-load efficiency curves are presented from [60]. Different lines in the graph represented different gas turbines: Wärtsilä Simple Cycle, 25 C (orange), Wärtsilä FlexiCycle, 25 C (brown), Siemens SGT6-500F Simple cycle, 25 C(electric), GE 7FA,05 Simple cycle, 25 C (grey), Siemens SGT6-500F Combined (light blue), GE 7FA,05 Combined cycle, 25 C (blue). We can see that single cycle gas turbines are less efficient across all part-load levels. As an example, GE 7FA,05 Simple cycle, 25 C (grey) has efficiency of around 26 % at 40 % load level ($W = 0.4MEL$) and 38 % efficiency at full power $W = MEL$.

In order to approximate the part-load efficiency curves of dissimilar power plants, we use a power function as specified in (3.1).

$$\varepsilon(W) = \begin{cases} \varrho(W)^{\gamma} * \varepsilon_{max} & \text{for } \varrho(W) \geq \varrho_{min} \\ \varepsilon_{min} & \text{for } \varrho < \varrho_{min} \end{cases} \tag{3.1}$$

where $\varepsilon(W)$ is the efficiency of the power plant given the current power output W. Here we define $\varrho(W) = \frac{W}{W_{max}}$ as the percentage power output relative to full load, $\varepsilon_{max} = \frac{W_{max}}{Q_{max}}$ is the maximum power plant efficiency, W_{max} is the maximum power output, Q_{max} is the rate of fuel consumption at full load and γ is the power function parameter to account for the slope at which the power plant efficiency curve approaches maximum efficiency. We assume the lowest efficiency achievable in the power plant is ε_{min} when ϱ approaches ϱ_{min}, where $\varrho_{min} = SEL$ and is the stable exporting limit (this can be seen as discontinuities in the part-load efficiency curves in figure 3.4). We assume that the efficiency of the power plant is constant ε_{min} when the part-load level of the power plant is less than ϱ_{min}. The minimum output as discussed in the literature is around 30-50 % for CCGT power plants and 20-50 % for OCGT power plants [61].

3.3 Costs of Power Plant Operation

We specify several costs that would impact the operation of the power plant; these are fixed costs, fuel costs, and synchronisation costs. A further explanation of these costs is as follows.

Fixed Costs - costs that are not dependent on the current level of power production W of the power plant. We assume these costs are charged to the power plant during the power production as well as a start-up (the time it takes for the power plant to synchronise power production to the grid) and shut-down (time it takes for the power plant to stop producing power) periods. These would include labour, operation and maintenance, as well as regulatory costs such as the cost of emissions such as NOx and SO_2 [55]. In this thesis, we do not explicitly separate fixed costs into individual components but rather consider them as a single lumped cost for the power plant operator that is inferred from the real-world operational data of these power plants as discussed in Section 3.7. Power plant operators are not charged the fixed cost when the power plant is offline.

Synchronisation Costs - costs incurred as the power plant is being synchronised to the grid. Power plant synchronisation is a highly energy-intensive process [58]. We assume that the longer the power plant has been offline, the longer it will take for it to synchronise to the grid. Synchronisation costs are further discussed in Section 3.4.

Fuel Costs - costs attributed to the fuel consumed by the power plant (e.g. cost of coal or gas). These are charged depending on the fuel consumption of the power plant as £/MWh of fuel consumed. Fuel cost calculation is further discussed in Section 3.7.2.

3.4 Power Plant Operation Optimization

The objective of the power plant operator is to maximise its profit over the time horizon of operation given a set of prices of electricity, and a set of costs that we outline in this chapter. We are going to assume that the generator operator can control the rate of fuel input Q MW into the generator and also make decisions on whether to change the operating state of the generator.

The fuel input will be modelled as a continuous variable that, together with the operating state, can determine the power output of the plant. This requires us to be able to translate the rate of fuel used to power produced and vice-versa.

Formally, we can derive one-to-one functions of power to output and power to input using the efficiency of the generator as defined in (3.1), but special care must be taken when below ϱ_{min}. Let F be the function that converts fuel input to power output, then we have

$$W = F(Q) = \begin{cases} \left(\frac{Q}{Q_{max}}\right)^{\frac{1}{1-\gamma}} W_{max} & \text{for } Q > Q_{min} \\ Q\varepsilon_{min} & \text{otherwise} \end{cases}, \tag{3.2}$$

where Q_{min} is the fuel rate when power plant power production approaches ϱ_{min}. The inverse of this function can be used to derive the fuel input as follows

$$Q = F^{-1}(W) = \begin{cases} Q_{max} \left[\varrho(W)\right]^{1-\gamma} & \text{for } \varrho(W) > \varrho_{min} \\ \frac{W}{\varepsilon_{min}} & \text{otherwise} \end{cases}. \tag{3.3}$$

Now consider $Q(t)$ MW as the rate of fuel input at time t, which is a dynamic variable that can be controlled in our power plant operation model. This is our state variable which through the function F keeps track of the current power output rate from the power plant. However, this is not enough to completely track the current state of the power plant; we must further introduce a discrete variable $U \in \mathcal{U}$, which defines the current operating state of the power plant at time t. According to the combination of the fuel input level into the power plant Q, and its current state U, we can define the set of allowable control decisions that are available to the operator at that instant in time.

Let us first list these different states along with a short explanation. These are as follows:

- $U = 0$, or "Off" state, i.e. the power plant is offline. In this region, we expect the power plant not to consume any fuel at all and

$$Q = 0.$$

- $U = 1$, or "Synchronisation" state, the power plant is synchronising to the grid. The time it takes will depend on the length of time since the unit last delivered power to the grid. During synchronisation, the fuel supplied to the power plant is above null and below ι. ι represents the fuel level at which the power plant would be synchronised to the grid. This means that fuel input levels are

$$0 < Q < \iota.$$

- $U = 2$, or "Warm-up" state, the power plant starts producing power (i.e. exits the synchronisation level into production region) and moves towards the SEL. During the warm-up state, the fuel supplied to the power plant is above ι,

and below the fuel consumed at SEL power output $W = SEL$ represented by $F^{-1}(SEL)$, so we have

$$\iota \leq Q < F^{-1}(SEL).$$

- $U = 3$, or "Normal operation" state, the power plant operates above the stable export limit and can choose to either increase or decrease the production of power. During normal operation, the fuel supplied to the power plant is above $F^{-1}(SEL)$ and below fuel consumed at MEL power output $W = MEL$ represented by $F^{-1}(MEL)$. This gives

$$F^{-1}(SEL) \leq Q < F^{-1}(MEL).$$

- $U = 4$, or "Cool down" state, the power plant has been committed to de-synchronise and moves below the SEL production level. During the cool down the fuel supplied to the power plant is above ι and SEL power production

$$\iota \leq Q < F^{-1}(SEL)$$

- $U = 5$, or "De-synchronisation" state, the power plant is not producing any power. During the de-synchronisation state, the power plant needs to reduce the fuel input into the power plant to ν before it can choose to switch to the synchronisation state or the power plant operator can decide to switch the power plant off completely. The quantity ν represents the fuel input at which the power plant has been in the de-synchronisation state for a period of half the Minimum Zero Time (MZT). This is to make sure that if the power plant has stopped producing power $Q < \iota$, it stays in this region for a period of MZT minutes. As the speed of synchronisation and de-synchronisation are the same, we can restrict the power plant operator to stay in the de-synchronisation state for at least half of the time as we know that if the power plant decided to enter the synchronisation state, it would then take half of the MZT time again to start

producing power. This will ensure that the total time not producing power has been MZT. During de-synchronization fuel input levels in this state are:

$$0 < Q \leq \iota.$$

During the synchronisation and de-synchronisation stages, the power plant should not be producing any power, i.e. $W = 0$ but it is still consuming fuel, and we would like to maintain having a one-to-one function $W = F(Q)$ and $Q = F^{-1}(W)$. For this purpose in our models, the value of ι is chosen to be very small. This is to ensure that the power output of the power plant during the synchronisation and de-synchronisation stages is negligible. An example could be setting $\iota = 0.0001$ MW, minimum efficiency of the power plant of 20% $\varepsilon_{min} = 0.2$. This would lead to rate of power production of the power plant

$$W = F(Q = \iota) = \varepsilon^{min}\iota = 0.2 \times 0.0001 = 0.00002 \quad MW.$$

The minimum efficiency value in our example has been arbitrarily chosen by considering the real world part-load efficiency curves of the power plants, where the efficiency data is not provided for lower loads than 30-40%, and at 30-40% load the efficiency of the power plant was 0.2. This power plant efficiency does not include the costs and fuel consumption during start-up as these costs are accounted for by the start-up costs variable.

Now assume that our generator is modelled by a continuous time switching hybrid problem, which may be described by the following dynamics:

$$\begin{aligned} \frac{dQ}{dt} &= f(Q, U, c) \\ U(t^+) &= \eta(Q(t), U(t), c) \end{aligned} \tag{3.4}$$

where $Q(t) \in \mathbb{R}$, $U \in \mathcal{U} = \{0, 1, 2, 3, 4, 5\}$, and $c \in \mathbb{R}$ is the control variable. Here, the effective control $f : \mathbb{R}^{\not\vDash} \times \mathcal{U} \to \mathbb{R}$ that is enacted will depend heavily on the operating

state of the power plant U as described previously. The discrete dynamics of U are described by the function $\eta : \mathbb{R}^2 \times \mathcal{U} \to \mathcal{U}$.

An overview of how the power plant can move between these states according to the current value of Q, and the current state of the power plant U, is shown in figure 3.4. An arrow from the top of one box pointing to another indicates that the power plant will be able to transition to that state once Q reaches its upper limit, whilst an arrow from the bottom of a box indicates that the power plant will be able to transition to that state once Q reaches its lower limit. An arrow from the side indicates there may be flexibility over when the transition may take place. Boundaries for the power output, fuel output and control variables available in all states are also presented.

Now, consider that we are currently in an operating state, say $U = 2$ (warm-up), we have limited decisions that can be made. From this state, we are compelled to increase fuel input (with the maximum fuel input possible $c = c_{max}$), where c_{max} is the maximum increase in the fuel input that corresponds to the appropriate ramp rate. Once we reach $Q = F^{-1}(SEL)$ we must enter normal operation state with $c \geq 0$ and therefore we switch to state $U = 3$. Once in normal operation we can choose control anywhere between the maximum decrease in fuel input (c_{min}) and the maximum increase in fuel input (c_{max}), $c_{min} \leq c \leq c_{max}$ without changing the state $U = 3$. The power plant operator can also choose to enter the de-synchronisation state with $c < 0$ as the fuel input of the power plant approaches $Q = SEL$, which would cause a state switch to $U = 4$.

Conversely, c_{min} refers to the maximum decrease in the fuel input over the time step that meets the ramp down conditions. Ramp rate limits and load levels at which these changes are imposed by the technical structure of the power plant, we use rates and

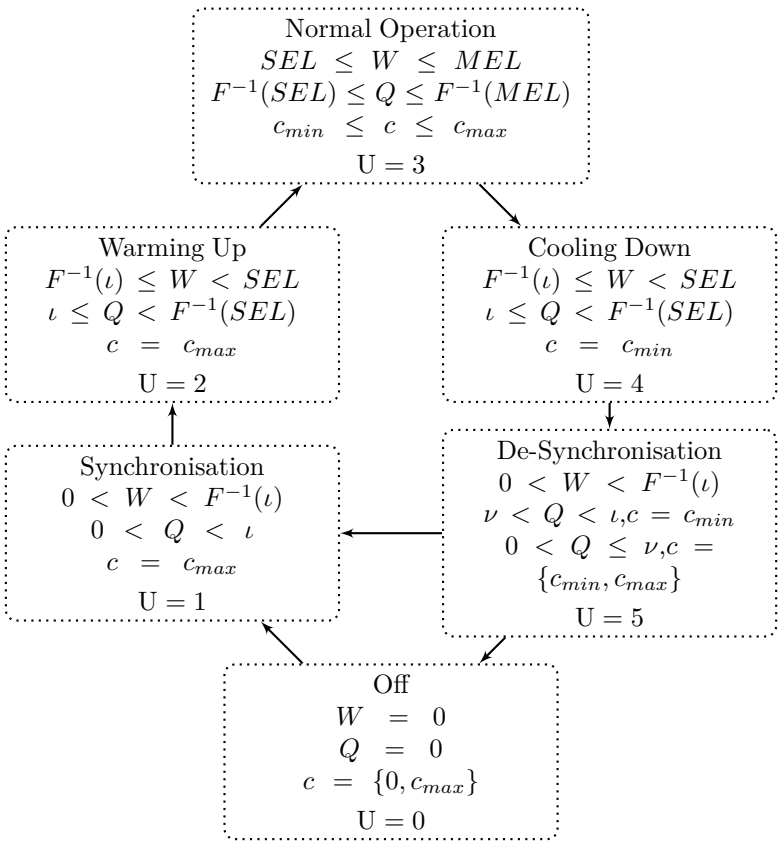

Figure 3.5: A diagram of the power plant transition between different states of operation.

levels as provided by NG and discussed in section 3.2. A more detailed description of the options available to the operator follows in the next section after we have introduced our objective function.

3.4.1 General model of the power plant optimisation

Let us define the objective of our problem, which is to maximize the profits from operating the power plant. We calculate the rate of profit Γ £/h realised at each

instant in time, by taking the power output of the generator W MW multiplied by the current market price of electricity $\pi^{wholesale}(t)$ £/MWh, minus fuel costs λ £/MWh per unit of fuel, minus the running costs per unit time given the current fuel input and state of the generator $AC(U)$ £/h,

$$\Gamma(Q, U, t) = \pi^{wholesale}(t)W(Q) - \lambda Q - AC(U). \tag{3.5}$$

Here AC is defined as

$$AC(U) = \begin{cases} \varsigma(\psi^{fcOM} + \psi^{fc}) + l & \text{if } U = 1, 5 \\ l & \text{if } U = 0 \\ \varsigma\psi^{fcOM} + l & \text{otherwise} \end{cases} \tag{3.6}$$

where $\varsigma = \lambda Q_{max}$ £/h is the rate of fuel cost at maximum power generating capacity ($W = MEL$). During the synchronisation phase, power plants consume significant amounts of energy in addition to other costs attributed to the synchronisation of the power plant. In our model, we set up the ψ^{fc} % to represent the ratio of fixed costs of synchronising the power plant, and the fuel cost at maximum power output. In this formulation, synchronisation costs become proportional to the size of the power plant. Similarly, we define ψ^{fcOM} % to represent the ratio between fixed costs for operation and maintenance and the fuel cost at maximum power output. Fixed costs of operation and maintenance should include all other costs, apart from fuel costs, that are incurred by the power plant when it is synchronised to the grid and is producing power ($W > F^{-1}(\iota)$). We assume labour costs $l = 0$, as we assume the labour costs do not differ between different states; the cost chosen should not significantly affect the optimal operation of the power plant.

Then we define J as the discounted integral of the profits over the time horizon from t to T, where T is the terminal time of the optimization, given that the current fuel

input is $Q(t)$, the current operating state is $U(t)$, and the current time is t

$$J(t) = \int_t^T e^{-\rho(s-t)} \left\{ \pi^{wholesale}(s) W(Q(s)) - \lambda Q(s) - AC(Q(s), U(s)) \right\} ds. \qquad (3.7)$$

assuming that we have determined a particular control to apply at each instant in time

$$c \in \mathbb{C}_t = \left\{ \; c = \{c(s)\}_{t \le s \le T} : \forall_{t \le s \le T} \quad c \in \mathbb{R} \; \right\}.$$

We use ρ as the discount factor to adjust the cash flows for time value of money. Time value of money can be regarded as percentage interest that could be earned by putting the money in a different, similar risk investment, rather than using it to buy fuel to produce power. This allows us to discount the value of the power plant to the net present value (NPV). In our simulations, we only consider short periods of time (a month), where the value of ρ is not of particular concern as the discounting is for a short period. For this purpose we set $\rho = 0$. For long term power plant valuation and longer period power plant operation, ρ is of critical importance and care should be taken to use an appropriate value therefore the models below are provided with the ρ values stated. The value of ρ will depend on the current economic climate and the riskiness of the investment.

To derive the Hamilton-Jacobi-Bellman (HJB) [62] equation for the optimal solution of this problem we use the value function

$$V(Q(t), U(t), t) = \max_{c \in \mathbb{C}_t} J(t) \qquad (3.8)$$

to represent the optimal value. Then assuming that $\eta(Q, U, c) = U$, we can re-write the value function as follows,

$$V(Q, U, t) = \max_{c \in \mathbb{C}_t} \left[\int_t^{t+dt} e^{-\rho(s-t)} \Gamma(Q(s), U(s), s) ds \right. \\ \left. + e^{-\rho dt} \int_{t+dt}^{T} e^{-\rho(s-(t+dt))} \Gamma(Q(s), U(s), s) ds \right].$$

Using (3.7) we can write

$$V(Q,U,t) = \max_{c} \left[\int_{t}^{t+dt} e^{-\rho(s-t)} \left\{ \Gamma(Q(s),U(s),s) \right\} ds + e^{-\rho dt} V(Q+dQ, U(t^{+}), t+dt) \right],$$

where we hold the state U constant.

Then applying a Taylor expansion around Q and t and holding the state U constant we obtain

$$V = \max_{c \in \mathbb{C}_t} \left[\Gamma(Q(t),U(t),t)dt + (1-\rho dt)V + (1-\rho dt)\left(\frac{\partial V}{\partial t} + f(Q,U,c)\frac{\partial V}{\partial Q} \right) dt \right] + o(dt).$$

Rearranging the above and eliminating values going to zero faster than dt and dividing by dt leaves us with the following

$$0 = \max_{c \in \mathbb{C}_t} \left\{ \Gamma(Q,U,t) - \rho V + \frac{\partial V}{\partial t} + f(Q,U,c)\frac{\partial V}{\partial Q} \right\}, \tag{3.9}$$

where c defines the optimal control strategy. If we apply a control that enacts a switch in the current state, we will have

$$V(Q,\eta(Q,U,c),t^{+}) = V(Q,U,t).$$

Then according to standard theory [63] we can solve the equivalent set of quasi variational inequality problems, where V is a solution to PDE (3.9) along with the condition that

$$V(Q,U,t) \geq \max_{c} V(Q,\eta(Q,U,c),t^{+}).$$

In the following sections, we define the functions f (the control) and η (the state) for all different states of the problem in detail. The ability to model the power plant operation as a continuous variable allows us to account for intermediary costs and the dynamics of power plant operation whilst moving in-between states and during start-up. We agree with [57] that in a world where we have an increasing number of renewable power generation and the need to cycle power plants increases, the inclusion of power plant start-up costs will be required to determine optimal operation.

3.4.2 Off state of the power plant

We allow the power plant to be off-line, this means that the state is $U = 0$ and our dynamic functions are as follows

$$f(Q = 0, U = 0, c) = \begin{cases} 0 & \text{if } c \leq 0 \\ c_{max} = \frac{\iota}{NDZ} & \text{if } c > 0 \end{cases} \tag{3.10}$$

$$\eta(Q = 0, U = 0, c) = \begin{cases} 0 & \text{if } c \leq 0 \\ 1 & \text{if } c > 0 \end{cases}. \tag{3.11}$$

In the off state, the power plant operator does not incur any costs. The power plant operator will choose to stay in the off state if the value of the power plant operation in the synchronisation state $V(Q, U = 1, t)$ is less than the value of staying offline $V(Q, U = 0, t)$.

3.4.3 Synchronisation state of the power plant

The power plant operator can choose to enter the synchronisation state ($U = 1$) from the off-line state ($U = 0$) or de-synchronisation state ($U = 5$). When in the synchronisation state, the time it takes for the power plant to synchronise to the grid depends on the time the power plant has been off-line. The dynamics of the power plant are defined as follows

$$f(Q, U = 1, c) = c_{max} = \frac{\iota}{NDZ} \tag{3.12}$$

$$\eta(Q, U = 1, c) = \begin{cases} 1 & \text{if } 0 < Q < \iota \\ 2 & \text{if } Q = \iota \end{cases} . \tag{3.13}$$

We assume the cold start of the power plant is when it has been off-line for NDZ minutes. During the synchronisation phase the operator is charged the fixed costs ($\varsigma\psi^{fcOM}$) £/h of running the power plant and synchronisation costs ($\varsigma\psi^{fc}$) £/h .

The power plant in synchronisation will approach the warm-up stage at which point it will switch to the state $U = 2$.

3.4.4 Warming up state of the power plant

As the power plant enters the warm up phase we require the power plant to increase its output to the stable exporting limit, subject to constraints imposed by allowed ramp rates. Limits can be inferred from the ramp rates and elbows provided by the power plant as shown in figure 3.2. These rates are provided in terms of allowed delivery rates of power. We need to use (3.3) to convert to limits on fuel burn rate. During

the warm up state, power plant dynamics are governed by

$$f(Q, U = 2, c) = c_{\max}(Q, U) \tag{3.14}$$

$$\eta(Q, U = 2, c) = \begin{cases} 2 & \text{if } \iota < Q < F^{-1}(SEL) \\ 3 & \text{if } Q = F^{-1}(SEL) \end{cases} . \tag{3.15}$$

In the warm-up phase, the power plant produces power $W(Q)$ and receives revenue for the power produced $\pi^{wholesale}(s)W(Q)$. The costs charged during the warm-up phase include the costs of fuel consumed (λQ) and the fixed costs of power plant operation and maintenance ($\varsigma\psi^{fcOM}$).

The power plant operator will continue increasing the fuel input into the generator up until a stable exporting limit is reached at which the power plant will enter the normal operation region ($U = 3$).

3.4.5 Normal operation state of the power plant

Once in the normal operation state, the power plant operator can choose to increase or decrease the fuel input Q MW. The dynamics are governed as follows

$$f(Q, U = 3, c) = \begin{cases} c_{min} & \text{if } c < c_{min} \\ c & \text{if } c_{min} \leq c \leq c_{max} \\ c_{max} & \text{if } c > c_{max} \end{cases} \tag{3.16}$$

$$\eta(Q, U = 3, c) = \begin{cases} 3 & \text{if } F^{-1}(SEL) < Q \leq Q_{max} \\ 3 & \text{if } Q = F^{-1}(SEL) \text{ and } c \geq 0 \\ 4 & \text{if } Q = F^{-1}(SEL) \text{ and } c < 0 \end{cases} . \tag{3.17}$$

Costs charged to the power plant include the fuel cost (λQ) £/h that depends on the amount of fuel input Q MW and the cost of unit of fuel λ £/MWh as well as the fixed costs of power plant operation and maintenance $\varsigma\psi^{fcOM}$ £/h.

When a power plant operator reduces the power production to a stable exporting limit, it can decide to stop producing power, changing to state $U = 4$.

3.4.6 Cooling down state of the power plant

After the power plant operator has decided to stop producing power, the plant enters the cool-down phase of operation. During the cool-down phase, the plant is still producing power $W(Q)$ MW and will still receive revenue for the amount of power it produces which can be calculated as $\pi^{wholesale}(t)W(Q)$ £/h.

The speed at which the power plant operator can reduce the fuel input into the power plant depends on the current fuel input Q MW and is set by the operation limits of the plant. The dynamics are provided by

$$f(Q, U = 4, c) = c_{\min}(Q, U) \tag{3.18}$$

$$\eta(Q, U = 4, c) = \begin{cases} 4 & \text{if } \iota < Q < F^{-1}(SEL) \\ 5 & \text{if } Q = \iota \end{cases} . \tag{3.19}$$

The power plant will incur the fuel costs (λQ) £/h for the fuel consumed and the fixed costs of power plant operation and maintenance ($\varsigma\psi^{fcOM}$) £/h.

If power plant operator moves the power plant to the cooling down phase, it will have to reduce its fuel input to ($Q = \iota$) at which point it will automatically enter the de-synchronisation state ($U = 5$)

3.4.7 De-synchronisation state of the power plant

When a power plant enters the de-synchronisation state, it must remain in this state for a period of at least $\frac{MZT}{2}$, before the plant can start a new warm-up cycle. During the de-synchronisation phase, the power plant will incur the fixed costs of power plant operation ($\varsigma\psi^{fcOM}$) £/h and synchronisation costs ($\varsigma\psi^{fc}$) £/h attributed to the costs during de-synchronisation.During the de-synchronisation stage, the plant has several options available to it. It can either be run down the de-synchronisation stage until the power plant is fully off, or it can restart the synchronisation. The power plant dynamics are provided as

$$f(Q, U = 5, c) = \begin{cases} -\dfrac{\iota}{NDZ} & \text{if } c \leq 0 \\ \\ \dfrac{\iota}{NDZ} & \text{if } Q \leq \nu \text{ and } c > 0 \end{cases} \tag{3.20}$$

$$\eta(Q, U = 5, c) = \begin{cases} 5 & \text{if } \nu < Q < \iota \\ 5 & \text{if } Q < \nu \text{ and } c \leq 0 \\ 2 & \text{if } Q < \nu \text{ and } c > 0 \\ 0 & \text{if } Q = 0 \end{cases}. \tag{3.21}$$

where $\nu = \frac{mzt}{2}\frac{\iota}{NDZ}$.

3.5 Numerical Method

In this section, we describe a numerical solution for our optimisation problem. Our numerical solution method is inspired by Semi-Lagrangian techniques introduced by [64]. In our optimisation, we model the power plant output rate as a function of the fuel input rate. We use multiple operational states for the power plant that influence the controls available to the plant operator and the costs incurred, as previously discussed in this chapter.

3.5.1 Semi-Lagrangian Discretization

We first introduce the notation used in this section. We have chosen to use a non-equally spaced grid for fuel input Q for the PDE discretization (discussed below), so assume that we have a set of $m+1$ unequally spaced points such as $\{Q_0, Q_1, Q_2, \ldots, Q_j \ldots, Q_m\}$. We use N equally spaced steps in time, using the variable $\tau = T - t$ so that

$$\tau_n = \frac{n}{N} T$$

We let $V^u_{j,n} = V(Q_j, U = u, \tau_n)$ be the approximation of the solution of the power plant at time τ_n, fuel input Q_j and state $U = u$.

$$0 = \min_{c \in \mathbb{C}_t} \left\{ -\Gamma(Q, U, \tau) + \rho V + \frac{\partial V}{\partial \tau} - f(Q, U, c) \frac{\partial V}{\partial Q} \right\}, \tag{3.22}$$

where Γ is the instantaneous rate of profit.

Now let us define the total derivative $\frac{DV}{D\tau}$ as

$$\frac{DV}{D\tau} = \frac{\partial V}{\partial \tau} + \frac{dQ}{d\tau}\frac{\partial V}{\partial Q} \tag{3.23}$$

where $\frac{dQ}{d\tau}$ is

$$\frac{dQ}{d\tau} = -f(Q, U, c) \tag{3.24}$$

and

$$U(\tau^+) = \eta^{-1}(Q(\tau), U(\tau), c). \tag{3.25}$$

Using equation (3.23) allows us to re-write our optimization problem (3.22) as

$$0 = \min_{c \in \mathbb{C}_t} \left\{ -\Gamma(Q, U, \tau) + \rho V + \frac{DV}{D\tau} \right\}, \tag{3.26}$$

which means that the control c, the change in the rate of fuel input, no longer appears in front of a derivative term, greatly simplifying the model.

Now we denote by $\{\mathcal{Q}(\tau, c), \mathcal{U}(\tau, c), \tau\}$ a path satisfying both $\frac{dQ}{d\tau}$, as defined in equation 3.24 and the discrete dynamics of U which arrives at the discrete point $\{Q_j, U\}$ at time $\tau = \tau_{n+1}$, assuming that the control c is held constant over the time interval τ_{n+1} - τ_n.

Let

$$\{\mathcal{Q}(\tau_n, c; Q_j, \tau_{n+1}), \mathcal{U}(\tau_n, c; U(\tau_{n+1}))\}$$

be the departure point, as defined in [7] at τ_n. For a given value of c, this departure point can be found by solving the ODEs

$$\frac{d\mathcal{Q}}{d\tau} = -f(\mathcal{Q}, \mathcal{U}, c) \tag{3.27}$$

$$\mathcal{U}(\tau^+) = \eta^{-1}(\mathcal{Q}, \mathcal{U}, c) \tag{3.28}$$

subject to the terminal conditions

$$\mathcal{Q}(\tau_{n+1}; Q_j, \tau_{n+1}, c) = Q_j \tag{3.29}$$

$$\mathcal{U}(\tau_{n+1}) = U \tag{3.30}$$

Now we can integrate (3.26) over the time interval τ_n to τ_{n+1} to obtain

$$\int_{\tau_n}^{\tau_{n+1}} \min_{c \in \mathbb{C}_t} \left\{ -\Gamma(\mathcal{Q}, \mathcal{U}, \tau) + \rho V + \frac{DV}{D\tau} \right\} d\tau = 0, \tag{3.31}$$

where $\mathcal{Q}$ and $\mathcal{U}$ solve the ODEs in (3.27). Next, we can calculate the integral of $\frac{DV}{D\tau}$ as

$$\int_{\tau_n}^{\tau_{n+1}} \frac{DV}{D\tau} d\tau = V(Q_j, U, \tau_{n+1}) - V(\mathcal{Q}(\tau_n), \mathcal{U}(\tau_n), \tau_n). \tag{3.32}$$

Therefore by assuming that the integral and min operators are interchangeable, and by substituting (3.32) in to (3.31), we have

$$V(Q_j, U, \tau_{n+1})) = \max_{c \in \mathbb{C}_t} \left\{ V(\mathcal{Q}(\tau_n), \mathcal{U}(\tau_n), \tau_n) + \int_{\tau_n}^{\tau_{n+1}} (\Gamma(\mathcal{Q}, \mathcal{U}, \tau)) d\tau - \int_{\tau_n}^{\tau_{n+1}} \rho V d\tau \right\}. \tag{3.33}$$

3.5.2 Fully-implicit timestepping

Now assuming that the control c does not change during $\Delta\tau$, we split the time interval $\Delta\tau$ into K substeps so that the discretised version uses the following time step

$$\Delta s = \frac{1}{K} \Delta\tau.$$

Using an Euler method we can solve the ODEs (3.27), and therefore we can approximate the path $\{\mathcal{Q}, \mathcal{U}\}$ by

$$Q_j^{i+1} = Q_j^i + f(Q_j^i, U^i, c)\Delta s, \tag{3.34}$$

$$U^{i+1} = \eta(Q_j^{i+1}, U^i, c). \tag{3.35}$$

As a result, we are able to derive the integral of the profit function according to

$$\int_{\tau_n}^{\tau_{n+1}} (\Gamma(\mathcal{Q}, \mathcal{U}, \tau)) d\tau \approx \sum_{i=0}^{K-1} \Gamma(Q_j^i, U^i, \tau_n + i\Delta s)\Delta s. \tag{3.36}$$

Substituting (3.36) into (3.33) we finally arrive at the following

$$V^u_{j,n+1} = \frac{1}{1+\Delta\tau\rho} \max_{c\in\mathbb{C}_t} \left\{ \sum_{i=0}^{K-1} \Gamma(Q^i_j, U^i, \tau_n + i\Delta s)\Delta s + V_n(Q^K_j, U^K) \right\}. \quad (3.37)$$

Here the value $V_n(Q^K_j, U^K)$ must be found via interpolation unless $\{Q^K_j, U^K\}$ is an existing grid point.

3.6 Numerical scheme with real-world parameters

In this section, we provide steps taken to adapt the fully implicit time stepping solution introduced in Section 3.5.1 to the discretised version of power plant operation using real-world parameters that we will be using to simulate GB wholesale market in Chapter 5. We start the section by going through the details of the discrete-time problem. We then follow on to introduce the non-evenly spaced grid steps used for the rate of fuel Q in the optimisations. Last, we introduce the power plant parameters available from the NG together with a discussion of ramp rates and an example power plant operation using an artificial set of parameters as outlined in table 3.6).

3.6.1 Electricity Prices

To demonstrate the behaviour of the optimised power plant in different scenarios, we insert a test series of wholesale electricity prices, as shown in figure 3.6. Prices

Parameter	Value	Units
MEL	90	MW
SEL	50	MW
NDZ	720	min
MZT	360	min
ι	0.0001	MWh
ν	$\frac{\iota}{NDZ}\frac{MZT}{2} = 0.000025$	min
γ	0.413185	
η_{max}	0.5	
η_{min}	0.2	
ψ^{fcOM}	0.2	
ψ^{fc}	0.2	
RURE1	1	MW/min
RURE2	0.1	MW/min
RURE3	2	MW/min
RUEE2	30	MW
RUEE3	60	MW
RDRE1	2	MW/min
RDRE1	0.1	MW/min
RDRE1	1	MW/min
RDEE2	60	MW
RDEE3	30	MW
$\Delta\tau$	$\frac{1}{60}$	*hours* equivalent to 1 minute
Δs	$\frac{1}{60}$	*hours* equivalent to 1 minute

Table 3.1: Arbitrarily chosen set of parameters for a power plant to qualitatively demonstrate the correct behaviour derived by power plant optimization models introduced in this thesis.

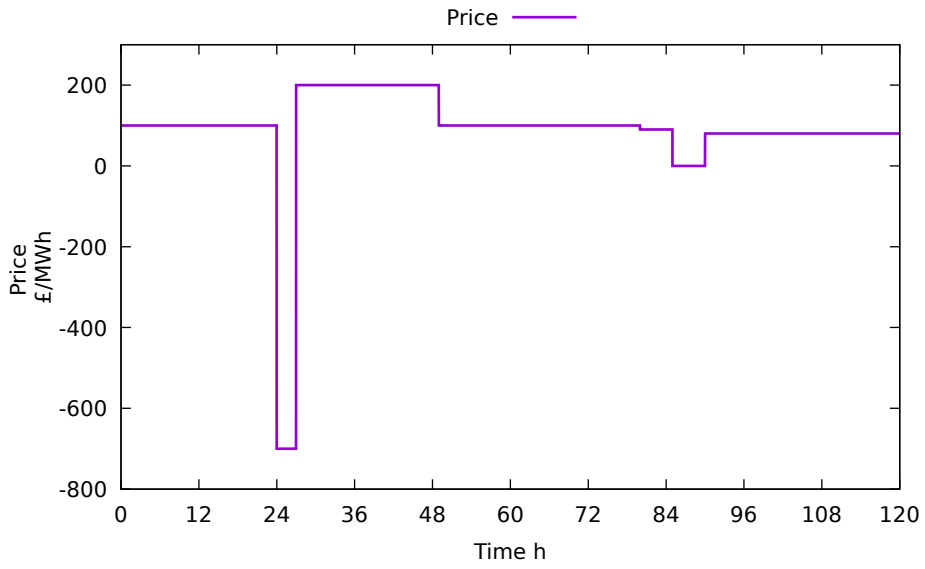

Figure 3.6: A set of arbitrary wholesale electricity prices used in the power plant operation simulation.

have been chosen arbitrarily to provide qualitative evidence to support our optimisation algorithm and to show that the optimal controls devised provide the expected outcomes. We reiterate that the optimisations discussed in this subsection assume that power plants react to forward agreed prices (power is sold in advance at given quantities and prices). Therefore no uncertainty or external forces are affecting these wholesale prices.

3.6.2 Discrete time control problem

In Section 3.5, we introduced a power plant optimisation as a continuous problem, where we assumed that controls are applied over an instantaneously small time frame. However, once we start to try and calibrate our model to the wholesale market, we see that the controls applied by a real power plant will need to align to the market

framework which imposes a fixed window over which power is bought and sold, currently half-hourly in GB ($\Delta\tau = \frac{1}{2}$). By using the control actions (only considering controls every half-hour), we are able to reduce the computational complexity of the power plant operation optimisation significantly, whilst achieving a reasonable level of accuracy.

Later in this section, to verify the integrity of our numerical scheme, we allow the time step $\Delta\tau$ to be gradually reduced and show that our solution converges. Generator operational constraints in GB are recorded at a one minutely resolution (MW/min) [32]. As a result, we choose the default sub-time-step Δs to be one minute unless the time step $\Delta\tau$ is smaller than one minute, i.e.

$$\Delta s = \begin{cases} \frac{1}{60} & \text{for } \Delta\tau \geq \frac{1}{60} \\ \Delta\tau & \text{for } \Delta\tau < \frac{1}{60} \end{cases} \tag{3.38}$$

From table 3.2, we can see that the power plant value as derived from the solution to the problem (3.37) converges to a true value of the power plant as $\Delta\tau \to 0$, confirming that the solution to (3.37) using parameters as outlined in table (3.6) is stable. In these calculations, only Δt has been varied, and grid points Q_j were kept constant across all values of Δt. The difference between the value of the power plant with $\Delta\tau = 0.5$ and $\Delta\tau = 0.00104$ is only £969 (0.26% difference) providing us with confidence that we can use $\Delta\tau = 0.5$ whilst simulating the behaviour of the power plants in GB wholesale market as if the power plant operation significantly differed between the $\Delta\tau$ the estimated value of the power plant would have also differed.

In figure 3.7 we also present a qualitative comparison of the output and controls of

Δ t	Value £
0.5	371920
0.033333333	372965
0.016666667	373072
0.011111111	372982
0.008333333	372947
0.005555556	372920
0.004166667	372909
0.002083333	372895
0.001041667	372889

Table 3.2: Convergence of the value of the generator when $\Delta\tau \to 0$.

the power plant between a case where $\Delta\tau = \frac{1}{60}$ (Case 1) and $\Delta\tau = \frac{1}{2}$ (Case 2) whilst operated under electricity prices as introduced previously. We can observe that the power plant is qualitatively similarly operated under both scenarios. It goes offline during the significant price decrease period, and power is only reduced to the stable exporting limit during the smaller price decrease period. We note that there is a slight misalignment of the turn off times between the two scenarios in figure 3.7 where the power plant in the case of $\Delta\tau = \frac{1}{60}$ turns off earlier than the same power plant when $\Delta\tau = \frac{1}{2}$ is used.

3.6.3 Variable grid

We observed that the rates at which the power plant can ramp power production differ significantly across the operating ranges of the power plant. We also know that interpolation can be both an expensive and sometimes inaccurate process so we would like to minimise this as much as possible. To reduce the amount of interpolation required in our scheme, we split the Q space into intervals according to the different ramp rates and behaviour of the available controls in different states. Within each

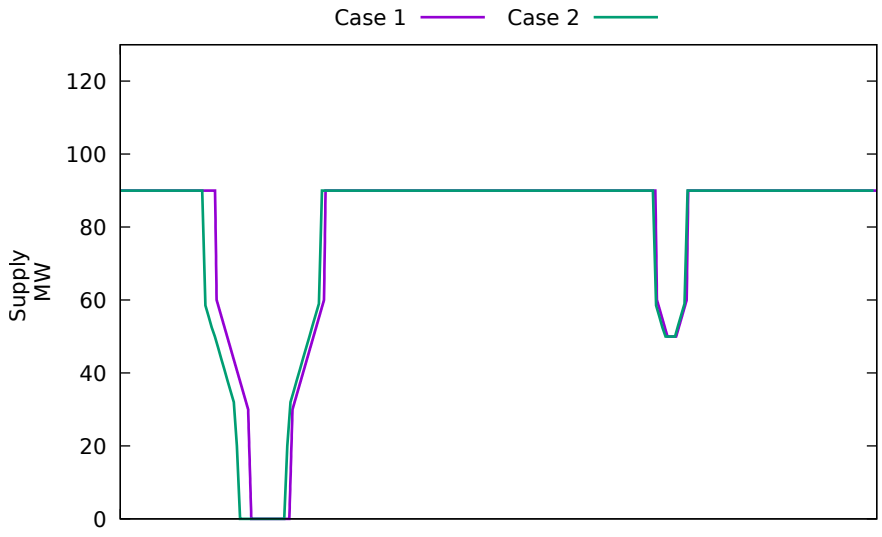

Figure 3.7: Power plant operation with different time stepping. Operation is very similar in both scenarios $\Delta\tau = \frac{1}{60}$ (Case 1) and $\Delta\tau = \frac{1}{2}$ (Case 2).

interval, we apply a fixed spaced grid, usually aligning the grid spacing so that

$$\Delta Q \approx f(Q, U, c)\Delta s,$$

where c is the typical control applied in that region.

Typical number of steps (rounded up)	Region	State
NDZ	$0 \leq Q \leq \iota$	$U = 1, 5$
$\frac{MEL-RDEE2}{RDRE1}$	MEL$\leq Q \leq$ RDEE2	$U = 2, 3$
$\frac{RDEE2-RDEE3}{RDRE2}$	RDEE2 $\leq Q \leq$RDEE3	$U = 2, 3$
$\frac{RDEE3-\iota}{RDRE3}$	$\iota \leq Q \leq$ RDEE3	$U = 2, 3$
$\frac{MEL-RUEE2}{RURE3}$	MEL$\leq Q \leq$RUEE2	$U = 3, 4$
$\frac{RUEE3-RUEE2}{RURE2}$	RUEE2$\leq Q \leq$RUEE3	$U = 3, 4$
$\frac{RUEE3-\iota}{RURE1}$	$\iota \leq Q \leq$RUEE3	$U = 3, 4$

Table 3.3: A table outlining a typical grid scheme.

From table 3.3, we can observe that between the fuel input ι and 0 we create NDZ numbers of points. This is to accurately account for the time spent in the synchronisation and de-synchronisation states. Within the elbows of the power plant operation, we create the number of steps required to transit the elbow. We have also added a grid point at $Q = F^{-1}(SEL)$ as this is a particularly important point in the solution, where the power plant operator needs to decide whether to commit the power plant to go offline for at least MZT or stay operating.

3.6.4 Ramp rates

A graphical depiction of operational limits is presented in figures 3.8 and 3.9. We can see in both figures that ramp rates change at ramp rate elbows as specified in Section 3.2. During each ramp elbow, we can see that the ramp rate in terms of power is constant, but due to the increasing efficiency of the power plant, the ramp rate in terms of fuel input is decreasing with load level.

3.6.5 An Example to Illustrate the Effect of Electricity Prices on the Power Plant

In figure 3.10, we show that a drop in the price of electricity to -700 £/MWh causes the power plant to turn off. To do so, the operator needs to ramp down as provided by the operation characteristics (ramp-down rates). We can see how these ramp rates change at different output levels (ramp down elbows).

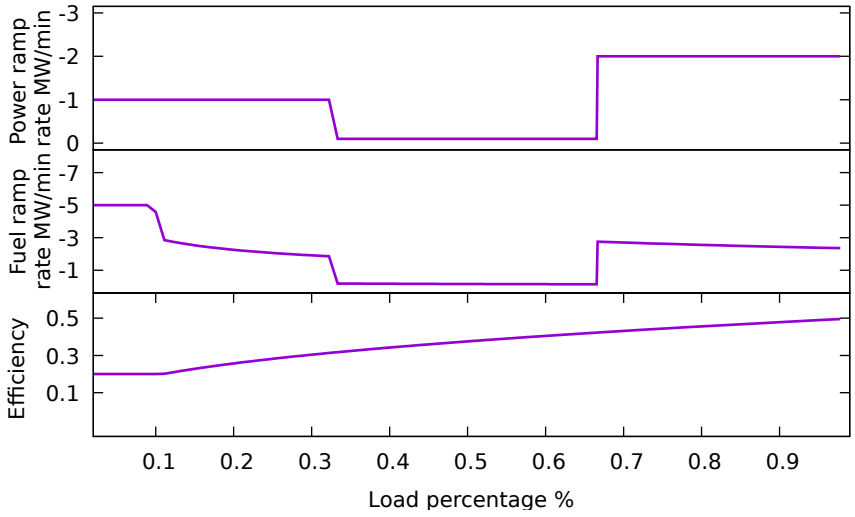

Figure 3.8: Plot of ramp-down rates at different load levels as provided by NG in their BM data [32]. The top graph represents ramp rates in MW/min power output for an artificial power plant as described in (3.1). The middle graph represents ramp rates in terms of fuel input MW/min; this is taking into account the power ramp rates and adjusts these for the efficiency level at the specific part load level. The bottom graph shows the part-load efficiency of the power plant at different load levels.

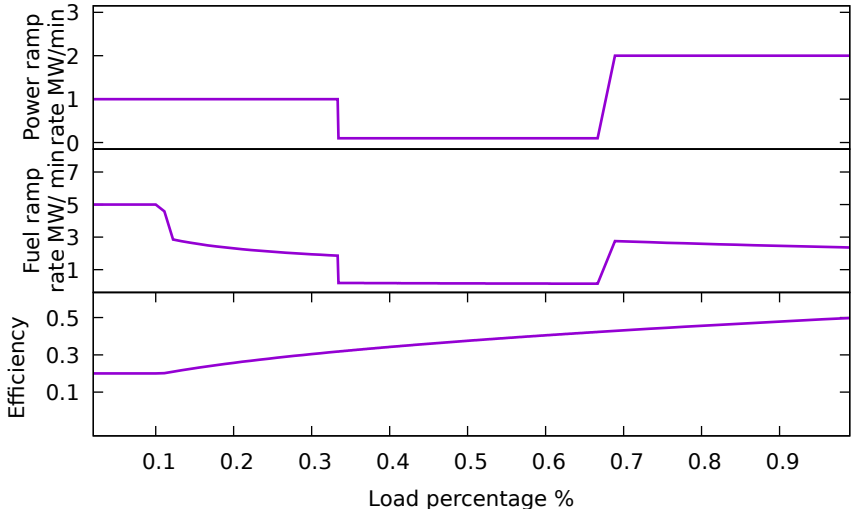

Figure 3.9: Power plant ramp down rates at different load levels. Top graph represents ramp rates in MW/min power output. Middle graph represents ramp rates in terms of fuel MW/min. Bottom graph shows efficiency of the power plant at different load levels.

As the power plant goes offline we can observe that it needs to stay offline for a MZT. The wholesale electricity price is lower 100 £/MWh before the negative price period compared to 200 £/MWh after. The power plant operator chooses to turn off the power plant before the first price decrease and stays offline for the MZT. The power plant then turns back online as soon as the price goes positive, as the electricity price is higher than before the price drop. As the power plant goes online, we can observe that it does so while respecting the operation characteristics of the power plant (ramp-up rates).

In figure 3.11, we show that if there is a short, low magnitude decrease in the wholesale electricity price, our power plant chooses to reduce its power production but only to the SEL. This is to avoid going offline and staying offline for the MZT.

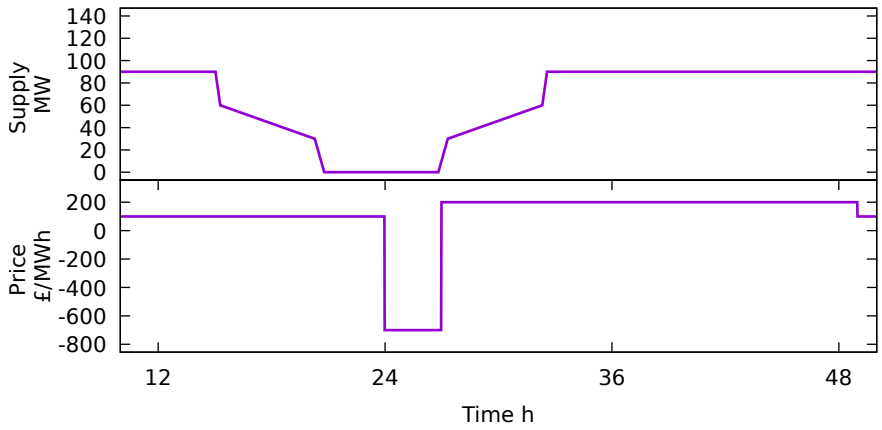

Figure 3.10: Power plant operation simulation during an artificial scenario where the price drops significantly. The power plant turns off to avoid the cost of operating during the negative price period. While turning off and turning back on, it needs to respect the operational restrictions of the plant (ramp rates). The stepped power supply function represents this before and after the negative price. The power plant needs to stay offline for a minimum of MZT minutes. This is represented by 0 supply of the power plant before the price decrease.

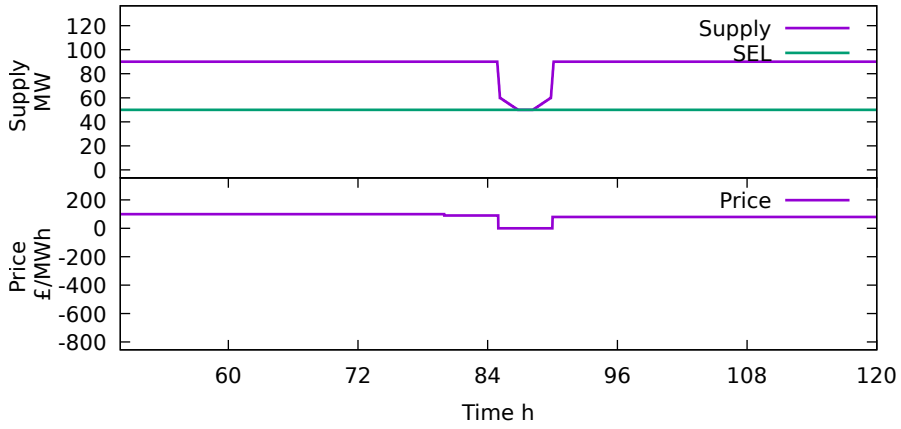

Figure 3.11: Power plant operation during a small price decrease. Low magnitude price decrease does not warrant the power plant to be turned-off completely. Power supply is reduced to SEL (green line)

The algorithm evaluates the cost incurred whilst producing power at a loss during the price decrease period. This cost is then evaluated against the revenues lost by producing during the positive price period. In this scenario, the loss made during the price-decrease period is lower than the revenue that would be lost if the power plant had to turn off.

3.7 Power plant operational data fitting

For meaningful results in our market simulations in Chapter 5, we need an accurate representation of the operation of power plants for a given schedule of prices of wholesale electricity, i.e. accurate characteristics of these power plants. Some of the operational information is already readily available from the BM as previously discussed. Other

information is proprietary and is not publicly available, such as:

- Maximum Efficiency - η_{max}.
- Minimum Efficiency - η_{min}.
- Fixed Cost - ψ^{fcOM}.
- Fixed Cost Operation and Maintenance - ψ^{fc}.
- Part-load efficiencies - in our model approximated by a power function x^{γ}.

In our model of the power plant operation, this is necessary information, and we need reasonable estimates of these. We were aware that there is a possibility that NG might hold some of this information, such as the input of gas to the power plants. However, after speaking to some NG representatives, it seems as though the information is commercially sensitive; therefore, we were not able to obtain it.

In our model, we used the Balancing Mechanism Reporting Service (BMRS) operational data where possible and estimated the unknown parameters of the power plants by using the historical operational data of the power plants to estimate the unknown parameters that best match the observed power plant behaviour. Further details of how these quantities are inferred are presented in this section.

BMRS data was used for power plants that were operating between October and December 2018 inclusive. At the same time, we were able to collect wind speed forecast data. Although the wind speed forecast data is not used in the current model, it can provide useful insights into the way wind speed affects wind power production and will allow us to analyse wind curtailment (power generated by wind restricted to

below the actual capacity available) in our future work. The time period selected also corresponds to a period of high demand for heating in GB, so we would expect HPs to be operating. As we are trying to evaluate the impact of increased HP uptake, capturing the heating season is of critical importance.

To retrieve data from the BMRS we followed the documentation in [65], noting that the data can also be explored using a graphical interface on [32]. We were primarily interested in the four data sources outlined below. We provide the list of specific information that has been used from these reports. Definitions of particular parameters are provided in the power plant characteristics section 3.2.

- Physical Data (identifier: PHYBMDATA) - MEL.
- Dynamic Data (identifier: DYNBMDATA) - NDZ, SEL, up to three run-up and run-down rate(s) in MW/minute with respective elbow(s) expressed in MW.
- National Output Usable by Fuel Type and BM Unit (2-52 Weeks Ahead) (identifier: UOU2T52W) - Fuel Type for specific BM Units. In addition we also used [66] and [67] for the fuel type of the generators.
- Half Hourly Out turn Generation by Fuel Type (identifier:FUELHH) - historical power generation per specific fuel type.

3.7.1 Part-load efficiency

Part-load efficiencies are not publicly available for the power plants operating in GB. Figure 3.12 presented in [68] was used for estimating part-load efficiencies. This relative efficiency curve is for a 60 MW gas turbine.

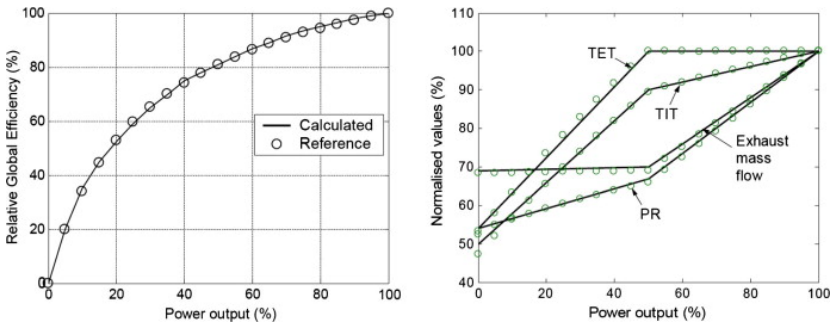

Figure 3.12: Relative global efficiency curve for a medium size 60 MW gas turbine. [68].

Using $\varrho(W)^{\gamma}$ as the relative power plant efficiency as introduced in Section 3.2, we estimate that $\gamma = 0.413$ is the value that best fits the data points in figure 3.12, and the fitted function is shown in figure 3.13.

We used the same γ for all power plants considered. With better information, these could be adjusted for different power plant types. As previously discussed, we assume the lower limit of power plant efficiency is 20% to prevent our efficiency curve going to zero.

An alternative to finding efficiency curves is to use commercial software Epsilon Professional as discussed by [57]. In their paper, examples of part-load efficiency curves are derived from the design features of the power plants.

3.7.2 Fuel Costs and Emission Charges

Fuel cost is the most critical determinant of operation a fossil fuel power plant. In our simulations we use average prices £/MWh of the fuel purchased by the power producers in Q4 2018 [69] in GB, this report is the best source of fuel costs paid by

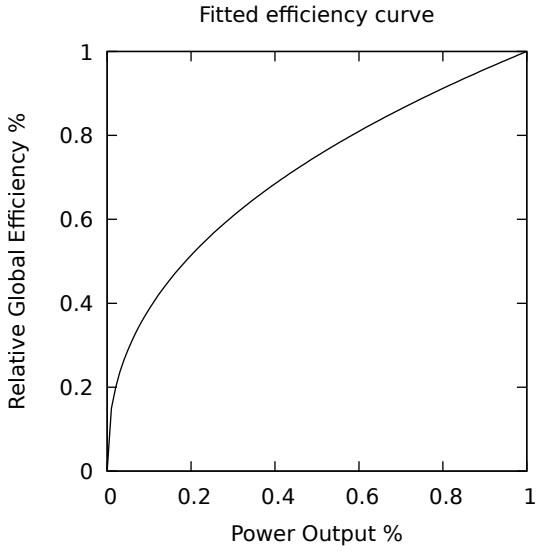

Figure 3.13: Fitted relative global efficiency curve, $f(x) = x^{0.413185}$.

the power plants that we could access.

GB power plants are also charged a carbon price, which comprises the EU traded cost of carbon and carbon price support. As of 2013 the carbon price support is set at 18.08 £/ ton CO_2 [70]. During the 4th quarter of 2018, the carbon price average on the EU exchange was 20.67 €/ ton CO2, which was recorded by [71]. The EUR/GBP interbank exchange rate average during Q4 of 2018 was 0.8908 using information from the currency exchange [72]. As we are trying to find out the carbon emissions for particular fuels, we use conversion factors from [73]. Natural gas has 0.18396 kg CO_2e/kWh (Gross CV), where CO_2e stands for carbon dioxide equivalent. CO_2e attempts to measure the impact of different greenhouse gases in terms of the amount of CO_2 that would create the same amount of warming. Gross CV stands for gross calorific value for which coal has 0.31112 kg CO_2e/kWh.

Therefore the cost arising from CO_2 charges is given as below for natural gas:

$$0.18396 \times ((20.67 \times 0.8908) + 18.08) = 6.71 \quad £/\text{MWh} \tag{3.39}$$

and for coal it is as follows:

$$0.31112 \times ((20.67 \times 0.8908) + 18.08) = 11.35 \quad £/\text{MWh}. \tag{3.40}$$

We can therefore estimate the total fuel input cost for gas to be $\lambda_{gas} = 28.33$ and for coal, we have $\lambda_{coal} = 22.24$.

3.7.3 Ramp Rates

The ramp rate and elbow information (previously defined) as provided in BMRS reports is stated in terms of the limits of power production as

$$\frac{dW}{dt}_{up} = \begin{cases} RURE1 & \text{for } 0 \leq W \leq RUEE2 \\ RURE2 & \text{for } RUEE2 < W \leq RUEE3 \\ RURE3 & \text{for } RUEE3 < W \leq MEL \end{cases} \tag{3.41}$$

Ramp down rates are as follows.

$$\frac{dW}{dt}_{down} = \begin{cases} RDRE3 & \text{for } 0 < W \leq RDEE3 \\ RDRE2 & \text{for } RDEE3 < W \leq RDEE2 \\ RDRE1 & \text{for } RDEE2 < W \leq MEL \end{cases} \tag{3.42}$$

We need to convert these to fuel rate changes as we are modelling the fuel input into the generator as a continuous variable. Conversion can be done using the chain rule as

$$\frac{dQ}{dt} = \frac{dQ}{dW}\frac{dW}{dt} \tag{3.43}$$

where

$$\frac{dQ}{dW} = (1-\gamma)\left(\frac{Q_{max}}{W_{max}}\right)\left(\frac{W}{W_{max}}\right)^{-\gamma} \tag{3.44}$$

3.7.4 Inferred power plant parameters

To estimate the unknown parameters (η_{max},ψ^{fc},ψ^{fcOM}) we have decided to use the real-world historical data of power production of the power plants (Physical Half Hourly notifications) and wholesale electricity prices (Market Index Prices) to find a set of parameters that best fit the real-world data using data from [32]. We understand that Market Index Prices are not necessarily representative of the prices the power plants agreed to sell their power due to the following reasons:

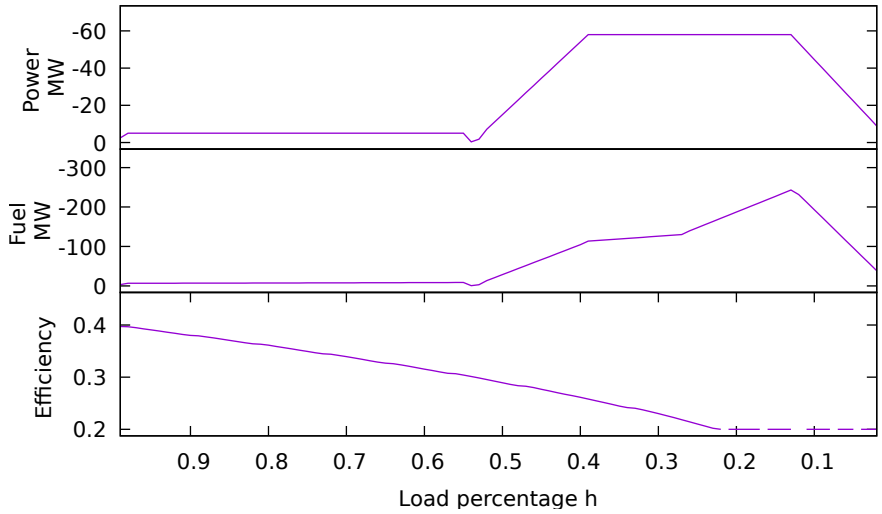

Figure 3.14: Simulation ramp down rates

- Long term contracts - the vast majority of power is bought and sold using bi-lateral contracts (direct contracts between the electricity producer and user). These can be entered years in advance and would not be represented in market index prices.

- Other markets - power plants might be participating in other markets such as capacity market, short term operating reserve. These markets allow power plants to provide flexibility to the NG for managing the electricity network. If power plants have agreed to provide flexibility during the settlement period, they might operate part-loaded to be able to increase their power production quickly.

Taking into account all of the considerations above, we still believe that in expectation, the Market Index Prices (MID) should represent the price of electricity at which power plants sell their power produced. If the prices agreed between the power sellers and power buyers in the forward market were not the same in expectation as the power

exchange prices, there would be an arbitrage opportunity. If there were an arbitrage opportunity traders would soon correct the market and realign forward prices to time adjusted short term market prices.

We are not concerned with the exact reasons why the forecasted power plant operation does not perfectly match the real-world historical data. We want our power plant optimisation model to provide a reasonable approximation to the real-world behaviour of the power plants. This would provide us with sufficient evidence that we can use our model to predict the behaviour of the wholesale electricity market.

To find the unknown power plant parameters η_{max},ψ^{fc} and ψ^{fcOM}, our first approach was to use the Nelder Mead [74] algorithm. Here we tried a set of parameters of the power plants to simulate the operation of the power plant using our power plant optimisation model. We then compared the forecasted operation of the power plant using the guessed parameters and a schedule of observed wholesale electricity prices (the real-world market prices) to find the set of parameters that cause the power plant to behave the same way as observed historically given the historical prices of electricity. We faced issues with this method as even slight deviations of prices were causing a power plant to have large shifts in operation. As we were comparing the difference between the simulated power production with the observed power production in each period, the step changes caused significant difficulties in fitting the model.

Our second approach was to match the price of electricity as derived through our market price search algorithm, as introduced in Chapter 2 to the market price observed when only one power plant was being controlled. Power production production of all other power plants and demand of the system was kept as provided in historical data. This is in contrast with the first approach, where we fitted the optimised power plant

operation given the estimated parameters to the observed power plant operation. This provided better results than the first approach. It still proved challenging to match the exact behaviour of individual power plants due to the potential mismatch between the price agreed by the power plant and MID.

We realised that matching prices as derived through our price search algorithm provided better results, but we still struggled to infer parameters for individual power plants. To overcome this, we have decided to search for parameters for collections of power plants. By collection, we mean that parameters were found for groups of all CCGT & all coal power plants separately. We expected this would allow the averaging amongst the same types of power plants to reduce the need to know exact prices at which these generators traded power. In this section, we provide the support that this argument holds.

To find the unknown parameters for the given power plants we have tested all combinations of the following parameters to find the ones best-fitting the real-world data:

- Upper limit of the efficiency distribution (η_{max}^{upper}) - [20,30,40,50]%
- Lower limit of the efficiency distribution (η_{max}^{lower}) - [20,30,40,50]%
- Fixed Cost (ψ^{fc}) - [0,10,20]%
- Fixed Cost Operation and Maintenance (ψ^{fcOM}) - [0,10,20]%

Where upper and lower limits of the efficiency distribution were used to construct a uniform distribution for maximum efficiency of the power plant η_{max}.

$$\eta_{max} \sim U(\eta_{max}^{lower}, \eta_{max}^{upper}) \tag{3.45}$$

The set of parameters chosen at each iteration can be written as

$$\wr = \{\eta_{max}^{upper}, \eta_{max}^{lower}, \psi^{fcOM}, \psi^{fc}\}. \tag{3.46}$$

For each combination as in (3.46), we ran a market price search algorithm to find the prices at which the market would clear with the chosen set of parameters, as explained in Chapter 2. For every combination $\wr$ we drew η_{max} from the uniform distribution ten times to make sure that sufficient variation of individual power plant η_{max} values were attempted for all power plants before changing the distribution values η_{max}^{upper} and η_{max}^{lower}.

We then selected the set of parameters from all the attempted values that provided the smallest sum of the squared differences between the actual price of electricity π^{real} and the computed price of electricity $\pi^{wholesale,*}$ using our algorithm. A detailed discussion of how $\pi^{wholesale,*}$ is found is provided in Chapter 2. The objective of the function is as follows.

$$\wr = \arg\min_{\wr \in \mathcal{O}} \sum_{t}^{T} (\pi^{wholesale,*} - \pi^{real})^2$$

OCGT, CCGT and coal power plants were of particular interest in our analysis as these provide the majority of power produced in GB that can react to the prices of electricity. This is in contrast to power production from renewable sources where power production is dependent on the availability of wind or sun or from nuclear power plants which tend to operate at a constant level. An example of typical GB power generation can be seen in figure 3.15.

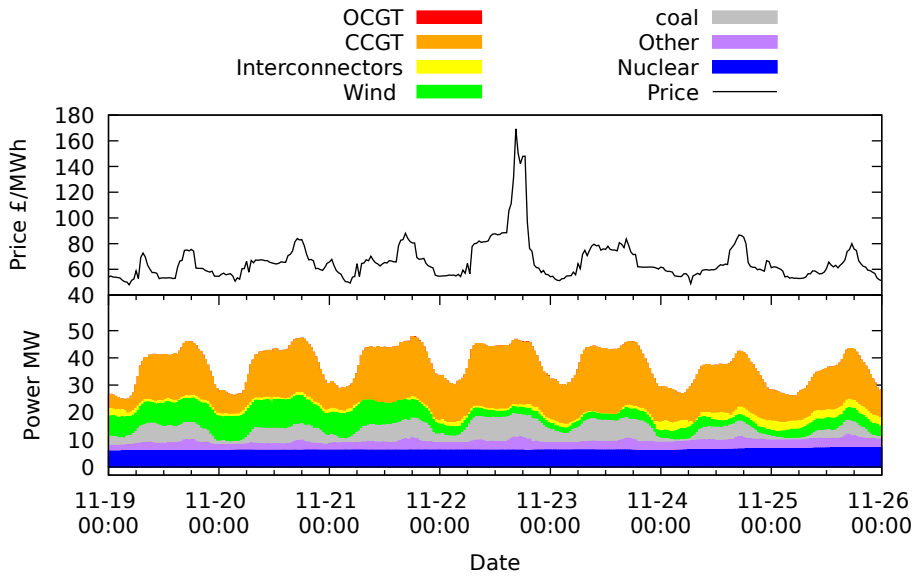

Figure 3.15: Power production by fuel type for period 2018-11-19 to 2018-11-26

The following steps were taken to clean the raw power plant and price data to estimate the parameters:

- Remove all the generation assets that have maximum MEL not available or zero.
- Remove generators with average SEL not available.
- If the average SEL was reported higher than the average MEL, we reduced the average SEL to the maximum MEL.

After cleaning the data, we were left with a total of 51 CCGT generators with a combined MEL of 26,156 MW and 24 coal generators with a combined MEL of 10,583 MW. This leads to the total MEL for all controlled power plants as 36.7 GW. Peak demand during the period was near 50 GW. This shows that CCGT and coal were available to produce up to 77.4% of all demand required during the peak half-hour.

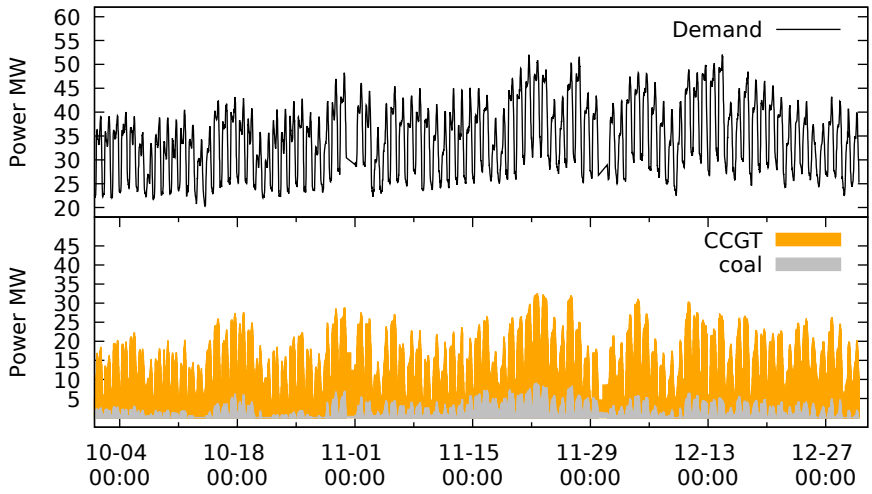

Figure 3.16: Power production by fuel type for period 2018-10-01 to 2019-01-01

The number of power plants operating varies through time and is dependent on the underlying total demand of the system. As we sought to capture the parameters of as many coal and CCGT power plants as possible, we were looking for a one week period that had the highest cumulative power production from coal and CCGT power plants. The period for analysis chosen was 2018-11-19 to 2018-11-26. We chose this period because the sum of CCGT and coal power generation was the highest as can be seen in figure 3.16. This meant that we could infer the parameters of more power plants. We used the first eight days of the period to find a set of parameters that best explain the behaviour of these plants (in-sample fitting). We then used the rest of the period to test our parameters on the set of data that was not used for fitting (out of sample testing). Supply data for the period is shown in figure 3.17.

We first found the dynamic data of the power plants that are provided to the BM. We used the average over the period for each BM unit for the following information: SEL, MZT, NDZ, ramp rates, and elbows as defined in section 3.2. The maximum

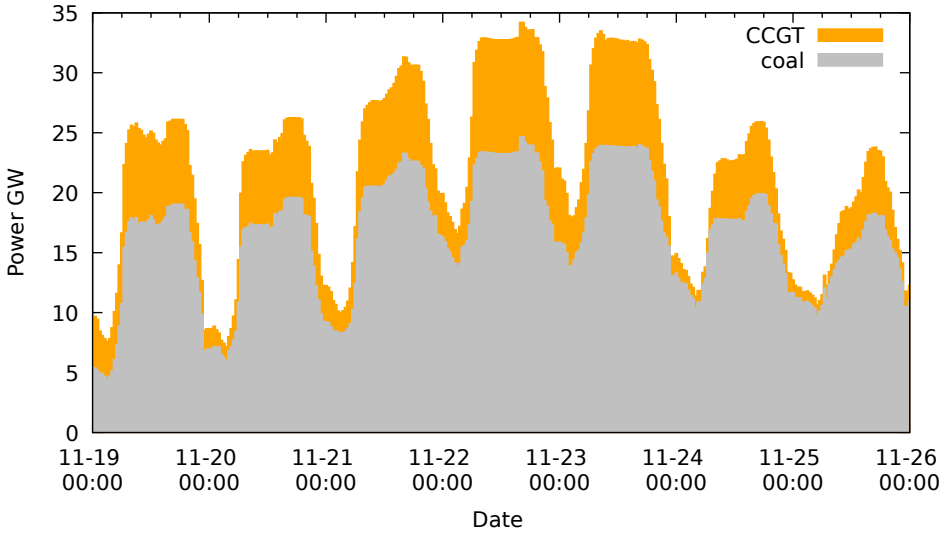

Figure 3.17: Power production from CCGT and coal power plants for the period 2018-11-19 to 2018-11-26.

value observed over the period was chosen for MEL. If ramp rates were provided for less than three elbows, we assumed the latest rate available applied for the rest of the operating region.

3.7.5 Combined Cycle Gas Turbine

The results of the best-fitting parameters for the CCGT power plants are shown in figure 3.18 and are given as follows:

- Upper limit of the efficiency distribution (η_{max}^{upper}) - 50%
- Lower limit of the efficiency distribution (η_{max}^{lower}) - 40%
- Fixed Cost - 10%

- Fixed Cost Operation and Maintenance - 0

Here we were attempting to estimate 4 parameters for each power plant (51 CCGT power plants in total). This means that we are estimating $4 \times 51 = 204$ individual parameters. For this, we used half-hourly wholesale price data over seven days and 18 hours, giving us a total number of points for the estimation as $7.75 days \times 24 hours \times twohalf - hours = 372$. We appreciate that this is not a large number of degrees of freedom. However, the method with which we attempt to find these parameters does not necessarily require an accurate approximation of each parameter, of the power plants. In this thesis, we are only interested in whether we can simulate the collective behaviour of the power plants in the GB market. Evidence of our model's ability to achieve this is provided in later in this chapter as means of out of sample model testing, using the parameters estimated.

From figure 3.18, we can see that the estimated prices (purple in the top graph) closely match the observed market index prices (green in the top graph). The mean difference between the observed and simulated price is 0.91 £/MWh, the standard deviation of the differences is 5.15 and kurtosis 1.21. This provides us with some confidence that the fitted parameters for the power plants are reasonable to make predictions about the behaviour of the sum of all coal power plants in GB. As explained previously, we would not expect the observed and simulated prices to match perfectly as the observed prices are not necessarily the prices at which the power plants sold their power.

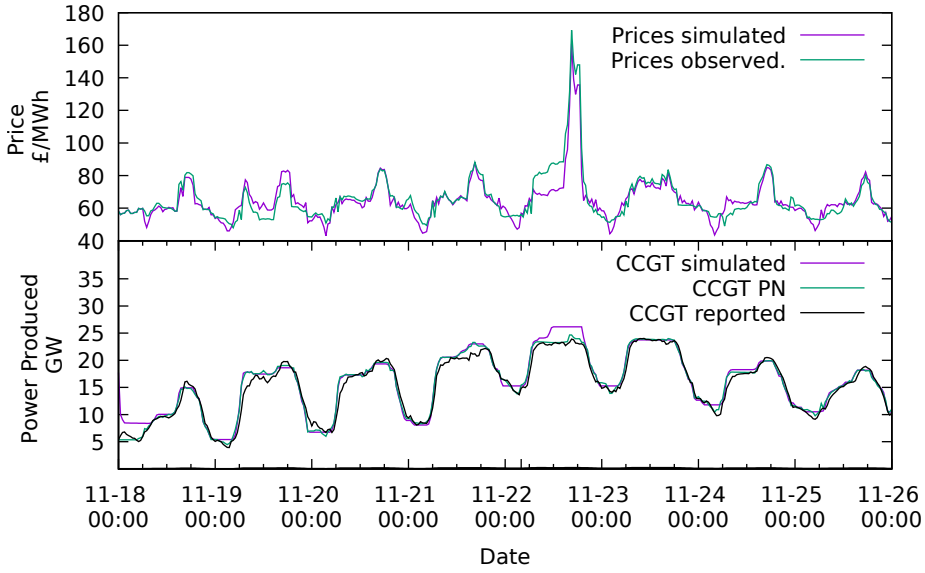

Figure 3.18: The top graph provides information about the result of the market price search algorithm wholesale electricity price (purple) and Market Index Prices (green). The bottom graph provides information on the simulated cumulated behaviour of the Combined Cycle Gas Turbine power plants (purple), physical notification data (green), and realised power production (black).

3.7.6 Open Cycle Gas Turbine

We were not able to derive parameters for open cycle gas turbines as there were insufficient physical notifications submitted to the BM, as shown in figure 3.19. OCGT power plants operated only for 35 half-hourly periods out of 372 periods in the sample. This is reasonable as the open cycle gas turbines tend to be only operated in cases when there is insufficient power available from other sources.

We present the physical notification and actual production of power by Open Cycle Gas power plants in figure 3.19. We can see from the figure that there were only a few instances where OCGT power plants were committed to producing power during the seven days of consideration. These periods were not necessarily corresponding to high-cost periods as shown in figure 3.19. The actual power produced by the power plants (OCGT reported) also differed from the physical notifications submitted.

Due to the lack of physical notification data and due to the operation periods not directly corresponding to higher cost periods, we have chosen not to estimate the distribution parameters for OCGT turbine power plants. Instead, we will be using the information as provided in the literature [75] where distributions of OCGT power plants are said to have operational efficiencies between 30% and 40%.

3.7.7 Coal Turbine

With the available data we were able to estimate $4 \times 24 = 96$ parameters for coal power plants using the price data for 372 half-hourly prices of wholesale electricity. The

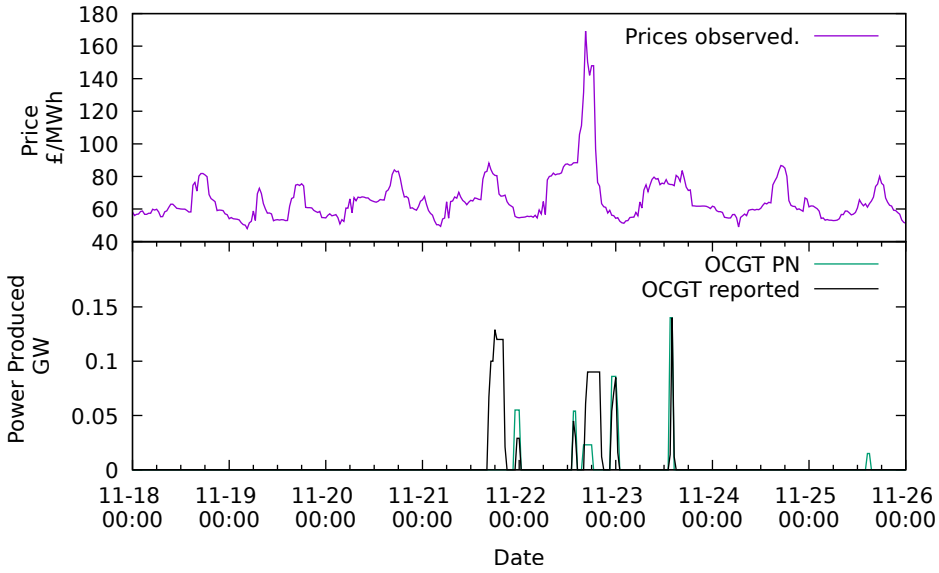

Figure 3.19: The top graph shows Market Index Prices (purple). The bottom graph provides information on the cumulated Physical Notification (PN) of the Open Cycle Gas Turbine power plants (green) and realised power production (black). Only in a few instances throughout the seven day periods, the OCGT power plants were called upon. These periods did not necessarily correspond to the highest price periods.

results of the best-fitting parameters are shown in figure 3.20. Best-fitting parameters were as follows:

- Upper limit of the efficiency distribution (η_{max}^{upper}) - 40%
- Lower limit of the efficiency distribution (η_{max}^{lower}) - 30%
- Fixed Cost - 10%
- Fixed Cost Operation and Maintenance - 0%

From figure 3.20, we can see that the estimated prices (purple in the top graph) closely match the observed market index prices (green in the top graph). The mean difference between the observed and simulated price is -0.07 £/MWh, the standard deviation of the differences is 5.66 and kurtosis 0.45. This provides us with some confidence that the fitted parameters for the power plants are reasonable to make predictions about the behaviour of the sum of all coal power plants in GB.

Throughout the period the physical notification (green bottom graph) seems to be consistently above the reported coal output (black bottom graph). We believe this might be due to coal power plants providing the lowest cost of reducing their output in the BM. This would warrant coal power plants to be the first ones to curtail their power.

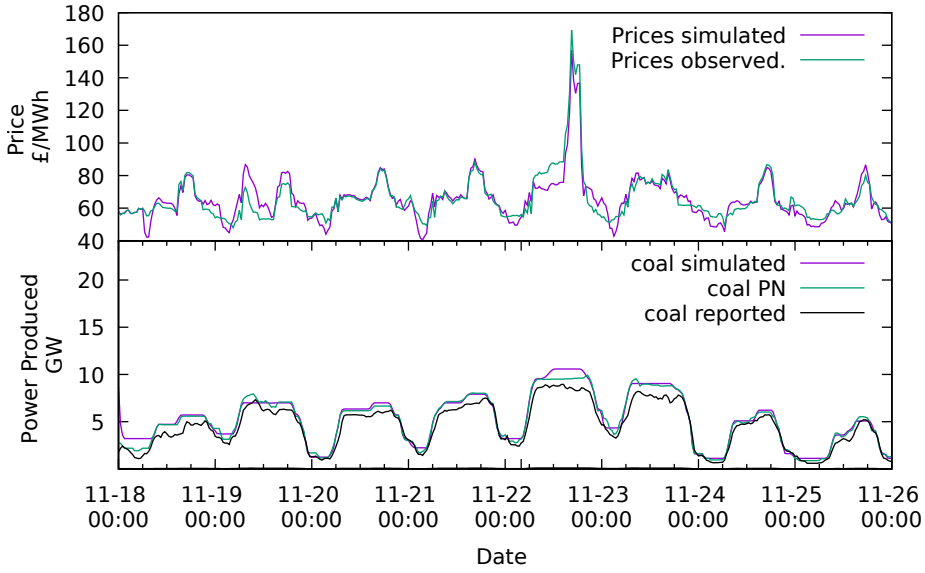

Figure 3.20: The top graph provides information on the result of the market price search algorithm wholesale electricity price purple and Market Index Prices (green). The bottom graph provides information on the simulated cumulated behaviour of the Coal power plants (purple), physical notification data (green), and realised power production (black).

	Simulated prices CCGT	Simulated prices coal	Real prices
Mean	64.8	65.6	65.7
Std.deviation	13.08	13.93	14.78
Max	160.9	157	169.3
Min	42.9	40.5	47.9

Table 3.4: Summary table of simulated prices for CCGT and coal compared to real prices.

3.7.8 Summary of maximum efficiency distributions

In table 3.4 we provide a summary table of the simulated and real prices for OCGT and CCGT for the period of the parameter fitting. We can observe that the prices that were derived using our price matching algorithm closely match the prices as observed in the real-market (Market Index Prices).

Maximum efficiency η^{max} distributions as estimated from the data were as follows:

$$\eta^{max} = \begin{cases} \mathcal{U}(0.3, 0.4) & \text{for } OCGT \\ \mathcal{U}(0.4, 0.5) & \text{for } CCGT \\ \mathcal{U}(0.3, 0.4) & \text{for } coal \end{cases}$$

These can now be used in our market simulations in Chapter 5.

3.8 In sample testing

Previously, we have found parameters for separate groups of power plants, namely coal and CCGT. To confirm the fit of our found parameters, we have decided to simulate

the behaviour of all (the combination of coal and CCGT) power plants during the training period using the previously found parameters. The results of the simulation are presented in figure 3.21. We can see that prices derived closely match the prices observed. Both the derived production of CCGT and coal closely match the observed information. We do observe that at the beginning of the week, we overestimate the production of power from CCGT and underestimate the production of power from coal power plants. This changes towards the end of the week where we tend to underestimate the production of CCGT and overestimate the production of coal. We believe this could be influenced by changes in fuel costs and emission certificate prices. We discuss these further in the next subsection.

3.8.1 Out of sample testing

As we are attempting to model wholesale electricity prices in the future energy scenarios we are also interested in the performance of our model and accuracy of the estimated parameters in predicting wholesale electricity prices in and out of sample situations. To test the robustness of the model, we simulated the behaviour of the power plants out of sample and again compared the derived wholesale electricity prices with those observed in the market.

To reiterate, we are using the parameters found in the previous subsection to test our results out of a sample. We have decided to simulate the behaviour of power plants for the period of 2018-12-01 and 2018-12-25 to see if the prices derived using our models closely match the prices observed.

We present the results which show that predicted and simulated prices closely match,

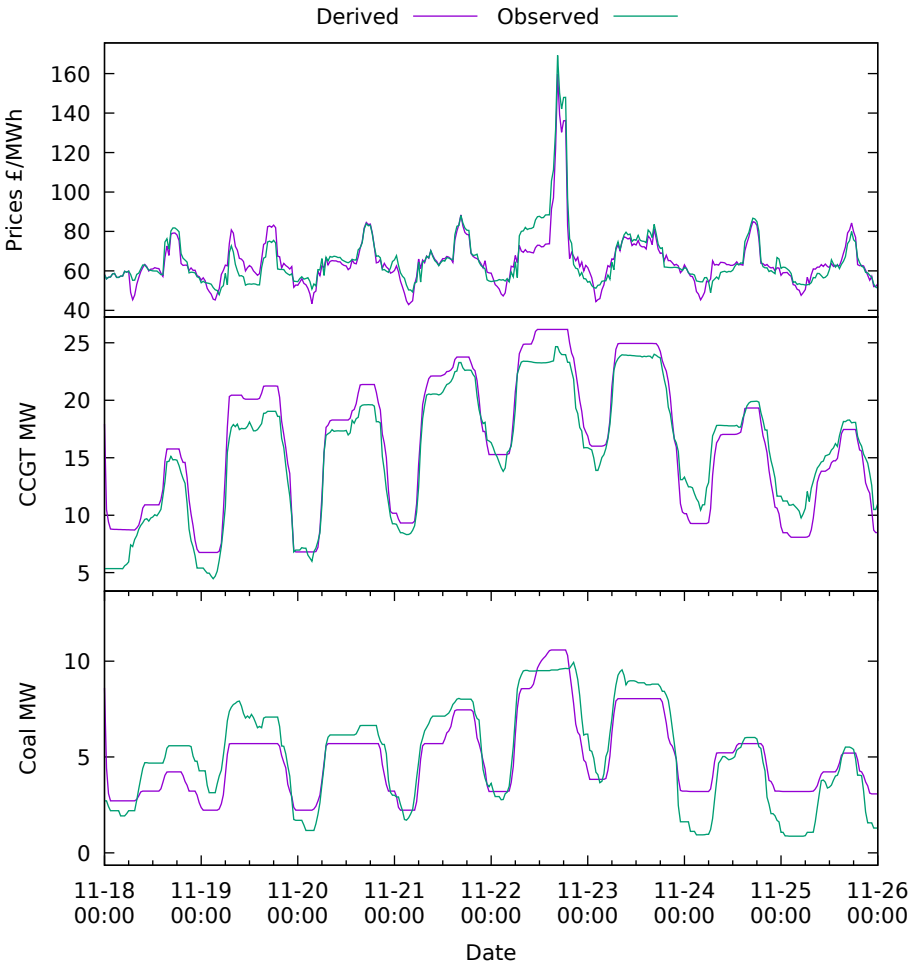

Figure 3.21: Production of power and derived prices using the combination of coal and CCGT power plants during the training period.

in figure 3.22. Production of power from CCGT power plants closely matches the observed power production. For coal power plants, this relationship between the observed and derived power production is not as evident. We can observe periods of divergence of the derived and observed power production.

Divergence of the coal power production from the observed data could be caused by the increase in the cost of carbon price. As we can see from figure 3.23, the cost of carbon increases in the second part of the month. As we are using the averaged price of EUA equal to 20.67 €/t, the increase in price could make it less economical to run coal power plants. This could be the reason why we are underestimating the cost of producing power using coal.

We have also presented an additional histogram of the differences between the derived and observed wholesale electricity prices as provided in figure 3.24. From the histogram, we can see that differences are normally distributed around zero. This provides us with confidence that simulated prices are not biased.

3.9 Conclusions

The purpose of this thesis is to provide a framework of modelling wholesale electricity markets of the future when the composition of power supply has significantly changed towards more renewable energy sources such as solar and wind. Even though we expect a significant increase in the power generation from renewable sources there will still be a need to run thermal power plants that can provide power when the wind is not blowing and the sun is not shining. Understanding how often these power plants will

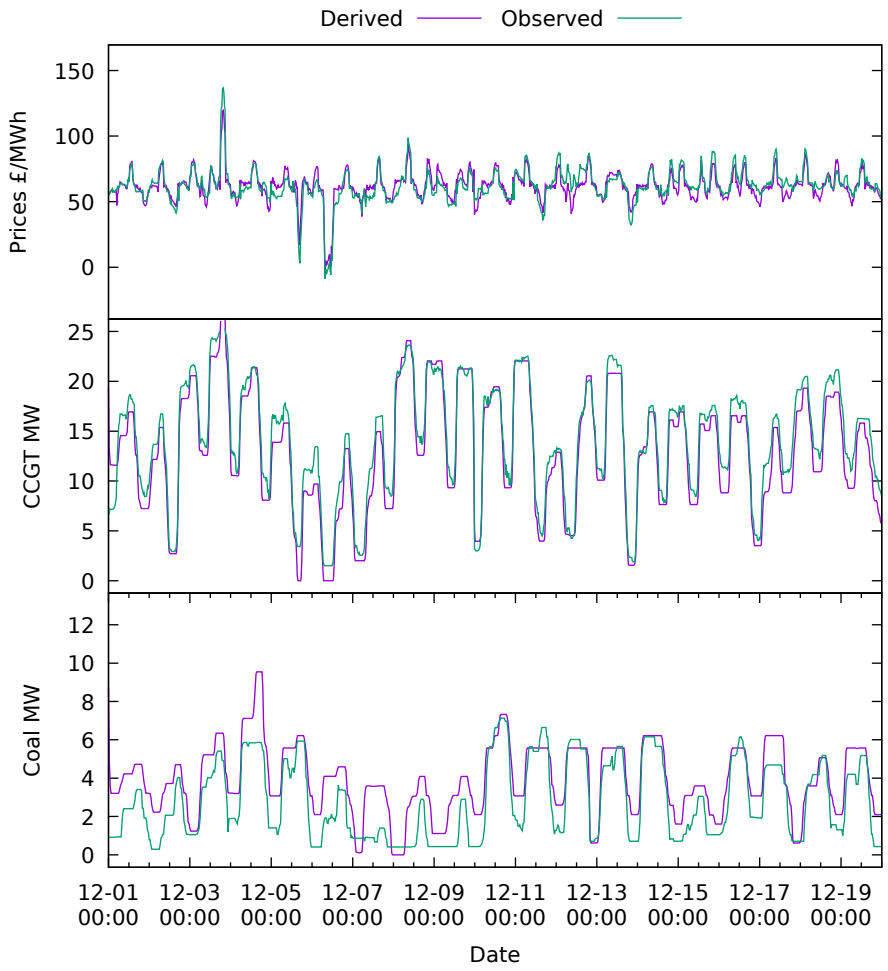

Figure 3.22: The top graph shows the price evolution of derived prices using our market search algorithm and the estimated parameters and observed wholesale market prices.

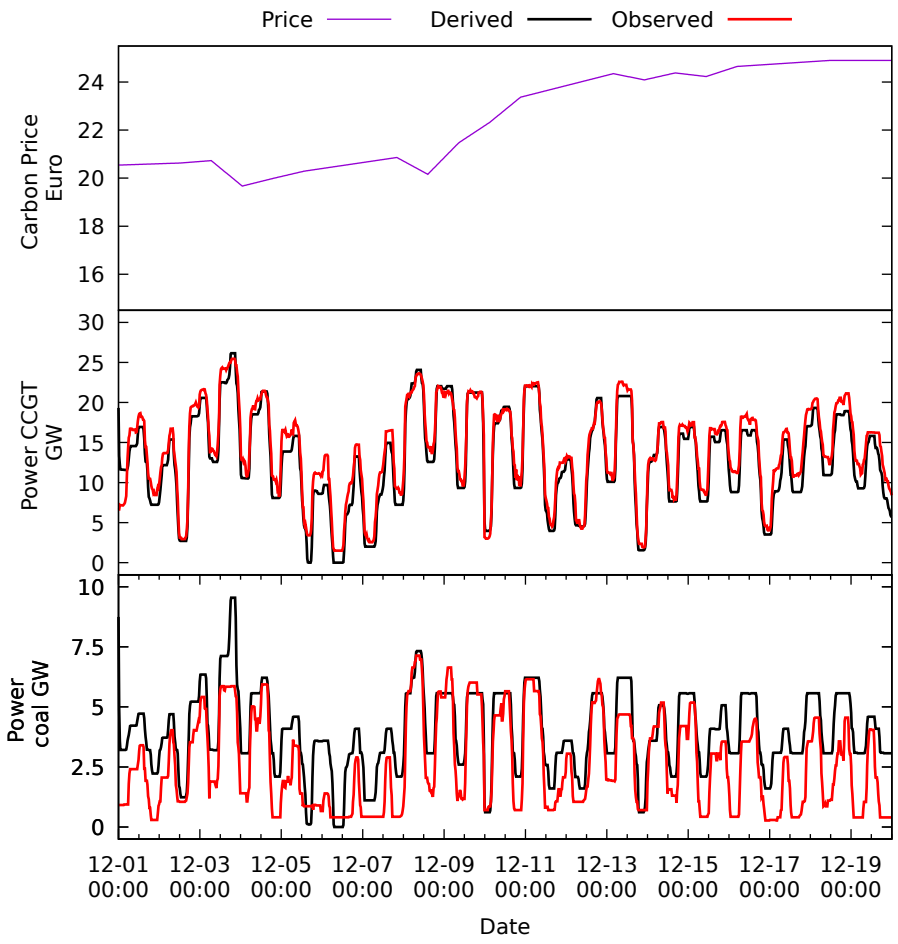

Figure 3.23: Out of sample parameter testing graph with carbon price (top graph), power production from power plants and coal power plants (bottom graph).

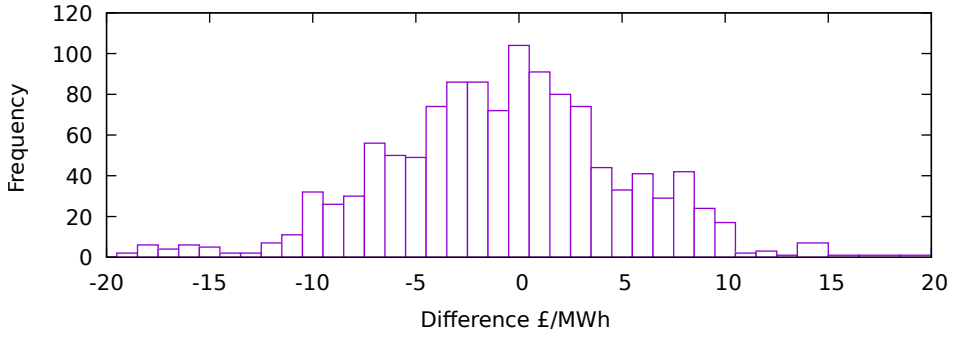

Figure 3.24: Histogram of the difference between the observed and derived wholesale electricity prices.

be utilised and how they will influence wholesale electricity prices is, therefore of great importance for policymakers.

In this chapter, we have introduced a generalised model for power plant optimisation as well as introducing the operational parameters that define individual power plants. Power plant modelling used is only an approximation to the real world power plant operation while using the information as provided by the NG [32]. Further investigation on how the simplified model fits actual instantaneous power plant dynamics could be studied in future research.

We have also discussed the parameters that are readily accessible for the power plants operating in the GB power market as well as the parameters that are not readily available. Our analysis has then focused on estimating these unknown parameters using real-world electricity market data. For the introduced models and estimated parameters, we have performed testing against real world data to evaluate the robustness of the modelling and estimation in predicting the behaviour of the power plants and the estimation of wholesale electricity prices.

Chapter 4

Control of Heating in Buildings

We assume throughout the thesis that significant electrification of space heating in buildings will have to take place in order to achieve the 2050 targets for carbon emission reductions. Temperature control in buildings is one of the key means to provide DSR in the future. It is the thermal mass of buildings that enables users to shift their heating patterns without incurring a significant deviation in the indoor temperature. We imagine a future in which intelligent controllers of HPs can participate in wholesale electricity markets, the BM and even provide frequency response. Introducing such agents to the market that are capable of interacting in this way will help with the integration of renewable energy sources by incentivising the shift of thermal loads to periods low demands and prices [76, 77].

In this chapter, we start by providing a brief overview of the literature concerning building energy management systems and the algorithms used for deriving optimal

heating schedules. Next, we build the framework for our model, as we introduce a domestic building heater dynamic optimisation algorithm similar to [8]. We are then able to show how to calibrate these optimisation models and find the real-world parameters that match the heating profiles of hundreds of different households documented in the Energy Follow Up Survey [78]. These parameters allow us to model representative households which can be used to obtain the consumption of energy for domestic heating households across England. The set of parameters we generate feeds later into the models in Chapter 5, to simulate the power consumption for heating in FES scenarios.

Lastly, we provide experimental results comparing the HP operation using fixed and DA-RTP tariffs using an HP at Salford University. Results from the experiment show that using dynamic tariffs with HPs could save domestic users 20% in heating costs during a typical week in the English wintertime. We are also able to achieve higher user comfort with temperatures that better match the user target temperatures.

4.1 Literature Review

As energy prices for domestic customers continue to increase, for instance in GB we saw the price rising from 1,000 £/year in 2012 to 1,254 in 2019 [79], and as domestic homes become more connected, the industry has seen an increase in the energy conservation offerings available, such as smart thermostats. These are usually internet-connected thermostats that can learn the behaviour of users in buildings by using installed sensors (motion and temperature) or through the users' interaction with the thermostat through a mobile phone app to schedule heating. This remote interaction allows users to make sure that their homes are only heated when needed, avoiding wasting energy

and reducing the overall carbon footprint. Popular smart thermostats available on the market include: Nest [80], Tado [81], Hive [82] and Heatsmart from EDF [83].

Commercially available thermostats tend to have focused on gas-based heating systems, as gas boilers are still the prevalent technology for heating homes across the world. In GB, gas boilers cover around 78.24% of the domestic heating market [3]. As gas is easy to store and does not need to be consumed straight away after production (in contrast to electricity), there was no need for a smart thermostat to consider DA-RTP prices. As we start seeing an increase in electric heating technologies, we will likely see an interest in providing smart thermostats that can react to DA-RTP electricity tariffs, that are becoming more widespread around the world. This thesis focuses on this type of control, where houses would be equipped with an electric heating technology, most likely HP, and would be able to receive DA-RTP tariffs. Our building heating optimisation algorithms can then use information on the price of electricity, weather forecasts, and user temperature preferences to find the most cost-efficient way of operating the system.

Variable electricity tariffs and optimisation algorithms have been studied in academia, preparing for the eventual shift of gas heating systems to electricity. Of particular interest in energy management systems was also the control of air conditioning in countries such as the United States. Several field studies conducted [84, 85, 86] used smart thermostats to confirm the willingness of consumers to allow their home energy management systems to be autonomously controlled, based on price signals or direct control algorithms as defined in Section 1.1.

Academics have mostly focused on the ability to aggregate several buildings to provide services such as regulation services for the grid (short-term grid response) [77] or

aggregation of a number of these loads to participate in wholesale electricity markets [87, 88, 27, 89, 90]. In this thesis, we do not consider the participation of individual buildings in short term grid response services. We assume that the buildings in our models are already a part of a consortium or a load aggregator, allowing them to access wholesale electricity markets. Modelling of the feedback between the wholesale electricity market and the market participant is one of the contributions of this thesis. The feedback we consider here is the ability of several controllers to affect the wholesale electricity prices; if several controllers shift heating to off-peak periods, they could increase the off-peak price, therefore, creating a new peak. By using the iterative market price search process discussed in Chapter 2.1, we can provide the estimation of thermostatically controlled loads effect on the grid (maximum load, average peak load) when the feedback between the market and the heating controller participation has been taken into account.

A number of algorithms have been used to optimize heating operation of buildings (minimizing the cost whilst maximizing the occupant's comfort), including mixed-integer linear programming [91, 92], Monte-Carlo methods [88], model predictive control [93], stochastic dynamic programming [8] and dynamic programming [94, 27]. In this thesis, we use the adapted model introduced in [8] without the stochastic weather predictions leading to a simplified dynamic programming method to solve the optimal heating control problem. Dynamic programming methods cannot solve problems with a high number of states, but they provide benefits of high computational speed and ability to incorporate building dynamics [8].

Other differences between studies are the inclusion of different factors in the optimisation models that would improve the accuracy of the optimal heating scheduling for individual users. Some papers have focused on including stochastic variables in their

optimizations such as stochastic weather predictions [8, 92, 95], electricity prices [92, 94, 90] or occupancy [95] others have attempted to better predict user temperature preferences [96] or to improve the thermal modelling of buildings by better learning the dynamic parameters [91] or by using more parameters risking over-fitting [87]. For an extended literature review on home heating controllers and optimisation algorithms, please see [97].

4.2 Heating Optimization

Our model for controlling and optimising the heating of a house is similar to that introduced by [8]. In contrast with that work, we assume weather forecasts are accurate and therefore do not include in our initial model any uncertainty around the evolution of the outside temperature and its effect on the building. Inclusion of stochastic weather predictions would improve the control although it would come at the cost of increasing the complexity of the modelling. This complexity would prohibit us from using our market search algorithm due to time constraints.

Discomfort coefficient

User preferences in terms of their flexibility (how sensitive they are to internal temperature variations) are specified in our heating optimisation through a coefficient p $£/°Ch$ similar to [98]. This coefficient is the weight attached to the temperature deviations $|I(t) - I^*(t)|$ where $I(t)$ is the current internal temperature, and $I^*(t)$ is the

time-dependent desired temperature. The discomfort cost function can then be specified as $p|I(t)-I^*(t)|$. We believe using the modulus of the temperature differences from the desired temperature allows us to use the formulation of the coefficient p as $£/^\circ Ch$ that is easy to understand and can be explained to the users of autonomous control devices with the proposed optimisation algorithms. An example question that the user could be asked is "What is the lowest amount of savings you would like to receive for keeping your temperature one degree lower than your set point for an hour?".

Other authors have used quadratic discomfort cost functions [94, 88, 90, 25, 8] or a temperature deadband around desired temperature without penalties [99, 95, 89, 27]. Our modelling is flexible enough to cater for alternative models discussed above.

4.2.1 Building Models

The optimality of our building optimisation solution relies on the accuracy of the internal building temperature modelling. For simplicity and to reduce the computational efforts we use the 1-dimensional model for the building dynamics. In future work, it would be possible to investigate extending building modelling to include additional dynamics such as solar radiation effects [98] or increasing the order of the model. Some authors suggest that second-order models should be used to accurately model the thermal behaviour of buildings [100, 101, 87]. We were unable to use higher-order building models as the increased computational complexity would have meant that our simulations would take significantly longer to perform and are left for future investigation.

Let the internal temperature dynamics of the building be modelled as in [77, 90, 88,

99, 89, 27, 25, 94, 102, 8] and be given by

$$\frac{dI}{dt} = a_{11}(\hat{T} - I) + a_{12}H \tag{4.1}$$

where

- I - a single point estimate of internal temperature of the building $^{\circ}C$.
- $\hat{T}(t)$ - single point estimate of the outside temperature $^{\circ}C$.
- H - rate of domestic heater power input.
- a_{11} - Heat transfer coefficient from indoor temperature to outside.
- a_{12} - Heat transfer coefficient from the heater to internal temperature.

Each building is defined by a set of building dynamics parameters a_{11},a_{12}, the time-varying temperature set-points $I^*(t)$ $^{\circ}C$, value for the trade-off between cost and temperature discomfort p £/$^{\circ}C$h and the times at which the set temperature is required $U(t)$. However, we must recognise that there are severe limitations in proceeding in this way. For instance:

- In our simplified model of the building, we have ignored solar radiation. Although we accept that it can be an important source of heat for the buildings, we have found it difficult to get accurate data of solar irradiation from available data sources.

- We assume that there is a constant HP Coefficient of Performance (CoP) across different flow temperatures (the temperature that is being supplied by the heater) and outside temperatures (the incorporation of CoP adjustment could be considered for future work).

In our work, we are looking to use real-world building data to estimate the behaviour of individual buildings in the electricity market with a high uptake of HPs. For this, we will be required to estimate the heat transfer coefficients, as discussed in more detail in Section 4.3.5. For reference, we have identified several papers that could be used to gather example building parameter data from real-world buildings [77, 102, 26, 90].

4.2.2 Optimization

The objective of the heating controller is to minimise the cost to the user. The optimisation algorithm finds the optimal control policy $H \in \mathbb{H}_t$ that is the amount of instantaneous energy consumed by the heater in the building. The optimal derived policy will depend on the current internal temperature of I and the time of the day t. We can represent this objective as a minimisation of the total discomfort costs (cost of electricity for the heater and discomfort of the user due to temperature imbalance) over the time horizon T.

We can note the cost of discomfort at any given temperature as

$$pU(t)\,|I(t) - I^*(t)| \quad £/h. \tag{4.2}$$

and $H(s)\pi^{domestic}(s)$ £/h represents the cost of electricity paid for using the heater, where $H(t)$ kW is the heater power input and $\pi^{domestic}(t)$ £/kWh is the price of electricity at that time step.

The value of the total discomfort given that current internal temperature I and time t can be written as

$$V(I,t) = \min_{H \in \mathbb{H}_t} \left[\int_t^T e^{-\rho(s-t)} (pU(s)\,|I(s) - I^*(s)| + H(s)\pi^{domestic}(s)) ds \right] \quad (4.3)$$

as first introduced in [8]. As discussed previously, we have chosen to remove the modelling of the stochastic weather predicitons to reduce the computation intensity of the calculations. For the purposes of grid cost modelling, we assume that the weather predicitons are accurate and therefore this omission is not expected to impact our whole grid modelling results in later chapters.

We let $\mathbb{H}_t$ be the set of all admissible control policies defined as follows

$$\mathbb{H}_t = \{H = \{H(s)\}_{t \le s \le T} : \forall_{t \le s \le T} \quad H_{min} \le H(s) \le H_{max}\}.$$

This defines the set of all heater inputs $H(s)$ between the current time t and final time T. At every time step s, the heater input is limited by an upper power bound H_{max} and lower power bound H_{min}.

To solve this optimal control problem we use (4.3) to derive our HJB equation using

the following steps

$$V(I,t) = \min_{H\in\mathbb{H}_t} \left[\int_t^{t+dt} e^{-\rho(s-t)} \left\{ pU(s)\left|I - I^*\right| + H(s)\pi^{domestic}(s) \right\} ds \right.$$
$$\left. + e^{-\rho dt} \int_{t+dt}^{T} e^{-\rho(s-(t+dt))} \left\{ pU(s)\left|I - I^*\right| + H(s)\pi^{domestic}(s) \right\} ds \right].$$

Using (4.3) we can also write this as

$$V(I,t) = \min_{H\in\mathbb{H}_t} \left[\int_t^{t+dt} e^{-\rho(s-t)} \left\{ pU(s)\left|I - I^*\right| + H(s)\pi^{domestic}(s) \right\} ds \right.$$
$$\left. + e^{-\rho dt} V(I+dI, t+dt) \right].$$

Using Taylor's expansion and assuming that the value function $V(I,t)$ is differentiable everywhere in t and I we can rewrite this as

$$V(I,t) = \min_{H\in\mathbb{H}_t} \left[pU(t)\left|I - I^*\right| dt + H(t)\pi^{domestic}(t)dt + (1-\rho dt)V(I,t) \right.$$
$$\left. + (1-\rho dt)\left\{ \frac{\partial V}{\partial t} + \left(a_{11}(\hat{T} - I) + a_{a12}H \right) \frac{\partial V}{\partial I} \right\} dt + o(dt) \right]. \tag{4.4}$$

We further use (4.4) and eliminate all terms going to zero faster than dt, divide through by dt and take the expectation which leads us to

$$0 = \min_{H\in\mathbb{H}_t} \left\{ pU(s)\left|I - I^*\right| + H(t)\pi^{domestic}(t) + \rho V + \frac{\partial V}{\partial t} + \left(a_{11}(\hat{T} - I) + a_{a12}H \right) \frac{\partial V}{\partial I} \right\}. \tag{4.5}$$

Given this HJB equation, we can use Semi-Lagrangian numerical schemes to solve this optimal control problem. Similar steps can be used to those provided for the generator optimisation in Section 3.6, as introduced in [64].

4.2.3 The discrete-time problem

When we perform the analysis of the energy system, we will assume the heating controls taken by the HP controllers are at discrete time steps. This will mean that once turned on, the HP can not change its operation for the specified time step (we will consider timesteps of 30 minutes in our analysis). These longer time steps will replace the ds as specified in (4.3) and will be denoted as Δt. During the Δt the power input to the heater H and the outside temperature is assumed to be constant. The restriction on the time intervals chosen for the heating controls is due to physical limitations of HPs as they have a minimum on and off times when operating and the granularity of DA-RTP tariffs.

When solving the optimisation problem, we need to calculate the temperature evolution throughout the period of Δt. The temperature change over period Δt can be calculated by solving the (4.1) leading to the temperature I at a time one Δt in the future as specified in (4.6).

$$I(t+\Delta t) = (I(t) - \frac{a_{11}\hat{T}(t) - a_{12}H}{a_{11}})e^{-a_{11}\Delta t} + \frac{a_{11}\hat{T}(t) + a_{21}H}{a_{11}} \tag{4.6}$$

where $I(t+\Delta t)$ and $I(t)$ is the temperature of the building at time $t+\Delta t$ and t

respectively, a_{11},a_{12} are the inferred house parameters, H is the power input of the heater and $\hat{T}(t)$ is the outside temperature at time t.

4.3 Real World Data Cleaning and Processing

To estimate dynamic parameters for representative domestic houses, we used data from Energy Follow Up Survey (EFUS) [78]. This study aimed to record the evolution of the internal temperature of domestic buildings across England to improve the government models on forecasting domestic energy consumption such as the BRE Domestic Energy Model (BREDEM)[103], and Department of Energy & Climate Change's (DECC) own National Housing Model (NHM) [104]. Temperature loggers were given to willing participants to record the internal temperature every 20 minutes in the year 2012 in up to three rooms: the living room, hallway, and bedroom. EFUS collected internal temperature data for 823 houses across England. We acknowledge the limitation that this provides the survey on English housing stock as the electricity supply information for the analysis is used for the whole of GB. We assume that the build of homes across GB would be fairly similar, and therefore we extrapolated the house information to represent the whole GB housing stock.

To be able to model the behaviour of heating systems across GB we needed information on the heating patterns of the users $U(t)$, the thermal parameters of the buildings a_{11}, a_{12}, desired temperatures $I^*(t)$ and trade-off between the discomfort and the cost of heating p as introduced in Section 4.2. Using the information provided in EFUS, we were able to calibrate all of these parameters to predict the behaviour of heating systems in GB.

For our parameter estimation, we used the living room temperature information provided in the EFUS dataset. We believe that the majority of houses will have their thermostats placed in the living room. Therefore, the set temperature on the thermostat will be corresponding to the living room temperature. It is also the position of the thermostat that is advised by HVAC installers "Placing your thermostat in one of the primary living areas of your home can allow it to collect the most relevant information about temperatures and comfort levels." [105].

For parameter estimation, we used the three months between 2011-11-01 to 2012-02-01. We have chosen this period as it is most likely to have the heating systems operating in buildings. In GB, the heating season generally starts at the beginning of November and finishes at the beginning of April.

The Nelder-mead algorithm [106] was used to estimate the thermal parameters of the buildings, according to the temperature model in (4.1).

4.3.1 Data Cleaning

Internal temperature data from EFUS required cleaning before the parameter search could be performed. The steps we took to clean the internal temperature data were:

- Check if living room temperature information exists. If it does not exist, remove the house.
- Check if internal temperature varies through time. Assume that the temperature logger was faulty if there is no variation and remove the house. It is impossible for

the internal temperature to stay constant throughout the whole of the reporting period.

- If temperature information is not recorded at 20-minute intervals it is approximated using linear interpolation, to get values for every 20-minute intervals.
- Use the EFUS main heating file to find heater on/off times. Houses can report up to 6 different times at which the heating turns on/off for every weekday. If a house has a thermostat but no timer then set on/off time as "on" for the whole day, so the temperature is only regulated by the temperature set point and not the heater on/off times. If the heating data not available remove the house.
- Use EFUS room file to find the number of bedrooms in the building. If the number of rooms information is not available, remove the house.
- Find the weight of the building in the interview file, express it as a percentage of England's total.

Weightings of the EFUS data were then used to scale up the logged data to represent the GB population. Weighting factors provided in the EFUS dataset have been calculated to align individual dwellings with national totals for tenure, Government Office Region and dwelling types as discussed in [107]. We assumed the housing stock and demographics across GB were similar to that in England. After data cleaning, we were left with 519 houses for which all the required information was provided.

4.3.2 User profile estimation

From manual inspection of the recorded internal temperature data, we found there were some houses where temperature set-points were constantly much lower than the internal temperature reported. This may have been caused by the wrong placement of the temperature logger (away from the thermostat) or misinformation (misstated set-points during the interview). We, therefore, employed the following method to devise the desired temperatures ($I^*(t)$) and $U(t)$.

We assumed the day is split into two periods, morning and evening. We considered the morning to be between 00:00 - 14:00. This was to make sure that the heating schedule captured by the morning does not include the evening schedule. Evening time was therefore considered as the rest of the day 14:00 - 00:00.

To find the desired temperatures of the buildings $I^*(t)$ and the times at which this temperature was required $U(t)$ we first found the time at which heating is first turned on in both the morning and evening periods. We then used the averaged daily temperatures for the specific weekday and looked for the temperature peak that occurred after the heater has been turned on. In some of the cases, the temperature at 00:00 was still higher than the morning peak temperature. This was because the temperature set point in the evening was much higher than that in the morning. By finding the peak of the temperature after the first instance the heater is turned on, we made sure that the temperature peak captured corresponds to the correct period of the day.

The peak temperatures found in respective periods of the day were assumed to represent the desired temperature of the occupants $I^*(t)$ in those particular periods. We, therefore, used one set-point temperature in the morning and a different set point for

the evening. We further assumed that the times at which this temperature is required $U(t)$ will be at the times when the averaged daily temperature is within 0.5 degrees from the peak in respective periods of the day.

Daily profile counts across different houses can be seen in figure 4.2. These show the percentage of houses of the dataset having their set-points ($U(t) = 1$) set at particular times of the day. We can see majority of users (85%) have their temperature set-points between 7:00 and 9:00 in the morning and 18:00 and 21:00 in the evening. All weekdays seem to have similar profiles (lines labelled 0-5). Weekend profiles (lines labelled 5 and 6) have a slightly different profile with the peak time shifted to 8:00 and more users having their set-points throughout the day.

We have noted some improvements that could be made for future EFUS studies:

- Loggers should have been placed next to the thermostat. We would expect the thermostat to control the internal temperature when the set temperature is reached. As the temperature loggers were not necessarily placed next to the thermostat, we did not know precisely when the heating would have turned off.
- Temperature set-points and timings of the heating should have been inspected by the surveyor on the thermostat and timer of the thermostat synchronised with real-time to avoid errors.
- Households should have been asked when they want their building to be warm and what is their desired temperature. In usual scenarios, users only choose the times during which the heaters in these houses would turn on. This is not an efficient control as the achieved internal temperatures would be affected by outdoor conditions. On a warmer day, the house could be overheated, and on colder

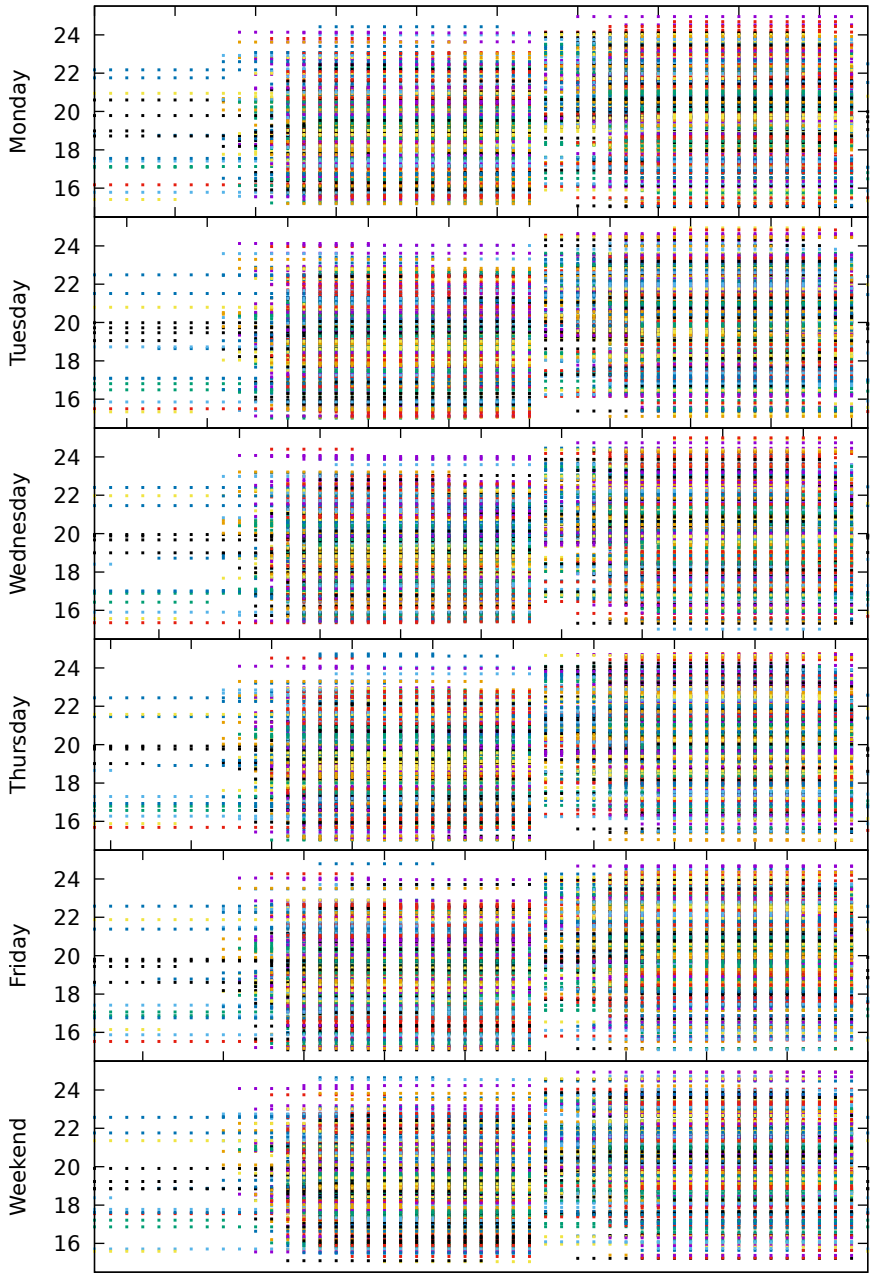

Figure 4.1: Daily internal temperature evolution profiles across England using EFUS data [107]

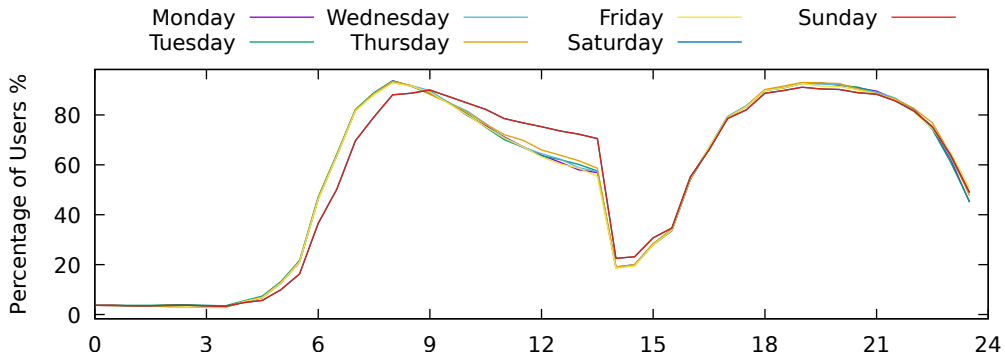

Figure 4.2: Daily profile counts across different houses

days, houses would be under heated. Knowing at what time the user required the set temperatures would have enabled us to assess the comfort realised by the user.

- It would have been interesting to find out the minimum temperature set point on the thermostat. This is the point at which the heater turns on even if it is outside the "on" times specified. Example: If the room temperature ever drops below 15°C, even if the heater is outside "on" times it will try to keep the temperature above 15°C.

4.3.3 Heater size estimation

As the size of the heaters installed in houses was not reported in the study, we had to make assumptions on the size of the system H_{max}. We assumed all houses were heated using gas boilers. For the sizing of the boiler, we assumed a simple method of 1 kW per 10 m^2 floor space, laid down in the building code basics [108]. However, information on the floor space was not provided in the EFUS. We estimated the size of the usable floor space of different buildings by regressing the usable floor space in terms of m^2

Rooms	Usable Floor Space m^2	H_{max} kW
1	45.75	6
2	64.87	8
3	84.72	11
4	130.67	16
5	195.27	24

Table 4.1: Mean usable floor space and heater sizes for different number of bedrooms.

on a number of bedrooms using the 2015-2016 English Housing Survey (EHS) data [109]. Usable floor space information is not provided in EFUS but provided in EHS, and the number of bedrooms is provided in the EFUS. We used the total number of bedrooms household has from the EHS interview file (variable = nbedsx) and usable floor area m^2 original EHS definition for the floor area from the EHS physical survey file (variable name floorx). Averages of the usable floor space and the corresponding H_{max} for a different number of bedrooms are provided in table 4.1.

From table 4.1, we can then choose a specific number of rooms and estimate what would be the expected average capacity of the installed heater in the building. For example, according to the table in the case of 1 room, it would be 6 kW, to provide the required amount of heat. Due to limited information, this estimate of the size of the boiler is the best we can achieve. Further improvements in the estimation could be made if we had access to more data. The following are the considered limitations of our method:

- We do not know what type of boiler is installed in the building.
- We do not know the actual efficiency of the boiler installed.
- We do not know if the boiler has been oversized. It is known that it is common practice to oversize domestic boilers.

4.3.4 External temperature

The location of the houses was not provided in the EFUS. For the estimation of building parameters, we used external temperatures for the following cities: London, Manchester, Birmingham, Leeds, Sheffield, Truro, Bradford, Durham, Liverpool, Wiltshire, Bristol, Kirkles, Carlisle, Newcastle, Norwich, Brighton, Sunderland, Wolverhampton, Plymouth. The majority of these locations have been chosen to represent the largest cities in England. Others have been included to make sure that different parts of England have been represented.

In figure 4.3, we present the variation of the temperatures across England for the period 2011-11-01 to 2012-02-01 that was used to collect internal temperature data in the EFUS. From this figure, we can see that temperature can vary significantly between different parts of the country. The average difference between the coldest and hottest part of the country during the period is observed to be 5°C, with the highest difference reaching 13°C and the lowest difference being 1.25°C.

4.3.5 Building thermal parameter estimation

Building parameter estimation was performed for all of the houses in the EFUS dataset, where temperature logger data was available. In each case, a set of thermal parameters was used to simulate the temperature of the building for each day in the estimation period (2011-11-01 to 2012-02-01), a total of 92 days. Equation (4.1) was used to simulate the internal temperature using the heater operation times as reported in the EFUS interview dataset. To find the best-fitting thermal parameters of the building,

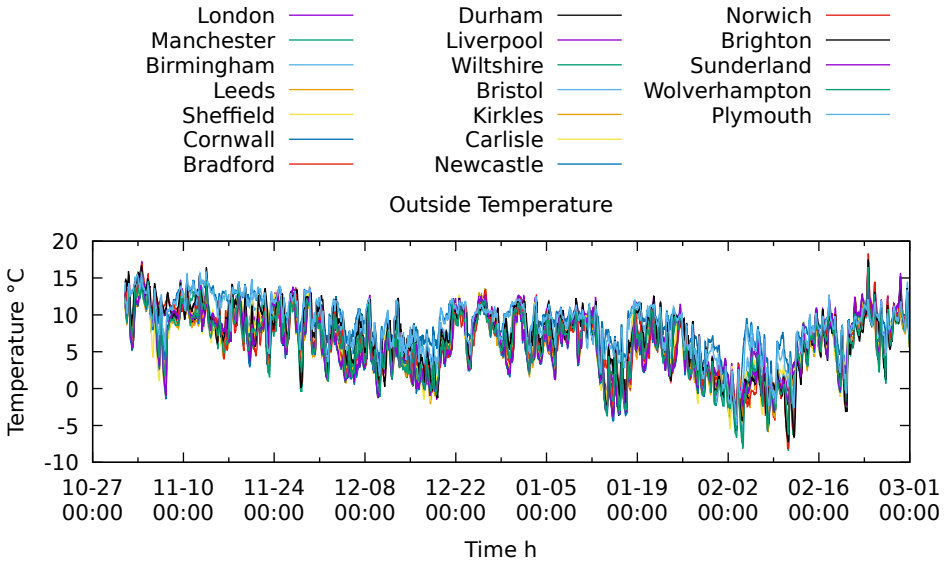

Figure 4.3: Recorded outside temperatures for different regions. We present the outside temperature evolution for the period of 2011-01-21 till 2012-03-01. Information was sourced from [110]

we used the Nelder-mead algorithm [106] from the LMFIT library in Python [111]. For the parameters, we have imposed restrictions on the range of the coefficients to be between 0.01 and 1, with an initialisation value of 0.5. This was to reflect the possible ranges of the building parameters as observed in the literature [77, 102, 26, 90]. The time step chosen for the simulation of the temperature evolution using 4.1 was 10 minutes (i.e. $\Delta t = \frac{1}{6}$). This was used as some of the users stated their temperature on times (heating controls) in 10 minutely periods (e.g. 3:00,3:10,3:20 etc) that would be outside those specified Δt if we were to use the 20 minutely periods (e.g. available only at 3:00 and 3:20) at which the data has been collected. When simulating the internal temperature, we assumed that if the internal temperature goes above the inferred set-point during the heating period as provided by the user in the survey the heating would not operate at the next time step.

Simulation of the internal temperature required knowledge of the outside temperature.

City	Occurrences
Cornwall	63
Norwich	58
Kirkles	33
Wolverhampton	33
London	32
Brighton	29
Birmingham	24
Plymouth	24
Wiltshire	21
Bradford	19
Leeds	19
Bristol	18
Liverpool	16
Durham	16
Sheffield	15
Sunderland	13
Carlisle	10
Manchester	9
Newcastle	8

Table 4.2: Estimated number of occurrences of houses for each each of the 19 cities.

We had to infer the location of the buildings as the information on the location of the building was not reported in the publicly available EFUS dataset. Best-fitting building parameters for each particular house were found for all of the different outside temperatures for different cities, as shown in figure 4.3. We then identified the city in which the sum of the differences between the observed internal building temperatures in the EFUS and the simulated internal temperatures, using (4.1), was minimised. We then assumed that the building was located in this city. Table 4.3.5 provides a summary of the number of houses that were estimated to be in specific cities. We can see that there is a number of houses that are assumed to be based in Cornwall and Norwich although the remaining split is

We present in figure 4.4 an example of the temperature evolution of a building as

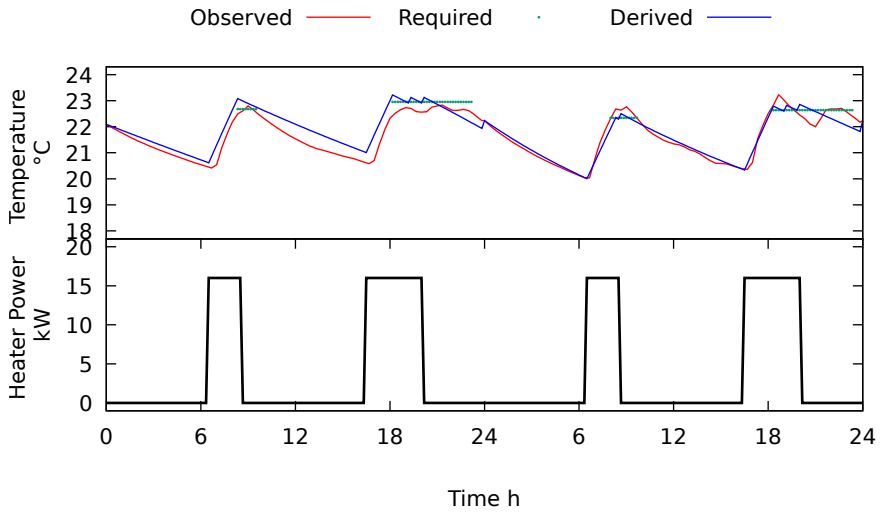

Figure 4.4: In the figure we present the observed temperature as recorded during the EFUS study (red line - top graph), required temperatures as inferred from the observed data (green- top graph) and the derived temperature using the building equations as specified in equation (4.1). The bottom graph black line shows the heater on times at which the user reported their heating system to be heating the house. We estimated the size of the heater to be 16 kW heating is therefore either off (0) kW or on (16) kW.

observed in the EFUS alongside the internal temperatures as inferred using the best-fitting parameters. We assume that even if the heater was reported to be on, but the required temperature set-point (green line) was reached, the in house controller would turn the heater off and wait for the temperature to drop below the set point before the heating is turned back on. This is reflected by the derived temperature line (blue line) going above the set-point and coming back down to the set-point even though the heater is reported to be on (black line bottom graph). As the observed temperature and derived temperature closely match each other, we can confidently say that the thermal parameters estimated for this building are representative of its behaviour. This is house 3, as indexed in the EFUS dataset [78], in the dataset with the first two days of the simulation data. The parameters determined were $a_{11} = 0.02172$ and $a_{12} = 0.09964$, the location of the building was estimated to be Leeds.

4.3.6 Discomfort coefficient estimation

We have then arbitrarily chosen half of the days that had the best-fitting parameters of the buildings as representative days of a particular house. Given this set of thermal parameters, we then attempted to estimate the discomfort coefficient p, as introduced in Section 4.2. We attempted to find the value of p that would achieve the same temperature discomfort in terms of temperature deviations from the desired temperatures as the one observed in the internal temperature data. This is assuming the thermal building model and the usage profile estimated are correct, and the house heater was operated optimally, as described in Section 4.2.2.

For each building, the objective of the value p search algorithm was to find the lowest value of p that achieved the sum of temperature deviations similar to those observed in the recorded internal temperature data. As the p value is the trade-off between the heating cost and the thermal discomfort of the user we had to find an estimate of the cost of heating the building during the time when the internal temperature was recorded.

We used the price of gas in 2012 (temperature data from EFUS study used was for the period 2011-11-01 till 2012-02-01) as $\pi^{gas}(t) = 0.0449$ £/kWh. This value was calculated using domestic energy price statistics [112]. The annual domestic energy bill average (from file QEP 2.3.2 in the [112]) for England and Wales in 2012 for all three payment methods (standard credit, direct debit, prepayment) was £673.33. This average is based on the consumption of 15,000 kWh/year. Therefore we can calculate the average cost of fuel by using

$$\pi^{domestic}(t) = 673.33/15000 = 0.0449. \quad (4.7)$$

A golden search algorithm was used to determine a p £$C^{-1}h^{-1}$ that achieves our objective of minimising the difference between observed and simulated temperature deviations. We restricted our search region to the range of $[0, 10]$ £$C^{-1}h^{-1}$ as we believe majority of heat users would be happy to forego one degree variation from their optimal temperature if they were able to save £10. House heating optimisation, introduced in Section 4.2.2, was used to find the optimal controls. An example of the determined temperature can be seen in figure 4.5. We show that the temperature evolution as derived using the building dynamics from section 4.3.5 and the estimated p value in sample closely matches the real-world, observed behaviour of the house internal temperature. In this scenario, we have not restricted the heating controls to be fully on or off (bang-bang control). We assume that heating could be operating for part of the half-hour. The p value found in this scenario was 0.012 £/°Ch. The observed temperature deviations recorded were 166.14 °Ch, and the derived temperature deviations were 161.23 °Ch. As it would be impossible to match the temperature deviations perfectly, we decided to restrict our p value search to the last value with which the derived temperature deviations (those found with the estimated value of p) are lower than the ones observed from the data. This is the reason why the derived temperature deviations are slightly lower than the observed temperature deviations.

4.3.7 Summary of processed data

From the EFUS dataset of 823 houses, we were able to estimate all the parameters discussed for 461 houses. Using the weightings provided for scaling this data to national level these would in total represent 57.3% of the population of houses in England.

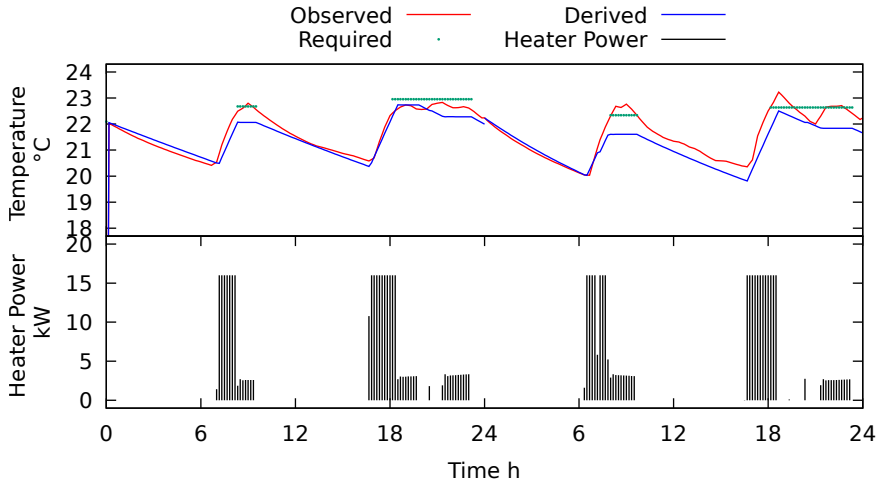

Figure 4.5: In the figure, we present the derived temperature evolution using the building dynamics parameters as found in subsection 4.3.5. In the top graph we present the observed temperature as recorded during the EFUS (red line - top graph), required temperatures as inferred from the observed data (green- top graph) and the derived temperature using the building equations as specified in equation (4.1) and the estimated discomfort value p. The bottom graph shows the heater on times as optimised using the estimated p.

Using the estimated size of the required heaters as discussed in section 4.3.3 and the weights as provided, we estimated a weighted average size of the heater in a house would be 11.56 kW. Assuming a CoP of the HP is 3, and the total number of houses in GB is 30 M there would be a potential for a peak HP demand of 66 GW.

4.4 Real-world control testing

A smart thermostat business (Homely Energy Ltd) has been set up during the project [113] enabling HPs to be integrated with dynamic electricity tariffs, peer-to-peer markets and real-time electricity prices. Through a mobile app, customers of the business can provide their temperature preferences. The system then uses this information in conjunction with weather forecasts and a knowledge of the building dynamics to control customers' heating in the most cost-efficient way, reducing the heating costs to the customer and supporting the integration of renewable power.

Currently, the thermostat is integrated with dynamic tariff provided by Octopus Energy (Agile Tariff) [34]. A further explanation of the tariff is provided in Section 1.2.5. To show the effectiveness of the algorithms developed in providing cost savings to HP users when using DA-RTP tariffs, we have conducted an experiment at Salford University and will discuss the results next, where we used an air source HP. We have shown that at least 20% savings can be made by using DA-RTP tariffs when compared to fixed tariffs.

4.4.1 Power consumption of the HP

The following experiment was carried out at the Smart Meters Lab at Salford University as part of their Energy House 2 engagement with local small and medium-sized enterprises (SMEs). The setup consisted of a Nibe brand air source HP with radiator heat emitters. Only the lounge in the Smart Meters Lab building was heated using the HP. We were allowed to control the operation of the HP for a week and monitor the internal temperature data of the room heated. We were also granted access to the consumption of the electricity as recorded by the smart meter, although the consumption provided also included the power consumption of different appliances (e.g., dishwasher, microwave, kettle) in the kitchen of the building as they were connected to the same smart meter.

As noted previously, the electricity consumption data that we were able to collect, through the smart meter included electricity consumption of other appliances, as discussed previously. We, therefore, needed a way to isolate the power consumption of the HP for us to compare the heating costs between the DA-RTP and the fixed tariff scenarios.

To estimate the isolated HP electricity consumption, we recorded HP pump speed, return flow temperatures and hot water temperature at a minutely granularity, as defined in [65]. We then compared the HP data collected with the minutely electricity consumption data from the smart meter. The data recorded is provided in figure 4.7. From the figure, we can identify that the observed power consumption (purple line - bottom graph) is closely related to the pump speed of the HP. This is particularly true when the HP is not producing hot water (top graph).

Figure 4.6: HP indoor unit at Salford Smart Meters Lab

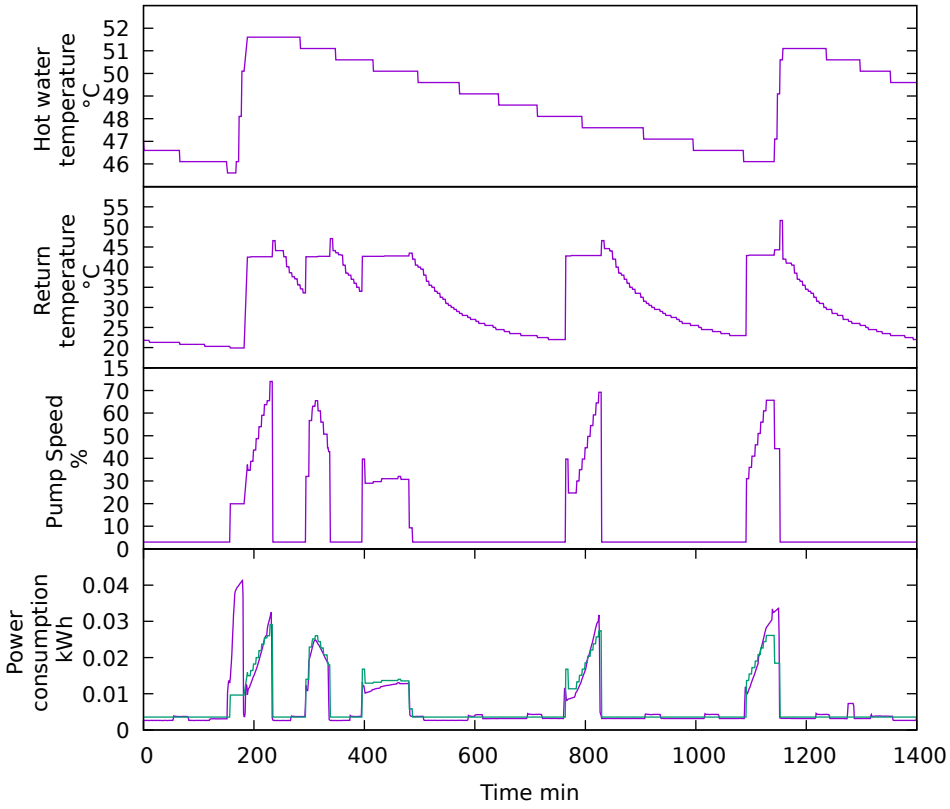

Figure 4.7: A plot of minute by minute temperatures and electricity consumption for the HP over a single day period. Purple lines indicate observed data points recorded by the HP. The green line in the bottom graph shows the predicted power consumption given pump speed.

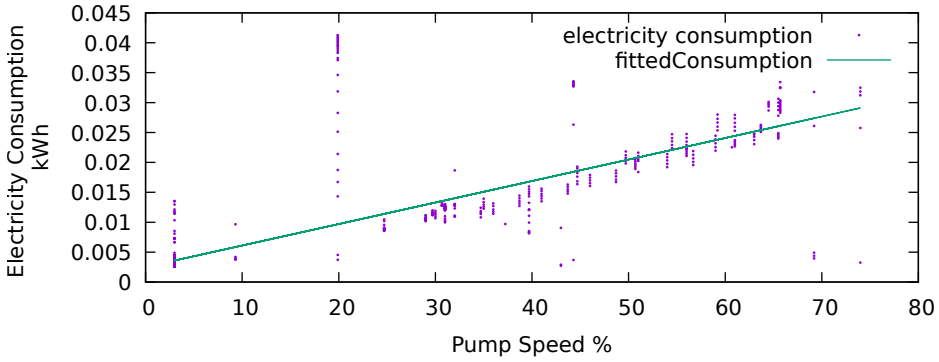

Figure 4.8: Plot of pump speed against the observed electricity consumption and fitted electricity consumption.

To identify a functional relationship between the pump speed and the electricity consumption of the HP, we have plotted the electricity consumption against the pump speed, as shown in figure 4.8. Given that the relationship seemed linear, we have decided to use linear regression to derive a model for expressing the electricity consumption of the HP when only the pump speed is observed. The best-fitting model was identified to be

$$\text{Electricity Consumption} = 0.00206291 + 0.00032819 \times \text{pump speed} \quad \text{kWh} \quad (4.8)$$

From figure 4.8, we can see that the majority of electricity consumption points lie around the fitted line (green line), which supports our hypothesis that the HP electricity consumption can be explained by recording the pump speed of the HP and using a one-to-one functional relationship.

The estimated electricity consumption of the HP using the linear regression estimated is shown by the green line in the bottom graph of figure 4.7. We can see that the estimated power consumption closely relates to the pump speed of the HP. The only significant deviations that appear are during the periods when hot water production

is active. This provides us with confidence that the HP speed can be used to estimate the electricity consumption.

4.4.2 Scenarios

Several HP manufacturers suggest users set a constant internal temperature throughout the day so that the HP heating the building would be able to operate at lower flow temperatures, improving the HP efficiency. We believe this could minimise the cost of operation in a scenario where electricity prices are fixed throughout the day. We do not believe this would be the case in a scenario where dynamic electricity tariff is available. We, therefore, define the base case (original controls) scenario as follows:

- HP adjusts its operation according to the outside temperature (weather compensation).
- Set temperature does not vary 00:00 to 24:00 - 21 °C.
- Fixed price of electricity throughout the day.

For the control when dynamic tariffs are used, we suggest that the HP should not be set to the constant desired temperature throughout the day, but rather the user should specify two periods of preferred temperatures, one for the morning and one for the evening. This is to allow for the heating controller to use the flexibility through the remainder of the day to either overheat or cool the building when the user is not present using the cheaper tariffs. We assume that the desired temperature chosen is the same as the base case scenario (21 °C). The electricity prices received by the user

are as observed from the Agile Octopus rate. We define this as our test scenario, and we refer to it as the Homely Control together with Agile Octopus tariff. A summary of the scenario is as follows:

- HP heats the house during cheaper electricity periods.
- Desired temperatures are set for morning and evening as follows:
  - 06:30 to 08:00 - 21 °C.
  - 18:00 to 22:00 - 21 °C.
  - Assume the user has no temperature preferences outside these times and therefore the temperature can be higher or lower than the set temperature for the two periods of 21 °C.
- Variable price of electricity throughout the day (Octopus Energy Agile).

4.4.3 Outside temperature

The testing was not performed under controlled weather conditions. To show that our results are still applicable, we decided to choose a warmer day for the original control and a much colder day for the Homely controls scenario, as shown in figure 4.9. This is to show that even on a colder day, Homely controls, as defined in the previous section, achieved 20% savings when compared to original controls.

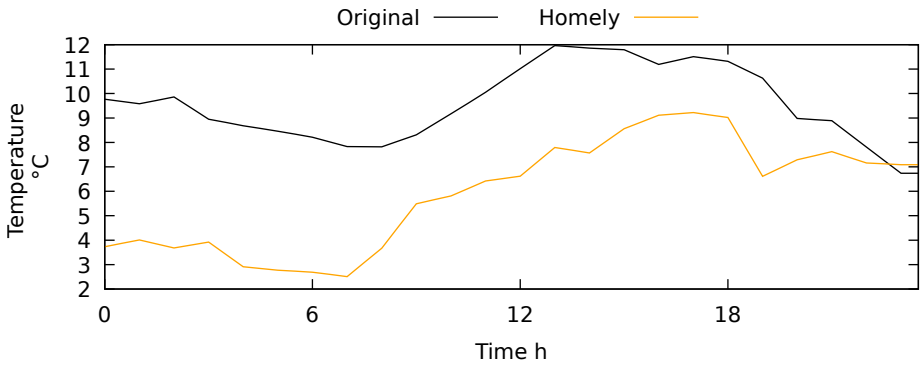

Figure 4.9: We show the outside temperatures of the two scenarios. We can see that the day in which we used original controls was much warmer than the homely controls day.

4.4.4 Original controls

In the original scenario temperature achieved throughout the day (top graph - green line) did not meet the desired temperature (temperature achieved was below the set temperature for the duration of the monitoring). This is due to the wrong placement of the temperature sensor for the HP. This particular HP was using a weather compensation operation mode where the outside temperature measurements determine the flow temperature of the heat pump. As the temperature outside decreases, the flow temperature is increased to meet the changing demand in energy. The temperature sensor was positioned in the sunlight and therefore was reading higher outside temperatures than actually present, leading to internal temperatures that were lower than the set points. As the price of electricity is constant throughout the day, we can observe the HP is operating throughout the day, regardless of the time.

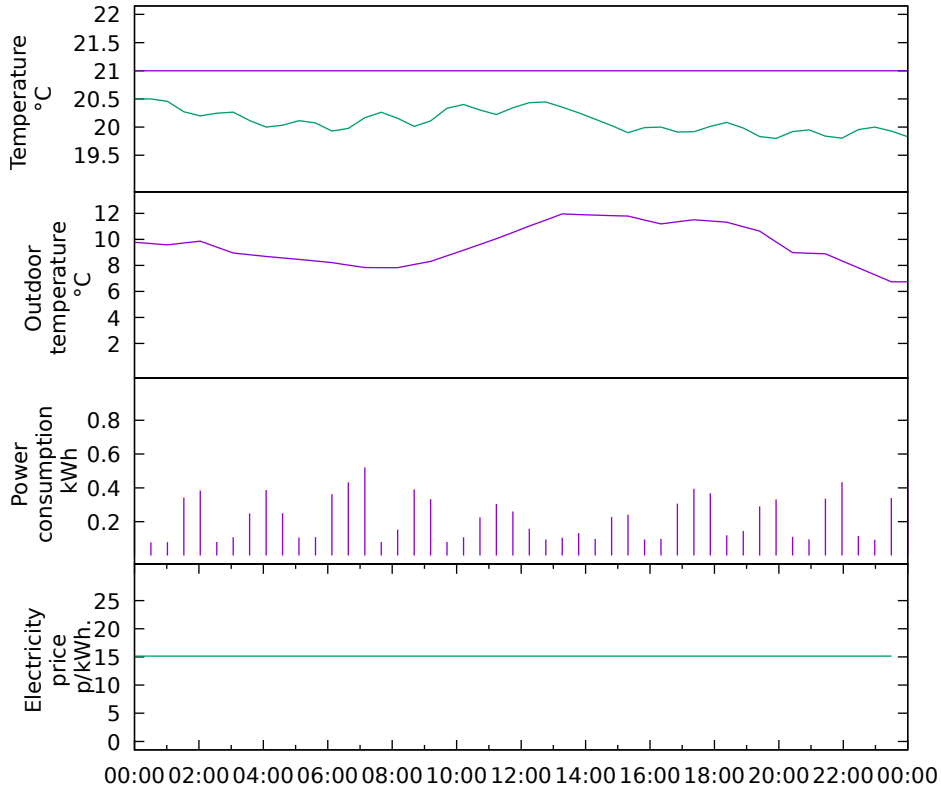

Figure 4.10: This plot presents the operation of the HP when original controls were used. The top graph presents the desired temperature (top graph- black line) achieved temperature throughout the day (top graph - green line). The second graph shows the outside temperature information. The third presents power consumption for the half-hourly periods observed and the bottom graph presents the fixed price of electricity throughout the day.

4.4.5 Homely Controls

In the Homely scenario, prices varied throughout the day, as shown in the bottom graph of the figure 4.11 together with the original constant price of electricity throughout the day. For the majority of the day, the DA-RTP price was lower than the fixed-rate, apart from the period between 16:00-19:00 when the Agile price increased above the fixed rate. In contrast with the original controls scenario, here the user specifies two separate temperature requirement periods, namely morning and evening. Even though the efficiency of operating the HP drops, due to heating to higher temperature throughout the day, the differences in the price of electricity make up for the lost efficiency of performance of the HP.

We can see that the temperature achieved in this scenario closely matched the set temperatures, therefore achieving the higher comfort for the user. With varying prices, we observe the heating system operating during the cheaper times and slightly overheating the building before the price peak, letting the temperature slowly decrease to the set temperature in the evening, avoiding electricity consumption during expensive times. We can see that half-hourly consumption during this period is higher as the day is much colder. This is negatively affecting the CoP of the HP. Even with this drop in the CoP, we still achieve 20 % cost savings by using the Homely system whilst also achieving higher user comfort.

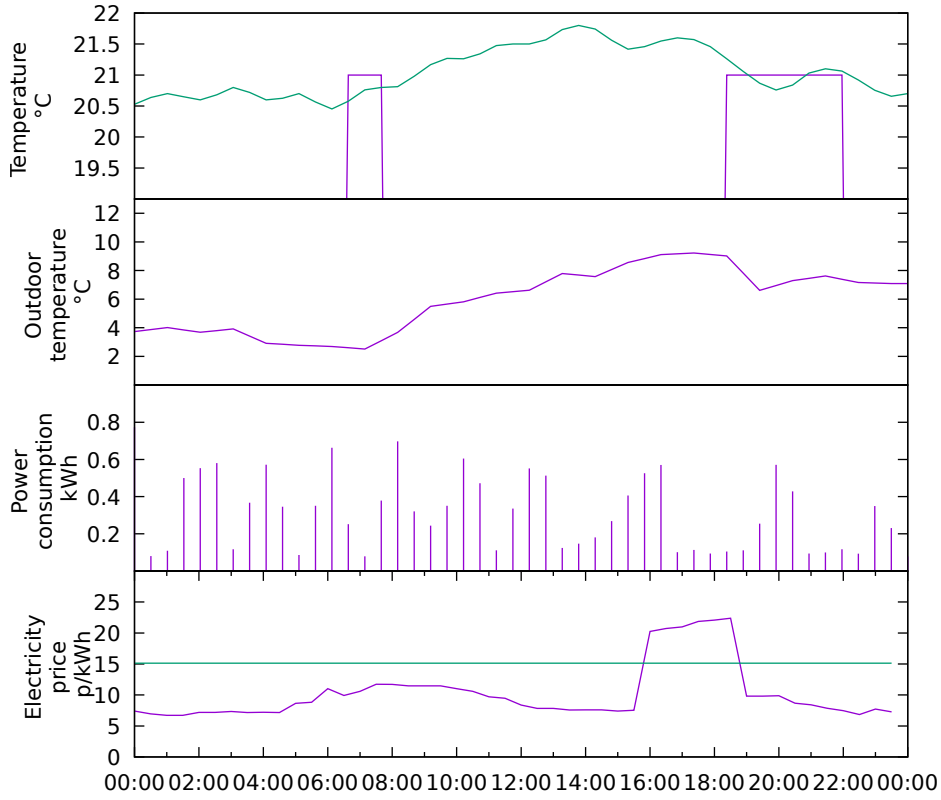

Figure 4.11: This plot shows the behaviour of the HP when Homely controls were used in conjunction with DA-RTP tariffs. Graph labels are the same as for figure 4.10.

4.5 Conclusions

In this chapter, we have introduced the model for the building optimisation that takes into account weather predictions, electricity prices and user preferences. We have introduced the data used to estimate the behaviour of buildings across England and the size of these heaters. We have finished the chapter with real-world experiment results as follows.

The estimated cost of running the HP using the original control scenario, fixed prices, and constant desired temperature was £1.57. The estimated cost of running the HP using a Homely Energy scenario, with the DA-RTP price of electricity and set temperatures only for morning and evening, was £1.26. The difference between the costs achieved was 20%, which is equivalent to £200 on a £1,000 yearly heating bill. These potential savings were achieved while providing higher comfort to the user, since as shown in figure 4.11 the temperature observed was much closer to the two set temperature periods than in the original control scenario as presented in figure 4.10. This provides evidence that using the HPs for heating the houses during the cheaper periods is technically possible and economically desirable as the cost of heating for buildings is decreased using the controls.

Chapter 5

GB Market Simulation

The great interest in HPs is due to their ability to displace high emitting gas boilers. Government's standard assessment procedure (methodology used to assess the energy and environmental performance of dwellings) recorded a reduction in the level of electricity grid emissions for space heating purposes to 0.233 kg CO_2/kWh (from 519 kg CO_2/kWh) compared to 0.210 kgCO_2/kWh for gas [114]. Lower grid emissions mean that even with a modest CoP of HPs of 3.33 [115] and assuming 100% efficiency of a gas boiler, the emissions of a heat pump are 70% lower per kWh of heat than a gas boiler to provide the same level of heating. For an average home with a yearly consumption of 12,000 kWh for space heating [116] this displaces 1,680 kg of CO_2 per year per property as the electricity requirement for HP would be 3,603 kWh.

With the increase in intermittent renewable power generation, the GB market will also see an increased need for flexibility to be provided by electric loads whose consumption can be shifted in the day (flexible users to achieve system balance). In order for HPs

to offer flexibility, users can be incentivised through price signals or take a control signal from a central control party such as an aggregator as defined in Chapter 1. Developments in smart home technologies have increased interest in making DA-RTP electricity prices available to domestic customers in GB. We have already shown in Chapter 4 how HPs can offer this flexibility if they are offered the DA-RTP tariffs already offered in GB by Octopus Energy.

At present, the decisions made by HPs to turn on or off are at a small scale (compared to the size of the whole network) and therefore the actions of HP users do not affect the peak power consumption of the grid, and there is no feedback of their decisions on the wholesale electricity prices. A key question to answer is how this will work once HPs reach 5% or 10% of homes on the grid when a simultaneous decision for all HPs to turn on at the same time could cause a demand spike.

Other researchers have attempted to model the impact of HPs on the GB grid using real-world HP data [117], although they do not attempt to capture the ability to shift consumption through the use of RTP tariffs. Many other studies have considered the impact of time-of-use or direct control of HPs by a central body and the impact of this behaviour on the grid [118], but these studies have not accounted for the feedback loop of user behaviour on electricity prices. Other studies have considered installing energy storage devices on a network scalable to time-shift the output from renewable sources.

To answer if HPs can help (or inadvertently hinder) progress towards a stable grid, we model dynamic interactions between agents (power plants, HPs, energy storage) in the market. In this thesis, we have shown in Chapter 2 how we can simulate the market, in Chapter 3 how to model supply-side agents, and in Chapter 4 how to model

demand-side agents that will adjust their production (or consumption) based on the price of electricity. We can evaluate the market impact of the new technologies by calibrating the model against scenarios predicted by NG defined as follows in 2019 report [3]:

- Community Renewables (CR) - local energy schemes and energy efficiency improvements are prioritised. Under this scenario GB achieves the 2050 decarbonisation target.
- Two Degrees (TD) - the focus is on large-scale solutions and customers are supported to choose renewable heat and transport options to meet the 2050 target. Under this scenario GB achieves the 2050 decarbonisation target.
- Steady Progression (SP) - the speed of low-carbon alternative implementation for heat and transport is assumed to continue at a similar rate to today but is also expected to slow down towards 2050. Under this scenario GB does not achieve the 2050 decarbonisation target.
- Consumer Evolution (CE) - local generation and increased consumer engagement are expected but largely come into effect from the 2040s. Under this scenario GB does not achieve the 2050 decarbonisation target.

More information about the FES energy scenarios can be found on the FES NG website [3].

We aim to test how alternative domestic pricing tariffs will feedback into market prices and the resulting total supply mix in 2030. We compare cases in which domestic users are contracted to fixed price tariffs throughout the day, with cases in which users receive DA-RTP tariffs.

In this chapter we remind about the model parameters for each agent, briefly reintroduce some concepts, and discuss the modelling results of the simulations of the wholesale electricity market in 2030, under DA-RTP and fixed domestic electricity tariffs. We also provide a discussion of the model which future work might enhance.

5.1 An Agent Based model for the GB Electricity Market

ACE is a sub-branch of ABM modelling as introduced in Chapter 1 and is concerned with computational modelling of economic processes (including whole economies) as open-ended systems of interacting agents [35].

In ACE, each agent is specified as a separate entity, which is modelled as an encapsulated software entity [35], with specific initial conditions. In our model, this would be each power plant or energy storage facility on the supply side, and each autonomous electric heater (HP), I&C facility providing DSR and electric storage facilities on the demand side.

In our energy price model, agents in the system make their decisions based upon the external variables arising from the interaction of all system agents. In our case, the external variable is the price of electricity in each half-hour period. This is affected by the interaction of the agents, namely power plants, I&C DSR, electric storage and HPs. Each agent is formulated as a separate optimal control problem and solved using a PDE-based approach.

Our future energy scenario modelling relies on searching for wholesale electricity prices that match the demand and supply in the electricity system in all half-hourly periods. To clarify the role wholesale electricity prices play in the market we have already introduced the various costs included in domestic user electricity bills and the prices that are paid to the generators by the users of electricity in Chapter 1.

In order to calculate the behaviour of domestic users (i.e. HP users) in our simulation, we need to be able to calculate the costs on which they base their decisions in the model. We assume that the HP controller solves a dynamic programming problem, balancing the real-time cost of electricity against the perceived cost of discomfort for the user as discussed in detail in Chapter 4. To estimate the power consumption for space heating across the GB and across many different households we estimated the set temperatures and thermal building characteristics for a sample of homes, details of which are provided in Chapter 4. Next, we briefly go through the cost of electricity for domestic users; further details can also be found in Chapter 4.

In our modelling, we assume that HP controllers pay electricity prices which are either different in each half-hour period (DA-RTP tariffs) or are fixed throughout the day (fixed tariffs). DA-RTP tariffs are a combination of the wholesale electricity price and the cost of delivering the power to the domestic customer. In fact, on average the wholesale electricity price is currently only around 33.5% of a domestic electricity bill [28], details of other costs are provided in Chapter 1.

5.1.1 Energy storage

Energy storage facilities are another flexible energy resource that competes with HPs in providing grid flexibility, helping to smooth the energy consumption throughout the day. We found that by using a simple adaptation of the house heating model (see Section 4.2), we were able to capture the dynamics of batteries connected to the grid. Our simple model can replicate simple strategies that can provide reliable simulations, without claiming to model all of their complexities. Within our modelling framework, energy storage facilities are modelled as agents that can draw power from the grid, store it and discharge it when required. The objective of the energy storage facilities is to maximise their profit given the prices of electricity; therefore, we expect them to charge during periods of low-cost electricity and discharge during expensive periods.

Now to describe our model of energy storage facilities, we assume that they can charge and discharge at its maximum rated capacity (C^{max}). Let the internal energy storage dynamics be given by

$$\frac{dC}{dt} = cC^{max} \tag{5.1}$$

where

- c - represents the control variable of the battery discharging (-1), charging (1), idle (0).
- C^{max} - represents the maximum capacity of the battery at which it can charge and discharge to the grid in MW. We include five types of energy storage facilities as per FES [3], namely: batteries, liquid air, compressed air, pumped hydro and

vehicle to grid. C^{max} represents the sum of the capacity of all of the energy storage facilities in a particular group.

- C - current charge level of the battery in MWh.

To obtain the behaviour of the batteries, we need electricity prices, and we assume that the prices received by all batteries are wholesale. We appreciate that this is not representative of the true market as some of this storage will be based at domestic user properties, and used for consumption. Modelling domestic storage together with domestic use would improve the accuracy of the simulations and this is left for future work. Therefore, model all batteries as if they were grid-connected, trading solely in the wholesale market of electricity.

The objective, as stated previously, of the energy storage facility is to maximise storage facility revenues. The optimisation algorithm finds an optimal control policy $c \in c_t$ that is the charging, discharging or staying idle of the energy storage facility. The optimal derived policy will depend on the current state of charge C and the time of the day t. As we have done previously, in Chapter 3 with the models for power plants and chapter 4, with the models for houses, we can represent this objective as a maximisation of revenues for the energy storage facility V over the time horizon T (hours).

We again include a discount factor ρ to adjust cash flows and account for the time value of money. We denote the revenues of the storage facility as

$$\epsilon c C^{max} \pi^{wholesale} \tag{5.2}$$

and ϵ % represents discharging $(1 - e^{loss})$ and charging $(1 + e^{loss})$ losses where e^{loss} is

a constant to account for battery degradation and the losses incurred when charging or discharging the battery. Prices received by all batteries are the wholesale prices $\pi^{wholesale}$ derived as part of the simulated market-making mechanism.

Therefore the value of the battery V given that the current battery charge level is C at time t can be written as

$$V(C,t) = \max_{c \in c_t} \left[\int_t^T e^{-\rho(s-t)} (\epsilon c C^{max} \pi^{wholesale} £) ds \right]. \tag{5.3}$$

We let c_t be the set of all admissible control policies defined as follows

$$c_t = \{c = \{c(s)\}_{t \leq s \leq T} : \forall_{t \leq s \leq T} \quad \{0, -1, 1\}\}.$$

Derivation of Hamilton-Jacobi-Bellman (HJB) equation is a straightforward extension of that in Chapter 4, and we can use Semi-Lagrangian numerical schemes, as introduced in [64] and discussed in Chapter 3, to solve the optimal control problem.

5.1.2 Industrial, Commercial and other DSR and wind curtailment

We assume that NG has agreements in place with large energy consumers (I&C DSR and aggregators) to provide demand turn-down (reduce the energy consumption) and demand turn up (increase energy consumption) to help manage the power delivery

to grid users. There are a number of DSR services that NG procures from these customers, but they all incentivise the change in customer behaviour in exchange for monetary incentives.

Demand turn down is the amount by which large energy users or aggregators of loads will reduce their energy consumption during high demand periods when the power supply of the system is insufficient to meet the needs of the energy users. Demand turn up is the opposite of the demand turn down and is defined as the incentive to large energy users or aggregators to increase the energy consumption during periods of high renewable power generation.

There is a lot of uncertainty around DSR markets in GB as these markets are currently developing. We believe that due to this, we would not be able to find an accurate representation of current or potential future functional demand price relationship of these services. For simplicity, we have assumed a logit function for this relationship.

We assume that DSR agents start reducing their loads as the price of wholesale electricity rises above 33 £/MWh. The 33 £/MWh was chosen as it was the average price of wholesale electricity in 2019. We assume that market participants can see anything greater than this average as expensive and anything below this price can mean that agents in the market would like to take advantage of the below-average prices of electricity.

Now let d^{dsr} be the absolute amount of power that is reduced/increased given the

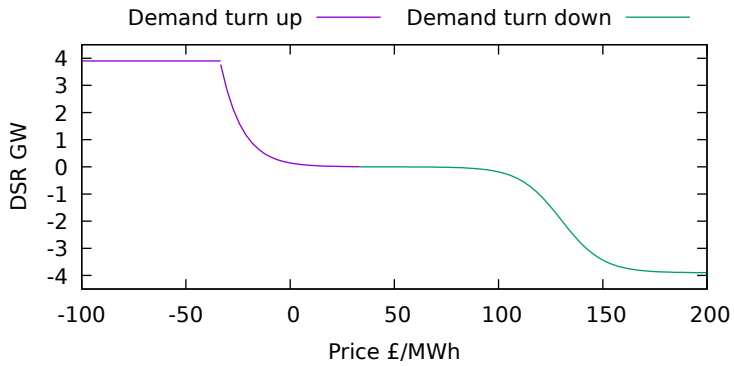

Figure 5.1: DSR function $d^{dsr}(\pi)$

current wholesale price $\pi^{\text{wholesale}}$, such that:

$$d^{dsr}(\pi^{wholesale}) \tag{5.4}$$
$$= \begin{cases} \frac{1}{1+e^{\pi^{wholesale}/a^{up}+b^{up}}} D^{dsr} & \text{if } \pi^{wholesale} > 33 \\ min\left(\frac{1}{1+e^{\pi^{wholesale}/a^{down}+b^{down}}}(D^{dsr}+S^{wind}), D^{dsr}\right) & \text{if } \pi^{wholesale} \leq 33 \end{cases}$$

where D^{dsr} is chosen to scale the I & C DSR across different scenarios and represents the maximum capacity of DSR in the specific scenario, $a^{up} = 10$, $b^{up} = 13$,$a^{down} = 10$, $b^{down} = 13$. D^{dsr} is the sum of I & C DSR and residential DSR. We assume that this domestic DSR that is included in D^{dsr} does not include HPs and is sourced through domestic load aggregators from other loads. S^{wind} represents total capacity of wind power production in a particular FES scenario. We have chosen parameters a^{up}, b^{up}, a^{down}, b^{down} so as to represent our expectation of DSR agents as explained next.

As an example we provide a graphical representation of this functional relationship in figure 5.1 for TD FES scenario where $d^{dsr} = 3900$.

The logit function has been used for the functional relationship as we expect low

DSR availability for very low prices of electricity (sub 100 £/MWh). We expect DSR availability to increase rapidly between 100 £/MWh and 150 £/MWh (3 times the average peak price of electricity) as factories decide to slow down their production processes to save on energy costs. We also expect there to be a limit to the amount of DSR that could be made available and at prices above 150 £/MWh we assume a limited effect on the availability of the additional DSR as most available agents would have already committed their DSR availability.

We have also assumed that the price of electricity can drop significantly or even go negative during periods of high renewable energy output and low demand. As wind farm revenues include other sources of income (such as Renewable Obligation Certificate (ROC)s) in some circumstances it makes sense for wind farms to operate even at negative prices as long as the payment to be made through negative electricity prices is less than the income derived through the alternative incentives.

In figure 5.1, we show that market participants would start reacting to prices as the price of electricity drops below 33 £/MWh (below the average price of electricity). The effect on demand will start increasing when the price of electricity goes below 0 £/MWh increasing rapidly as the price approaches -50 £/MWh (the current buy-out price for a ROC is £50.5.

Around the price of the ROCs we assume wind farm to start reducing their output and we formulate wind curtailment as follows

$$s^{curtailed} = max(min(\frac{1}{1+e^{\pi^{wholesale}/10+6}} * (D^{dsr} + S^{wind}), s^{wind}(t) - D^{dsr}, 0) \quad (5.5)$$

where $s^{wind}(t)$ is the available wind at time t.

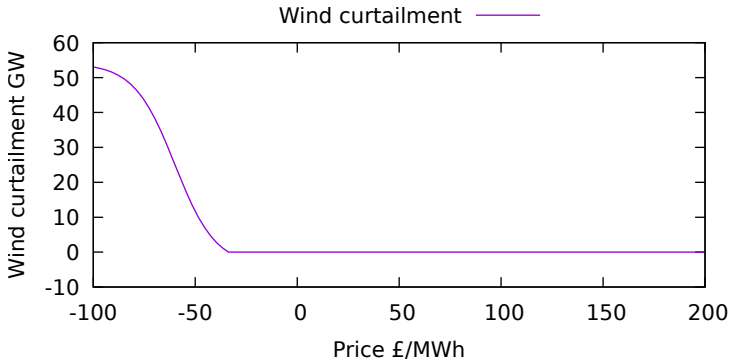

Figure 5.2: Wind curtailment $s^{curtailed}$ for TD scenario

In figure 5.2 we can see how wind curtailment rapidly increases to the amount of wind available $s^{wind}(t)$ at time t as prices drop below the levels of ROC.

As the multiplier D^{dsr} has a significant effect on the availability of DSR at all output levels we also provide sensitivity analysis further in this chapter's results section, where we have compared the results of market simulation as calculated using the $D^{dsr} = 14000$ (chosen to make sure there is sufficient DSR availability in all scenarios to clear the market) for all FES scenario simulations.

This concludes the overview of the parameters and agents used in our simulations. Next, we will continue with the overview of the model calibration to the real-world data followed by the results.

5.2 Model Calibration

In this section, we describe how we calibrate the model for each agent in our GB energy market simulation, using real-world input data. We use a period of 30 days in January

2019, from the 1st until the 30th as the input data for our simulations. This period has been chosen as it should provide a good representation of winter outdoor temperatures and the load levels in terms of electricity demand during these cold winter months. It also includes a public holiday that can provide some interesting behaviour in domestic and industrial energy consumption that should be catered for when planning energy networks.

5.2.1 Domestic electricity prices

In fixed tariff pricing, we assume that the price of domestic electricity $\pi^{domestic}$ is a pre-agreed fixed tariff, which charges the same amount for a unit of electricity at every time period during the 30 days of our simulation. Given that domestic suppliers will need to recover the cost of electricity supplied over the 30-day simulation (this would normally be a whole year but we are only simulating behaviour over the 30 day period), the tariff for all periods π^{fixed} is therefore calculated as the weighted average electricity price as received by domestic customers $\pi^{domestic}$ for the user's demand of HPs.

$$\pi^{fixed} = \frac{\sum_{t=0}^{t=T} \pi_t^{domestic} d_t^{hp}}{\sum_{t=0}^{t=T} d_t^{hp}} \quad \forall t. \tag{5.6}$$

where π^{domestic} includes all of the costs born by the supplier including wholesale price of electricity $\pi^{wholesale}$, network costs, operating costs etc, and d_t^{hp} is the total of all HP demands on the grid at period t.

We only use HP demand for the calculation of the fixed tariff. We assume that if there were an electricity supplier that is willing to offer the fixed price of electricity to

the domestic user but is exposed to all the other costs introduced, then the electricity supplier would need to estimate the predicted consumption of the portfolio of HPs and other electricity demand of the household and determine the fixed price of electricity on these demands. As we do not know what the consumption of power is for the other equipment in the house, we assume in our simulations that only the fleet of HPs is used across all of the houses to determine the fixed tariff offered.

We assume that HP controllers can also receive DA-RTP tariffs which consist of electricity prices that are varying for future half-hourly periods. HP users can receive these prices either through an aggregator, electricity supplier or by participating in the market. In all cases, the DA-RTP tariff will be communicated to the HP user. This means HP controllers will receive a set of prices as follows.

$$\pi^{domestic} = \{\pi^{domestic}(t)\}_{0 \leq t \leq T} : \pi(t) \in \mathbb{R} \quad \forall t, \tag{5.7}$$

Distribution Use of System charges

As we know from figure 1.1 network charges comprise a large part of the electricity tariff for domestic users, and they include DUoS and TNUoS charges. In our simulations we chose to explicitly model DUoS charges ($\pi^{distribution}(t)$) as a function of average national demand ($\bar{D}(t)$). The true calculation methodology for DUoS charges can be found in [119]. As there is no set function to relate the average national demand and the DUoS charges, we have evaluated a number of possible functions to replicate the current DUoS prices. In figure 5.3 we present the averaged DUoS half-hourly prices across all regions plotted against average half-hourly GB demand for the year 2019. For DUoS forecasting, in our models we have evaluated piece-wise linear, exponential

and squared exponential relationships between DUoS charges and national demand. We have used least squares methods to find the line of best fit to replicate the average demand/DUoS price relationship. Lines of best fit are presented in figure 5.3 and discussed next.

First we have evaluated a piece-wise linear relationship. We decided that a simple linear relationship would not be appropriate as the DUoS charges currently are much higher during the 16:00-19:00 period than the rest of the day as discussed in Chapter 1. We have therefore chosen to evaluate a separate functional relationships for low and high average demand periods

$$\pi^{distribution}(\bar{D}(t)) = \begin{cases} -406.315 + -22.1697\bar{D}(t) & \text{for } \bar{D}(t) > 39,358 \\ -22.1697 + 0.000886848\bar{D}(t) & \text{for } \bar{D}(t) \leq 39,358 \end{cases} \quad (5.8)$$

where $\bar{D}(t)$ is the average national demand for time half-hour t.

When using the piece-wise linear function we observed that due to the discontinuity at the switching point ($\bar{D}(t) = 39,358$) the piece-wise function was forecasting very high changes in DUoS charges. This meant that even small changes in average demand for specific time period t between iterations were causing very large changes in the domestic prices $\pi^{domestic}$, therefore leading to instability of the market price search method as the majority of market HPs were then reacting to this big price jump and trying to change their behaviour to shift to lower-cost periods as a group.

We next evaluated an exponential function so as to avoid discontinuities and to account for small DUoS charges at low average demand levels increasing rapidly once the

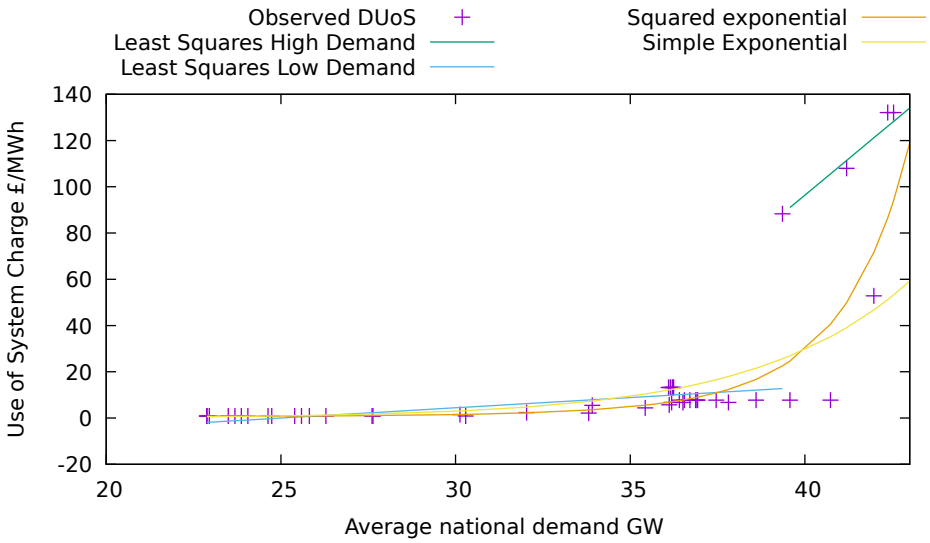

Figure 5.3: Exponential DUoS charge fit compared to observed average DUoS charges across GB for different DUoS regions

average demand reaches higher demand levels.

$$\pi^{distribution}(\bar{D}(t)) = 0.003e^{0.23\bar{D}(t)}. \tag{5.9}$$

We however observed that even the exponential curve was not able to account for the rapid increase in the DUoS charges as seen in figure 5.3. We can see how the line of best fit matches the low DUoS charges well but significantly underestimates the DUoS charges during high demand periods.

We then chose to use a squared exponential function to replicate the relationship between the average demand and DUoS charge. We first attempted to use the least squares fitting using the absolute average observed national demand $\bar{D}(t)$ and the observed DUoS charges $\pi(t)^{distribution}$. Squared exponential function performed best out of all the functions evaluated in terms of matching the DUoS charging behaviour.

Even though in sample fit seemed to perform the best, we faced challenges when considering the behaviour of the DUoS charge estimation in the future when average demand of electricity is going to be higher. Once we started using this function with increased future average demand the squared exponential function was predicting values that were outside of what we thought was realistic. The inability to predict DUoS charges at higher average demand levels was therefore unacceptable as we are modelling the electricity consumption in 2030 scenarios where additional loads could add an additional 10 GW on the average electricity consumption during peak periods. To address this issue we have decided to use the shape of the DUoS charging function as estimated using the least squares methods and apply it to the relative average national demand $\widetilde{D}(t)$ as follows

$$\pi(t)^{distribution}(\widetilde{D}(t)) = ae^{b(\widetilde{D}(t)+c)(\widetilde{D}(t)+c)} \tag{5.10}$$

where $\widetilde{D}(t) = \frac{\bar{D}(t)}{\bar{D}(t)^{max}}$ is the relative demand, $\bar{D}(t)^{max}$ is the maximum average demand observed during the period of estimation and $a = 0.855, b = 23.639, c = -0.541$ are the parameters that were estimated to best match the relative current national demand to the currently observed DUoS charges as shown in figure 5.3. The standard deviation of the fit observed was $\sigma = 16.824$.

From figure 5.3 we can observe that the squared exponential curve accounts for the very low DUoS charges at low demand levels (20-35 GW), it does underestimate the DUoS charges at higher demand levels (35-40 GW) but also rapidly approaches the DUoS charge levels at the peak average national demand of 43 GW, with the estimated DUoS charge of 100 £/MWh compared to 138 £/MWh observed.

Figure 5.4 presents the legacy DUoS prices and charges as calculated using the methods

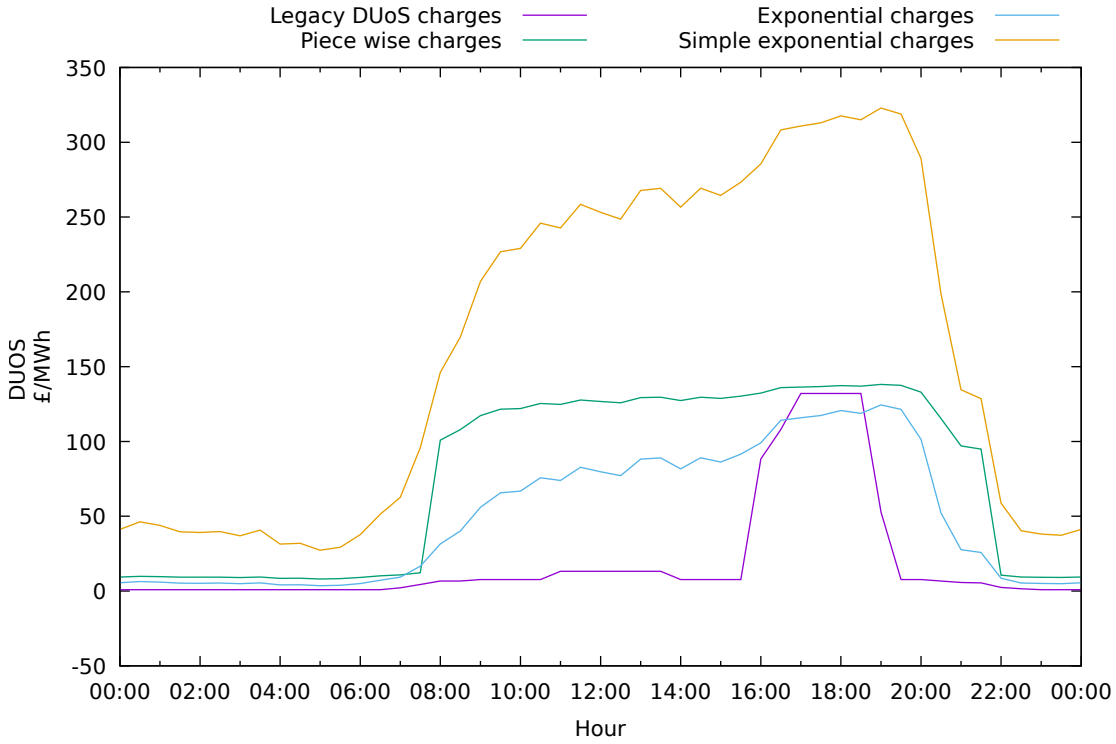

Figure 5.4: Comparison of the predicted DUoS charges using different DUoS charging structures in simulated CR scenario under the DA-RTP tariff

of estimation discussed previously for CR scenario using the DA-RTP tariff. We can see that DUoS charge calculated using the relative average demand is much closer to the legacy costs. Charges are slightly higher during the off-peak period as off-peak electricity consumption increases due to flexible resources being able to shift their consumption to cheaper periods.

Other Charges

In our simulations, other charges attributed to domestic electricity users are calculated by assuming they are proportional to the combined charge for wholesale electricity

$\pi(t)^{wholesale}$ and DUoS $\pi(t)^{distribution}$. We take a constant for the proportion of domestic electricity cost attributed to wholesale and DUoS, which was estimated to be 61.6% by [79] in August 2018. The price received by the customers $\pi(t)^{domestic}$ was therefore calculated as follows

$$\pi(t)^{domestic} = (\pi(t)^{wholesale} + \pi(t)^{distribution})/0.616 \tag{5.11}$$

5.2.2 Power demand

In our simulations, we attempt to match the total system supply $s(t)$ and total system demand in each half-hourly period. In this section, we will review the components of the system demand $d(t)$ followed by a review of the system supply components $s(t)$ in the next section.

The total system demand in our simulations can be represented as the following sum

$$D(\pi, t) = d^{baseload}(t) + d^{hp}(\pi, t) + d^{ev}(t) + d^{b\_charge}(\pi, t) + d^{dsr}(\pi, t) + d^{interconnector} \tag{5.12}$$

where all are in MW at time t:

- $d(\pi, t)$ -total national demand.
- $d^{baseload}(t)$ - base load demand.
- $d^{interconnector}(t)$ - interconnector flows.

- $d^{hp}(\pi, t)$ - aggregate HP demand.
- $d^{ev}(t)$ - aggregate EV load.
- $d^{b\_charge}(\pi, t)$ - aggregate of all grid batteries when charging.
- $d^{dsr}(\pi, t)$ - DSR turn up.

A brief overview of how these components are calibrated for the modelling is provided next.

Baseload demand

Rather than explicitly modelling the $d^{baseload}(t)$ (demand without HPs) we chose to use the actual demand in GB as recorded during the period 2019-01-01 to 2020-01-30 for the total system demand as currently the number of HPs installed in houses across GB is low, under 150,000 (the total number of dwellings in GB was around 27.2M in 2017)[120]. Suppose we were to assume that each HP has a maximum power draw of 3 kW. All of these HPs combined could only contribute around 0.3 GW of electricity demand. This is in comparison to the peak of the 2019 average GB demand of around 43 GW.

In figure 5.5 we plot the baseload electricity consumption for each individual week in January 2019. We observe two daily demand peaks as expected. The morning peak occurs just before households leave for work, and the evening peak occurs when people get back from work and turn on electric appliances. The two peaks are less distinct during weekends.

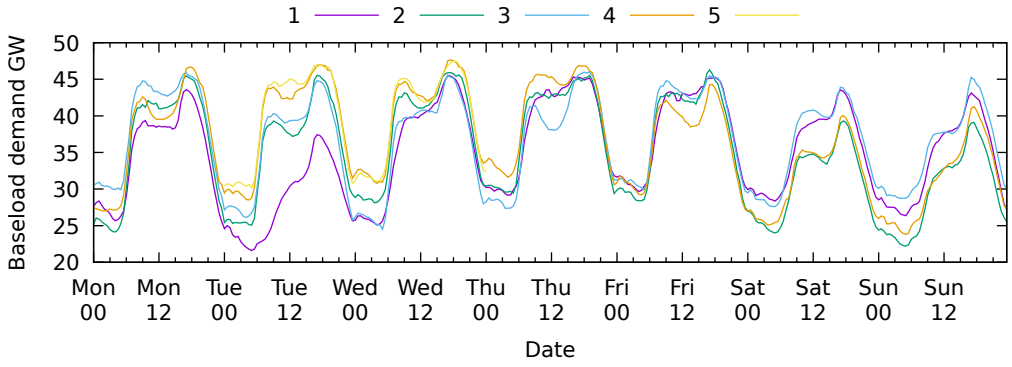

Figure 5.5: Weekly baseload demand for January 2019

Electric vehicles

To estimate the aggregate demand of EV's on the system $d^{ev}(t)$ we have used the residential charging point profiles from the FES report [3]. Total power consumption is presented in figure 5.6 across all FES scenarios. To calculate these profiles, we have multiplied the forecasts of the EV uptake in different scenarios as shown in table 5.1 by the profile data provided in the FES report.

From figure 5.6, we can see that there is a large difference in the potential load on the grid between the scenarios under which GB achieves its carbon reduction targets (CR and TD) and those where the developments in the uptake of renewable technologies are lower (SP and CE scenarios). In figure 5.6, we observe the maximum peak load of EVs is achieved under the TD scenario, where during the peak time of electricity use, the demand reaches 6 GW. Two daily charging peaks are present; first in the morning where users plug in as they arrive at work around 07:00 till 09:00 and the second peak is when users arrive back home after the day of work around 18:00 - 21:00. This is also a period where the current electricity peak demand appears. This means that there will need to either be other flexible loads that are taken offline during these periods

	CR	TD	SP	CE	Model input
% HPs	15.786	12.308	1.22	1.742	Agent
Number of EVs	11412630	13971462	2228617	1705360	Scaled
Maximum I&C DSR (GW)	4.5	3.5	1.4	1.2	Parameter
Maximum Residential DSR (GW)	0.8	0.4	0.3	0.8	Parameter

Table 5.1: Model input comparison across different scenarios

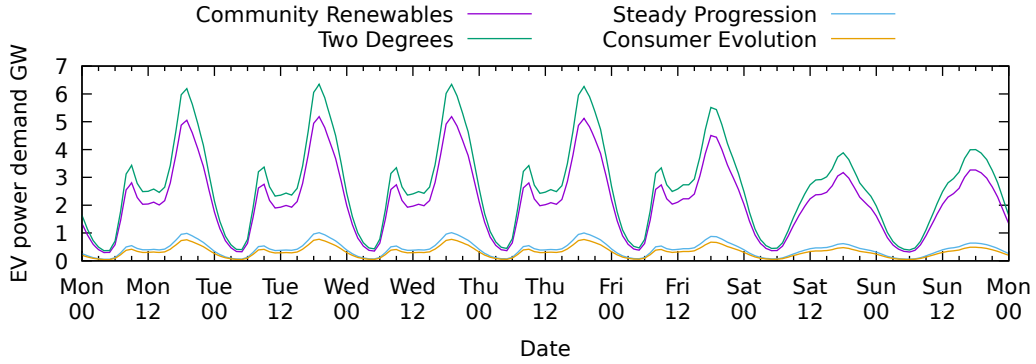

Figure 5.6: Electric Vehicle load on the grid for different periods of the week using the FES data [3]

to support EV uptake or EV charging will need to be shifted to off-peak periods. We do not attempt to model EV as consumers with DA-RTP in this thesis.

Heat Pumps

HPs are modelled as the primary active participants in the market in our framework. We evaluate HP effect on the electricity grid under the four scenarios as defined in the FES document [3]. The percentage of houses with an HP out of the whole population we set for each of the scenarios is presented in table 5.1 as per FES scenarios [3]. These numbers include Air Source HPs (ASHP), Ground Source HPs (GSHP) and hybrid HPs.

For the modelling of the internal temperature dynamics, we used the observed outside temperatures for 25 regions in England and allocated these to the respective houses in those regions for the period 2019-01-01 to 2019-01-30.

5.2.3 Power Supply

Our market simulation aim was to evaluate the benefit of flexible loads across different FES scenarios. To account for the changes in power supply in 2030 from the observed data in January 2019, we have made simple assumptions where possible (scaling the historical power production data) and have only used optimisation models for the power supply agents if we believed the agents are highly sensitive to price.

The total system supply of power in our simulations can be represented as the following sum

$$\begin{aligned} W(t) = {} & s^{ccgt}(\pi,t) + s^{ocgt}(\pi,t) + s^{wind}(t) + s^{solar}(t) + s^{biomass}(t) + s^{interconnector}(t) \\ & + s^{hydro}(t) + s^{b\_discharge}(\pi,t) + s^{other}(t) - s^{curtailment}(\pi,t), \end{aligned} \tag{5.13}$$

where all are in MW at time t :

- $W(t)$ -total national supply.
- $s^{ccgt}(\pi,t)$ - CCGT power plant supply .
- $s^{ocgt}(\pi,t)$ - OCGT power plant supply.
- $s^{wind}(t)$ - wind power supply.

	CR	TD	SP	CE	Model input
Interconnector	3.43	4.17	2.43	3.01	Scaling
Biomass	1.32	1.16	0.81	1.06	Scaling
Hydro	1.12	1.02	1.03	1.01	Scaling
Nuclear	0.49	0.49	0.41	0.86	Scaling
Wind	2.3	2.34	1.69	1.89	Scaling
Solar	2.269	1.76	1.46	1.2	Scaling
Other	10.16	11.53	9.86	8.62	Scaling
OCGT (GW)	10.27	4.7	5.47	11.78	Agent
CCGT (GW)	8.6	21.05	30.6	25.02	Agent
Other utilization factor (%)	0.7	0.7	0.7	0.7	Parameter

Table 5.2: Future Energy Scenarios energy production under different scenarios in 2030

- $s^{solar}(t)$ - solar power supply.
- $s^{biomass}(t)$ - biomass power plant supply.
- $s^{interconnector}(t)$ - interconnector power supply when importing.
- $s^{hydro}(t)$ - hydro power plant supply.
- $s^{b\_discharge}(\pi, t)$ - battery discharging into the grid.
- $s^{other}(t)$ - power supply from other sources.
- $s^{curtailment}(\pi, t)$ - wind curtailment due to negative prices.

and the treatment within the modelling of these supply agents is presented in table 5.2

We assume that only gas power plants can be controlled, i.e. scheduled to turn up and down when required. Historically, the majority of electricity production came from

CCGT power plants with OCGT power plants turning on only to meet the peak power consumption. We have chosen to combine gas reciprocating engines, OCGT and gas onsite generation into this category. We expect all of these plants to be less efficient than CCGT plants, but be much more responsive to electricity prices.

To simulate the behaviour of OCGT power plant agents, we chose to create random sets of agents using the following distributions (details of the parameters are defined in chapter 3):

- MEL - ξ where $\xi \sim U(5, 20)$
- SEL - $MEL - 1$ MW. This is to ensure that the power plants are operating at maximum capacity.
- NDZ - 4 minutes. We used the average NDZ time for OCGT power plants as observed from September to December 2019.
- RUER (1,2,3) - $MEL/2$. Having a ramp rate of half the full capacity allows the power plant to fully warm up within two minutes (observed average for the period September - December 2019)
- RUEE (2,3) - MEL. This means that the same ramp rate applies throughout the whole range of power production.
- RDER(1,2,3) - MEL. This means that the power plant can turn off immediately upon request.
- RDEE(2,3) - 0, meaning that one ramp rate applies throughout the whole range of power production.
- ψ^{fcOM} - fixed costs operation and maintenance 2,860 .

- γ - 0.413185
- η^{max} - ξ where $\xi \sim U(0.37, 0.42)$
- ψ^{fc} - 0

to meet the OCGT power production capacity as per table 5.2.

5.2.4 Energy storage

The composition of energy storage technologies across different scenarios is presented in table 5.3.

All electricity storage is assumed to have 10% losses on the energy coming into the battery and being discharged. Therefore the round trip efficiency is assumed around 81%. We appreciate that under some scenarios these loses might be lower, but we have chosen to risk the over-estimating the cost of storage rather than under-estimating to account for potential energy storage degradation from multiple charging cycles.

5.3 Results

In this section, we first provide a qualitative overview of the results and present figures of the predicted behaviour of the agents on the grid in 2030 under different FES scenarios and for both fixed and DA-RTP tariffs. We then follow on with the quantitative analysis of specific aspects of the simulation, including simulated wholesale

	CR	TD	SP	CE	Model input
Battery Storage (MW)	9300	6150	5030	4170	Agent
Liquid Air Storage (MW)	5	5	5	5	Agent
Compressed Air Storage (MW)	40	40	0.1	40	Agent
Pumped Hydro Storage (MW)	2954	5054	2744	2744	Agent
Vehicle to Grid Storage (MW)	642.7	519.6	89.8	112.2	Agent
Battery Storage (GWh)	16.8	10.5	8.24	8.11	Parameter
Battery Decentralised (GW)	7.04	3.83	2.82	3.18	Parameter
Battery Transmission (GW)	2.26	2.31	2.21	0.9	Parameter
Battery Efficiency (%)	0.1	0.1	0.1	0.1	Parameter
Liquid air Storage (GWh)	0.04	0.04	0.04	0.04	Parameter
Liquid Air Decentralised (MW)	5	5	5	5	Parameter
Liquid Air Transmission (MW)	0	0	0	0	Parameter
Liquid Air Efficiency (%)	0.1	0.1	0.1	0.1	Parameter
Compressed Air Storage (GWh)	0.32	4.3	0.1	0.32	Parameter
Compressed Air Decentralised (MW)	40	40	0.1	40	Parameter
Compressed Air Transmission (MW)	0	0	0	0	Parameter
Compressed Air Efficiency (MW)	0.1	0.1	0.1	0.1	Parameter
Pumped Hydro Storage (GWh)	32.2	88.8	29.59	29.59	Parameter
Pumped Hydro Decentralised (MW)	0	0	0	0	Parameter
Pumped Hydro Transmission (MW)	2954	5054	2744	2744	Parameter
Pumped Hydro Efficiency (%)	0.1	0.1	0.1	0.1	Parameter
Vehicle to Grid Storage (GWh)	0.6427	0.5196	0.0898	0.1122	Parameter
Vehicle to Grid Decentralised (MW)	642.7	519.6	89.8	112.2	Parameter
Vehicle to Grid Transmission (MW)	0	0	0	0	Parameter
Vehicle to Grid Efficiency (%)	0.1	0.1	0.1	0.1	Parameter

Table 5.3: Energy storage model inputs as per FES for 2030

and domestic electricity cost, peak grid demand, the power consumption of different agents and grid carbon emissions. We also present the impact on the grid of better insulated buildings, battery behaviour as well as providing sensitivity analysis for the I&C DSR function.

5.3.1 DA-RTP tariff

We begin our results section by presenting the predicted behaviour of all simulated and scaled agents under DA-RTP domestic electricity tariffs, as presented in figure 5.7. We can see the predicted wholesale electricity prices varying significantly between FES scenarios (a). In lower renewable energy production scenarios prices vary between -50 £/MWh and 80 £/MWh, whereas higher renewable power scenarios have periods where prices reach 350 £/MWh. We can also observe that even though overall demand (k) is higher under the TD scenario (green line) when compared to CR (purple line), the prices of CR are higher (a). This corresponds to the higher availability of storage (g) under the TD scenario and more efficient power plant operation (e and f) during the periods of low renewable power production periods such as those between the 2nd and 7th of January, 2019.

We know that renewable generation will play an essential role in decarbonising the grid in the future. In our energy predictions, we do not explicitly model the wind power generation in 2030 but rather scale the power generation observed historically during the corresponding dates in January 2019 using scaling factors presented in table 5.2.

Those scenarios with a large capacity of renewable energy (CR and TD) tend to rely on energy storage and higher renewable power utilisation to provide energy for the grid.

In figure 5.7 we can observe periods of very high estimated wind power production from the 7th till the 9th of January, between 12th and 14th of January and 25th and 28th of January, reaching a predicted value of nearly 30 GW of power production from wind alone. These high renewable power production periods drive the wholesale prices to the very low/negative levels causing thermal power plants to turn off and wind farms to curtail their power production driving the wholesale and domestic prices lower and causing batteries to charge (g). The use of electricity storage is useful for shifting the energy consumption within short periods as observed by the presence of reasonably smooth electricity prices under the TD, SP and CE scenarios for the majority of the simulation periods (a). The issue arises when we have a period of low wind power generation (b) and insufficient power supply from controllable power plants such as CCGT (e). We see prolonged low wind power production periods that cause prices to spike in the CR scenario that relies heavily on renewable energy power production. The results here are of particular importance as we can see that during this period, energy storage facilities are quickly depleted, and the grid is left to call on I&C DSR (i) to turn off industrial equipment to keep the grid in balance. Some of these periods (specifically 01/11 till 01/13 and 01/23 till 01/25) also correspond to low/negative interconnector flow periods driving the wholesale electricity prices even higher. Energy storage facilities attempt to smooth the demand throughout the period of the simulation, even under the CR scenario (g), but the battery capacity is insufficient for the supply of power during the prolonged periods of low renewable power generation. Using the storage capacity in table 5.3 as discussed in [3], we can see that under the CR scenario, energy storage would have a capacity of 50 GWh and a maximum discharge rate of 12.94GW. This would mean that at full capacity, the fully charged pumped storage facility could provide 12.94GW of power for a maximum of 3.86 hours, this should be compared to the period of low wind power production that lasted for five days from the 2nd of January until the 7th of January. Given that the

period of low energy production from wind is much longer than the available storage capacity, GB grid would have had to import a significant amount of power through the interconnectors. As this power might not be available elsewhere, GB could run out of power in this scenario.

Solar power production is another renewable energy resource that will provide an increasing share of power in the future, although as seen from figure 5.7 (d) the power production from solar is limited throughout the winter with the maximum possible solar output of 6 hours throughout the day due to shorter and cloudier days. The power produced can be seen, varying from 1 GW peak to 10 GW. Solar power reliance in the GB should therefore be considered in combination with storage, although seasonal energy storage remains prohibitively expensive and therefore unlikely to be feasible at this point.

As the average electricity demands are different across the scenarios, we can also discover the variation in DUoS charges across scenarios. Highest DUoS charges are seen in the TD scenario as EV charging profiles coincide with the peak electricity demand periods, therefore, driving the average peak demand of electricity, in turn raising DUoS charges.

5.3.2 Fixed tariff

Figure 5.8 presents simulation data for all FES scenarios, and this time, the prices for the domestic users are fixed and therefore HPs have no incentive to shift their consumption to lower demand/lower price periods. From the figure, we can observe similar behaviour to that discussed under the DA-RTP tariff apart from some notable

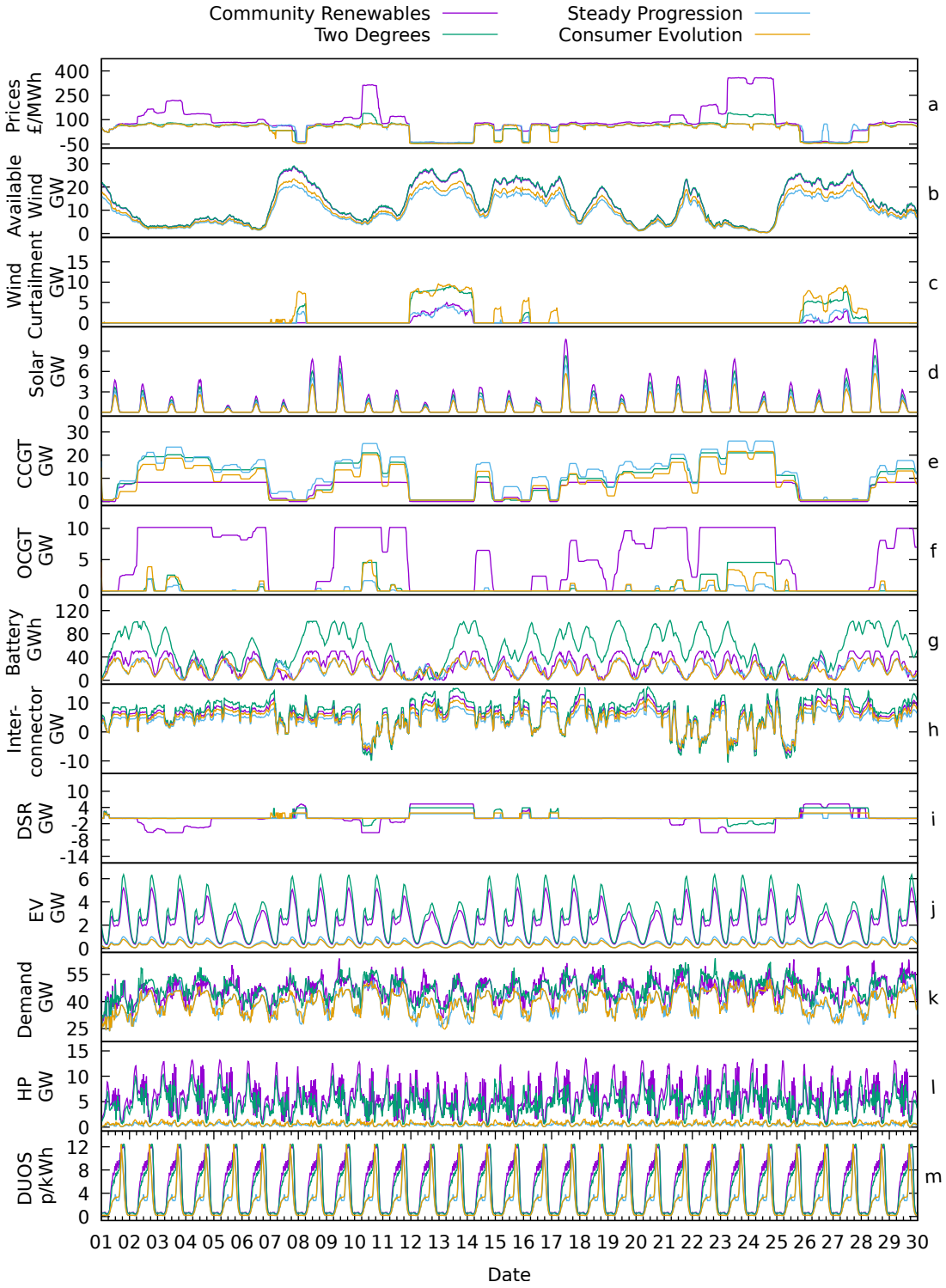

Figure 5.7: Comparison of the simulated power production and demand between in 2030 for the four FES scenarios under DA-RTP domestic tariffs using simulation parameters from tables 5.3,5.2,5.1.

differences. Under the fixed tariff scenarios, we can see that HP demand (l) is much more predictable and corresponds to the peak electricity demand from EV (j). Higher peak electricity consumption leads to higher wholesale electricity prices during periods of low renewable power generation, especially in high renewable scenarios such as CR and TD.

Under the fixed tariff scenarios, the SO needs to rely on I&C DSR more often. As I&C DSR cost is assumed to exponentially increase at higher DSR requirements, this disproportionally affects the low power production periods. As HP and EV peaks coincide with the baseload peak, we can see that peak DUoS charges (m) are disproportionally high under the fixed tariff scenarios when compared to DA-RTP tariff. Detailed analysis of DUoS charges between the fixed and DA-RTP tariff is provided later in this chapter.

Next, we will provide a thorough comparison of DA-RTP and fixed tariffs for specific scenarios with quantitative data.

5.3.3 Electricity cost

By performing market simulations, we are attempting to evaluate the benefits and disadvantages of DA-RTP tariffs when compared with fixed tariffs that are charged to domestic customers. We believe that only by driving the HP running costs much lower to make them economically compete with gas boilers will it lead to mass uptake of the HP technology and therefore lead to a big step in the decarbonisation of heat.

Our dynamic predictions of the wholesale market and behaviour of agents rely on

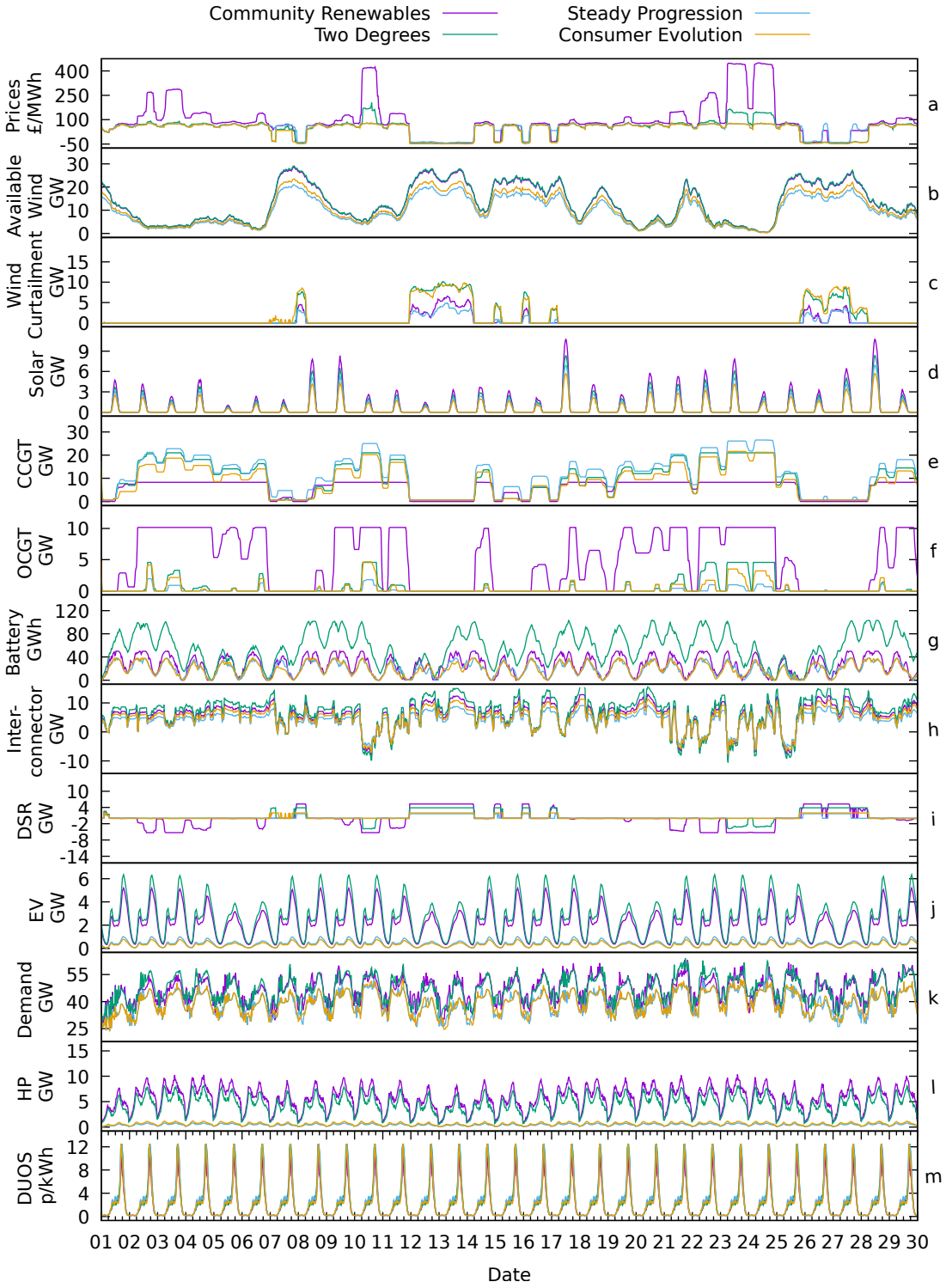

Figure 5.8: Comparison of the simulated power production and demand between in 2030 for the four FES scenarios under DA-RTP domestic tariffs using simulation parameters from tables 5.3,5.2,5.1.

	Average Electricity Price £/MWh	HP user total p/kWh	HP user wholesale p/kWh	HP user distribution p/kWh	HP user other p/kWh
CR DA-RTP	94.39	22.44	9.41	4.42	8.62
CR fixed	105.6	24.69	12.11	3.1	9.48
TD DA-RTP	51.03	14.2	4.98	3.77	5.45
TD fixed	52.62	14.47	5.93	2.99	5.56
SP DA-RTP	52.76	10.48	4.85	1.6	4.02
SP fixed	52.83	14.26	5.61	3.18	5.48
CE DA-RTP	44.87	9.61	4.09	1.83	3.69
CE fixed	44.77	12.62	4.93	2.84	4.85

Table 5.4: Comparison of electricity costs across scenarios

agents being rational and responding to prices when possible. This can be seen by the reduced average peak demands and lower wholesale prices under DA-RTP tariff where HPs can respond to price signals and shift their consumption away from the electricity use peaks.

Table 5.4 shows the comparison of electricity prices across the different FES scenarios. We can see that in all scenarios HP operating costs are lower under the DA-RTP tariff when compared to a fixed tariff with average savings across all scenarios of around 15.33%. This is due to the ability of HPs to shift to lower-cost periods where wholesale prices of electricity and DUoS charges are lower.

The shift of HP power consumption to lower demand periods also has spillover benefits for other users of electricity driving the average wholesale electricity prices by an average of 3.39% across all scenarios. This is driven by the use of HPs in off-peak periods driving the peak consumption of electricity lower and also shifting the consumption of power throughout the day to periods of higher renewable generation. This means that conventional thermal power plants need to be operated less, and more efficient power plants can be used to produce power by smoothing the electricity demand throughout the day. The effect on the wholesale prices is much lower for the scenarios with lower uptake of HPs (CE and SP).

While examining different components of the HP users' total p/kWh cost, we have

found that distribution charges increased in CR and TD scenarios when HPs were exposed to DA-RTP tariffs. This was due to the use of (5.10) for the modelling of DUoS charges where $\bar{D}(t)^{max}$ was simulation specific and in effect caused DUoS charges to be proportional to the average demand for that particular scenario and tariff combination (high DUoS charge during high average demand periods and vice versa). This seems to be appropriate when analysing the HP switching behaviour within a tariff and scenario combination but makes it difficult to compare the DUoS charges between the DA-RTP and fixed tariff cases for a particular FES scenario. We can see how even though the DA-RTP tariff simulation had lower average peak demand, as discussed later in this section and shown in table 5.5, the peak DUoS charges calculated for DA-RTP and fixed tariffs were similar at 12 p/kWh during the peak average demand periods as seen in figures 5.7 and 5.8. Other possible alternatives for the calculation of the DUoS charges that could help us compare the DUoS charges between fixed and DA-RTP cases could be the use of the same $\bar{D}(t)^{max}$ for the specific FES scenario. The use of the same $\bar{D}(t)^{max}$ across DA-RTP and fixed tariff cases would allow for lower DUoS charges when average peak demand is reduced as seen in table 5.5 under DA-RTP case (51.01 GW) when compared to fixed tariff case (54.58 GW).

5.3.4 Peak demand

An additional benefit of using DA-RTP tariffs is the ability to smooth the demand of electricity throughout the day to flatten the peak electricity consumption periods in order to avoid network reinforcements costs and reduce the reliance of the SO on DSR to manage the grid and the use of inefficient power plants. If the demand of the system is distributed throughout the day, it means that we can better utilise the

	Total Demand GWh	Average Peak GW	Peak GW
CR DA-RTP	33223.77	51.01	65.19
CR fixed	33097.02	54.58	63.82
TD DA-RTP	33515.65	51.86	63.83
TD fixed	33461.42	55.54	65.29
SP DA-RTP	27859.75	46.01	53.98
SP fixed	27864.43	46.05	53.93
CE DA-RTP	28030.99	45.9	53.46
CE fixed	28037.23	46.66	52.6

Table 5.5: Comparison of peak demand and average demand across different scenarios

electricity grid to deliver the power to customer homes.

From the results in table 5.5 we can see that under all DA-RTP tariff scenarios, the average peak demand (the average of daily peak demands over the simulation period) was lower when compared to the fixed tariff under the same FES scenario. The peak of daily half-hourly average demand is 6.58% lower under the higher renewable uptake scenarios CR and TD but only 0.09% and 1.63% lower under the low renewable scenarios SP and CE respectively. This is due to the limited number of HPs dispatched on the grid under the CE and SP scenarios. We can also see that in all scenarios, the peak electricity demand in GW was lower under the DA-RTP tariffs as expected.

Total energy demand under DA-RTP tariff was slightly higher under the DA-RTP tariff under the CR and TD scenarios and slightly lower under SP, CE when compared to a fixed tariff. This is unexpected, as we would have anticipated HPs that choose to operate during periods of low cost to consume more energy overall. As HPs are heating during the periods of low electricity prices, that would suggest they are overheating the property when not required, therefore wasting energy.

5.3.5 Power Supply

In table 5.6 we present the power supply composition across different scenarios as well as the called upon I&C DSR as these are the agents in our modelling that respond to electricity prices and can provide power to the grid. From the table, we can see that CCGT use increases slightly in CR, TD and CE scenarios when comparing DA-RTP and fixed tariff behaviour. This is expected as HPs are responding to prices and in effect are smoothing electricity demand throughout the day. This, in turn, leads to a reduced number of peaks, allowing the more efficient power plants (in this case CCGT) to warm up and provide a more stable power supply throughout the day. We also observe the expected behaviour of OCGT power plants across scenarios TD, SP and CE when comparing DA-RTP and fixed tariff cases where OCGT utilisation reduces due to the increase in the flexibility of power demand. The only exception for this is CR, where we can see an increase in CCGT and OCGT power consumption. For the CR scenario, this is expected behaviour as CCGT and OCGT power production is a more cost-effective option than I&C DSR. As the HPs shift their consumption away from the peaks, reducing the demand, this helps to drive the overall costs lower by reducing the required amount of DSR, the difference partly fulfilled by the price responsive HPs.

Comparison of energy storage power supply to the system shows that under all scenarios the utilisation of energy storage facilities reduces when comparing fixed and DA-RTP tariff behaviours. This would be expected as HPs and energy storage facilities are both providers of flexibility and the more flexible resources are dispatched onto the electricity network, the lower the benefits will be for all participants able to provide flexibility to the grid.

	CR DA-RTP	CR fixed	TD DA-RTP	TD fixed	SP DA-RTP	SP fixed	CE DA-RTP	CE fixed
Demand	33223.77	33097.02	33515.65	33461.42	27859.75	27864.43	28030.99	28037.23
Wind Available	8942.84	8942.84	9098.37	9098.37	6571.04	6571.04	7348.68	7348.68
Curtailed	189.36	349.17	711.4	892.58	248.82	266.15	936.86	967.62
Wind	8753.48	8593.67	8386.96	8205.79	6322.22	6304.89	6411.82	6381.06
Solar	607.54	607.54	471.25	471.25	390.93	390.93	321.31	321.31
Biomass	1781.98	1781.98	1565.98	1565.98	1093.49	1093.49	1430.98	1430.98
Hydro	366.23	366.23	333.53	333.53	336.8	336.8	330.26	330.26
Nuclear	2110.9	2110.9	2110.9	2110.9	1766.26	1766.26	3704.84	3704.84
Interconnector	4326.98	4326.98	5260.5	5260.5	3065.47	3065.47	3797.15	3797.15
Other	5019.29	5019.29	5693.6	5693.6	4869.21	4869.21	4258.12	4258.12
CCGT	4198.14	4172.34	7426	7334.07	8672.76	8683.69	6374.2	6346.38
OCGT	3894.59	3766.53	369.83	472.93	104.87	114.82	254.17	292.61
Battery Supply	1752.45	1780.63	1900.01	2020.82	1229.89	1245.1	1148.24	1172.64

Table 5.6: Comparison of demand and power production across different scenarios in GWh.

In table 5.6 we have also presented the sum of energy in GWh of wind curtailment. We can see that wind curtailment is reduced in all scenarios under DA-RTP tariffs, as expected. This is due to HPs shift of power consumption to lower cost/higher renewable periods.

5.3.6 Energy storage

All of the FES scenarios predict a significant uptake of storage over the next thirty years with the capacity of the energy storage increasing to 6.9 GW in CE and 12.25 GW in TD by 2030 from 4.14 GW today [3]. For comparison, the average peak electricity demand today is around 43 GW. Increases in grid flexibility and additional resources are useful for smoothing the electricity demands throughout the day. Energy storage can also help improve utilisation of renewable energy power by charging during periods of high solar and wind power production and discharging batteries during higher demand periods.

We have already observed in figure 5.7 that this ability to smooth electricity supply

leads to less volatile wholesale electricity prices. We have also seen that energy storage, even though able to provide a significant amount of instantaneous power, cannot provide power for extended periods (more than a day) when wind availability is in limited supply for several days.

There is also another complication that comes with including energy storage in wholesale market simulations, due to their ability to discharge up to 12.25 GW of power into the grid they significantly affect the supply and demand of power on the system. This means that, whilst trying to match the demand and supply of the system, price signals can make the energy storage facilities jump from -12.25 GW power demand to 12.25 GW power supply in very short periods. This is especially true if all energy storage facilities are responding to the same price signals, therefore turning on and off at the same time.

In figure 5.9, we show how battery behaviour changes when wholesale electricity prices change. We observe that even a small wholesale price change of 0.02 £/MWh causes the battery to shift its discharging period to nearby (more expensive) periods. If the nearby periods were periods when the battery was discharging, this shift would mean a power demand/supply changing by 25 GW. From these results, we can see that grid-scale batteries responding to wholesale prices and working optimally can have a detrimental (destabilising) effect on the market. As all batteries are exposed to the same market prices, they will tend to react in a similar way. This was of particular concern in our market simulations as supply and demand balance is achieved through the price search mechanism and relies on agents responding to price signals. This meant that batteries responding to our predicted wholesale prices caused our demand and supply to jump between iterations.

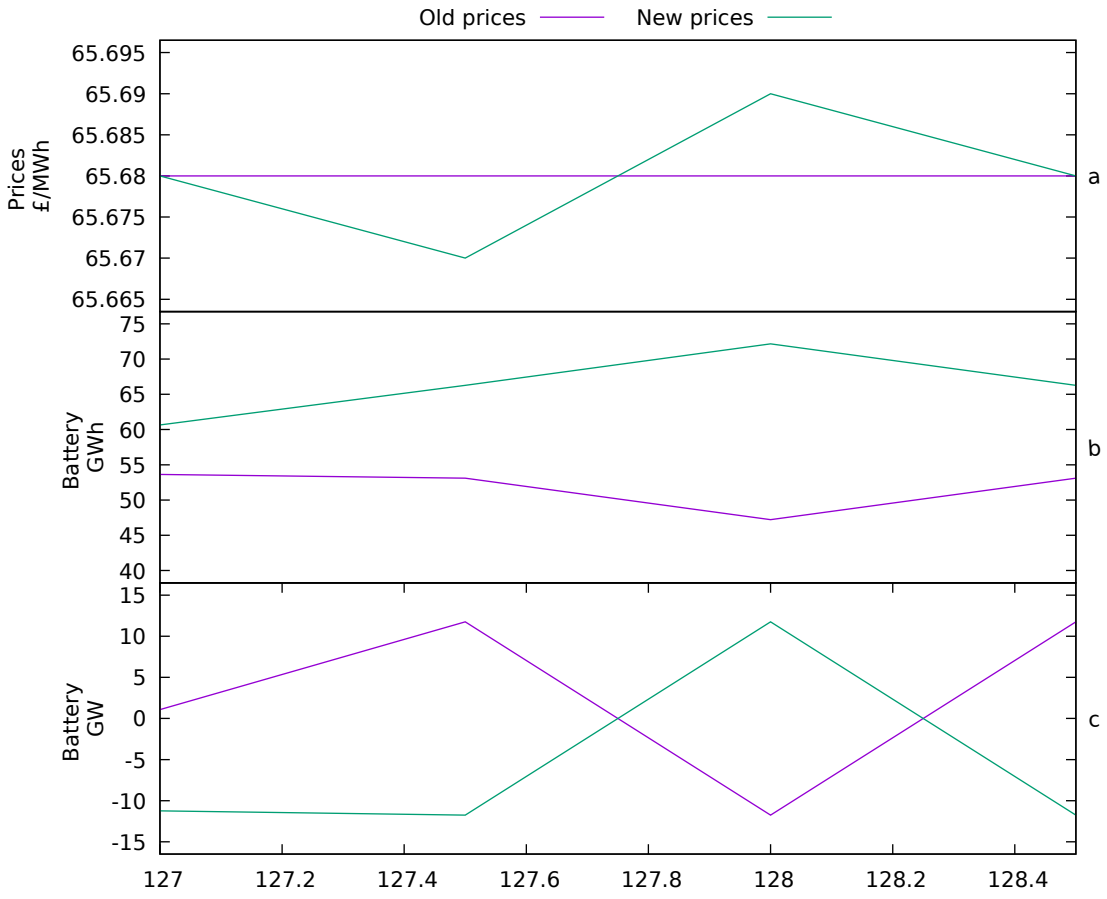

Figure 5.9: Battery behaviour change upon changes in prices

We have reduced this problem by using over-relaxation on the power output of the grid-connected batteries. By limiting the effect that newly optimised prices can have on the battery behaviour, we found that convergence of the system was smoother and faster.

5.3.7 Sensitivity analysis for DSR

At the beginning of this chapter, we outlined the price-demand relationship for the I&C DSR. We were unable to find additional supporting information for this functional relationship so instead we provide a sensitivity analysis for a different set of parameters for (5.4).

In the market simulations, we have found that I&C DSR has a significant impact on electricity prices under scenarios where thermal power plant availability is limited. This is especially true for the CR scenario. From figure 5.7 we can see that CR scenario heavily relies on renewable energy generation (mainly wind) with small amounts of power coming from CCGT and OCGT power plants.

Due to the limited thermal power plant availability, the grid also relies on I&C DSR during the periods of low power production to deliver the stability and balance of the grid. We can see that DSR under the CR scenario, reaches 6 GW in multiple periods. As DSR only turns on at high prices when compared to thermal power plant usage, we can see that wholesale prices rise to nearly 350 £/MWh during periods of lower wind power production periods in figure 5.7 (a).

The availability and the cost of I&C DSR, therefore, has a significant impact on the final wholesale electricity prices for all grid energy users. As we have assumed a logit function for the DSR, this also means that higher levels of DSR become disproportionally more expensive towards the limits of the available DSR.

To evaluate the effect of I&C DSR parameters on wholesale prices of electricity we have compared the original results of the wholesale market simulation for CE scenario

(where $d^{dsr} = 5300$) with a market simulation using an I&C DSR functions where available DSR is higher and therefore the cost of the same amount of DSR is lower. This is achieved by setting $d^{dsr} = 14000$.

We provide the market simulation results in figure 5.10 for different DSR functions. We can observe demand response changes significantly between scenarios reaching nearly -12 GW during periods of reduced power availability from renewable sources such as that observed between day 10 and 11, and between 23 and 25. As mentioned previously, the expected DSR in the CE scenario was insufficient to match the supply and demand of the system causing the price to rise indefinitely during the periods where there was insufficient power supply to meet demand (prices reaching 450 £/MWh). As we have assumed an increase in the available DSR, now the market matching algorithm was able to match the demand and supply. In figure 5.10, we can see that this has caused prices to drop to levels of around 270 £/MWh.

5.3.8 Carbon emissions

The most significant consideration for switching the space heating demand to HPs from fossil fuels is the ability of HP technology to displace carbon. In oder to assess the impact of HP uptake, electrification of heating and the use of different domestic tariff structures we have simulated total carbon emissions for all FES scenarios under fixed and DA-RTP tariffs. Carbon emission factors used in our calculations were sourced from [121, 122, 123] apart from the Belgium interconnector flow where we have used grid intensity of Belgium as stated in [124], all carbon intensity factors are summarised in table 5.7.

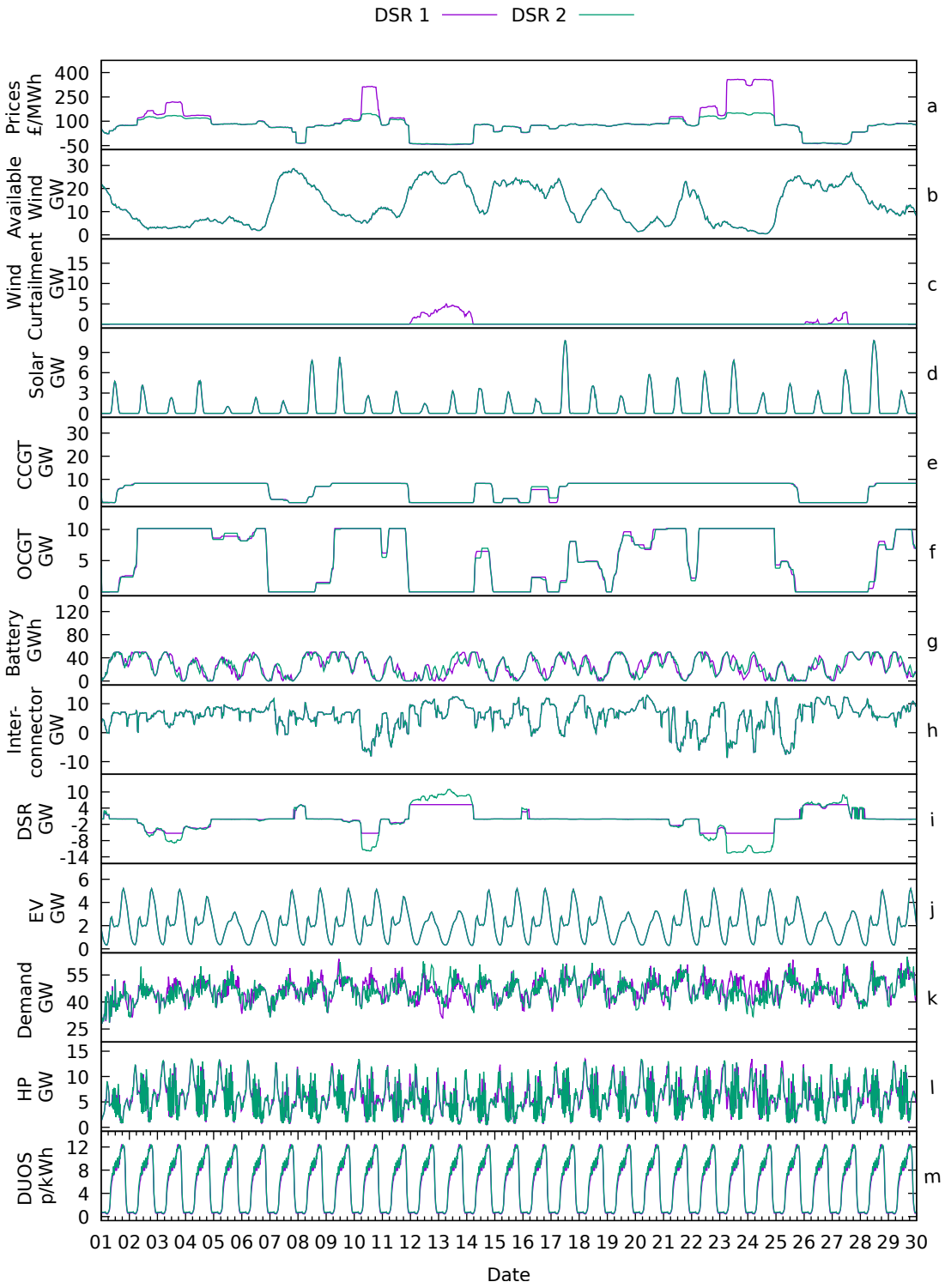

Figure 5.10: Comparison of the simulated power production and demand between artificially high DSR availability ($d^{dsr} = 14000$) and the original FES scenario ($d^{dsr} = 5300$) under DA-RTP domestic tariffs using simulation parameters from tables using all other parameters as per CR FES scenario.

	Carbon Intensity gCO_2/kWh
CCGT	394
OCGT	651
Wind	0
Solar	0
Biomass	120
Interconnector	206
Hydro	0
Nuclear	0
Other	300

Table 5.7: Carbon intensity of different sources of power [121, 122, 123]

To simplify the calculations, we have grouped all interconnector flows and used a volume-weighted average of carbon intensity to assess the carbon emissions of the interconnector. Volumes and grid intensities of interconnectors from 1 January 2019 to 30 September 2019 were as follows: France 9.0 TWh (53 gCO_2/kWh), Belgium 3.95 TWh (167 gCO_2/kWh), Netherlands 4.6TWh (474 gCO_2/kWh), Ireland 1.19 TWh (458 gCO_2/kWh) [125]. The calculated volume-weighted average of interconnector emissions was therefore 206 gCO_2/kWh.

To calculate transport emissions, we have assumed there will be 33.8M cars in 2030, calculated as the average sum of cars in individual FES scenarios. As we needed to assess the carbon emissions of the total number of cars, we needed to calculate the carbon emissions per vehicle for the 30 day simulation period discussed previously and compare carbon emissions of combination of internal combustion and electric vehicles. To find carbon intensity of internal combustion vehicles, we followed the following steps:

- We have divided the amount of TWh consumed by petrol/diesel vehicles by the number of vehicles stated in the specific FES scenario, giving us annual

consumption of 5947 kWh per vehicle per annum. [3]

- We then used diesel (10 kWh/l) and petrol cars (8.9 kWh/l) from [126] in combination with diesel (2.62 $kgCO_2$/l) and petrol (2.31 $kgCO_2$/l) [127] to find the carbon emission factors per kWh to be 0.262 $kgCO_2$/kWh for diesel and 0.259 $kgCO_2$/kWh for petrol.
- Assuming equal split between the petrol and diesel vehicles we used 0.260 $kgCO_2$/kWh to convert the annual kWh used by petrol/diesel cars to $kgCO_2$ giving us annual emissions of petrol/diesel vehicles as 1.56 tCO_2. Apportioning this for the 30 days out of the year gives us 0.127 tCO_2.

To calculate the emissions of EVs, we have used similar concepts apportioning the appropriate kWh consumption of the year for the 30 days and multiplying it by the simulated scenario-specific carbon intensity of the grid.

Next, to calculate the emissions of HPs, we have assumed houses to use an average of 12,037 kWh for their space heating needs [116]. We assumed that a fifth of this space heating demand would be consumed in January (the heating season is around six months in GB spanning October through to the end of March), although we assume a higher consumption of heat demand during the coldest months such as January. For the emissions of gas boilers, we used emissions of 0.233 $kgCO_2$/kWh as per [114]. We assume gas boilers to be 100% efficient; therefore, a house in January would produce 0.56 tCO_2 when heated with gas boiler. When calculating emissions associated with HPs, we have again used the simulated scenario-specific grid emissions and multiplied this by the assumed energy consumption of the house in January. As for the gas boiler we have assumed that a fifth of the space heating energy demand would be consumed in January, therefore assuming HP CoP of 3.33 [115] we calculate the kWh used by

	Heating Carbon $MtCO_2$	Vehicle Carbon $MtCO_2$	Power Carbon $MtCO_2$	Total Carbon $MtCO_2$	Grid Electricity gCO_2/kWh
CR DA-RTP	5.53	3.06	6.8	14.79	204.69
CR fixed	5.53	3.06	6.71	14.69	202.64
TD DA-RTP	5.67	2.77	6.15	14.03	183.38
TD fixed	5.67	2.77	6.18	14.06	184.61
SP DA-RTP	6.2	3.95	5.71	15.77	204.91
SP fixed	6.2	3.95	5.72	15.78	205.26
CE DA-RTP	6.17	3.99	4.91	15.01	175.1
CE fixed	6.17	3.99	4.92	15.02	175.56

Table 5.8: Carbon emissions under different scenarios

the HP for space heating in January as 723 kWh.

Using the calculations as outlined above, we then calculated carbon emissions of space heating, transport and grid, as shown in table 5.8 across different FES scenarios and tariffs. From table 5.8 we can see that total carbon emissions are lower in both of the high renewable energy scenarios CR and TD when compared to SP and CE. Lowest carbon emissions are observed in the TD scenario where users are exposed to DA-RTP tariffs as expected. In TD scenario, we have a large uptake of HPs and EVs whilst maintaining more efficient fossil fuel plants (CCGT) to produce power during periods of low renewable power generation, as seen in figure 5.7. Grid carbon savings are reflected in the gCO_2/kWh where TD grid intensity is 10% lower than that observed under CR scenario.

Grid intensity simulated across FES scenarios varies significantly. Lowest grid carbon intensity 175.56 gO_2/kWh is observed under CE scenario with DA-RTP tariffs. This is expected as CE scenario has lower electricity demand when compared to TD and CR due to lower uptake of HPs and EVs whilst still benefiting from the increased renewable energy sources allowing it to rely less on fossil fuel power plants (CCGT and OCGT) to deliver power requirements as per table 5.6. Highest grid carbon intensity 204.69 gO_2/kWh is observed under CR scenario where the high electricity demand, combined with reliance on renewable sources and reduced availability of CCGT power plants means that power needs to be sourced from less efficient OCGT power plants.

From table 5.8 we can observe that grid carbon intensity is lower under DA-RTP scenarios in TD, SP, CE scenarios as HPs are able to shift some of their electricity consumption to periods of lower cost/higher renewable periods. We do although observe that the carbon benefits are limited as batteries were already able to utilise the flexibility and cheaper energy generation; therefore, the difference between fixed and DA-RTP tariffs in terms of grid electricity carbon intensity is small. However, this does not include the fact that DA-RTP tariffs make HPs much more attractive to run (30% savings on the customer bills) and therefore would increase the number of HPs in the market in turn reducing the total carbon emissions of the grid.

Chapter 6

Conclusions

In this thesis, we have introduced a framework for evaluating dynamic electricity systems where electricity market participants, both domestic and non-domestic, are responding to price signals. The framework allows us to incorporate individual agent optimization and consider their individual inter-temporal dependencies when modelling the power market, allowing us to analyze the market behaviour in future energy scenarios.

In Chapter 2, we have introduced the market price search algorithm that uses ABM concepts to find equilibrium wholesale market prices where individual in-depth agent optimization can be parallelized. Our price search algorithm improved the equilibrium price search algorithms previously discussed in literature through the inclusion of the inter-temporal dependencies in the modelling of the agents. We have shown that the price search algorithm is stable and values of the variables of interest converge to a narrow bound after 1000 iterations.

We have then followed on to introduce individual agents of the market, starting with power plants in Chapter 3. The previous model of power plant optimization using a PDE-based approach [7] relied on temperature as a determinant of the power plant output and did not include the different states of the power plant as discussed in Chapter 3. As we move towards a more renewable future, power plants will need to be cycled, and the warm-up and cool-down costs will be of crucial importance in modelling the cost of power delivery. We have generalized the model introduced in [7] for fossil fuel power plants, and incorporated operational power plant constraints such as minimum zero time, stable exporting limits, notice to deviate from zero and ramp rates. We have shown that the simplified power plant modelling closely matches the observed market behaviour of the power plants in GB, providing us confidence for the use of our power plant models in evaluating future electricity markets.

Next in Chapter 4, we followed onto discuss the building optimization models used to find optimal heating schedule when agents are exposed to DA-RTP. The model introduced in [8] was adapted and simplified, to reduce the computation effort so that it can be included in our GB market simulations. The chapter mainly focused on the EFUS data processing in finding the optimal temperature schedules of the users in England and their thermal building characteristics. We believe that the use of real-world data in devising the building parameters in England significantly improves the accuracy of our future energy scenario simulations. We have concluded the chapter with results from a real-world experiment where we have shown that 20% customer bill savings can be made on a particular day by using such algorithms and subscribing to currently available DA-RTP tariffs in GB.

We have then brought all of these individual models together in Chapter 5 where we simulated the electricity market using all four FES scenarios under our dynamic

models for a single month in winter. Through the use of the framework, we were able to evaluate the ability of autonomous heating controllers to support the future smart grid by increasing the use of renewable energy produced, reducing the need for network reinforcement whilst reducing electricity bills for all electricity users. We also identified that issues might arise when renewable energy production was lower over the prolonged periods, and the capacity of batteries was insufficient to meet the demand of the grid to the point where (CE) scenario using our modelling was deemed not feasible.

6.1 Policy recommendations

Throughout the analysis, we have identified a few areas of potential policy intervention to help GB achieve carbon reduction. We outline our policy recommendations below. Please note that the author is a part-owner of renewables company involved in DSR provision, installation of HPs and the sale of smart thermostat for HPs.

1. Encourage uptake of HPs.

We believe that HP uptake across GB is crucial in achieving carbon reduction targets set out by the UK government. The issue of a mass uptake of HPs is still a high cost of installation and very low gas prices, making it hard for HPs to compete with gas boilers. DA-RTP is one potential avenue that customers can take to reduce their HP running costs. However, only one electricity supplier in the GB is currently offering these, and the many households across GB might still not be aware of the benefits these tariffs can achieve for the customer through reduced customer bills and for the economy through smarter use of our electricity infrastructure.

2. Promote DA-RTP tariffs.

We believe DA-RTP tariffs need to be promoted and more education needs to be provided on how these tariffs work and what benefits they can achieve. Other suppliers need to be encouraged to provide DA-RTP tariffs when high domestic loads are present at customers' property. We hope that current Ofgem review of the half-hourly settlement could provide the initial push for other suppliers to provide variable electricity tariffs [128] but additional support might be required to make DA-RTP tariffs the new standard.

3. Make DUoS charges reflect real-time demand.

The charging structure of DUoS charging could also be improved by making DUoS charges reflective of real-time demand rather than setting DUoS charges a year in advance. This would ensure that those customers who consume power during the peak times and are not willing to shift these loads to off-peak periods are paying the premium for the electricity consumption at those times as they will be the customers driving the needs for network reinforcement.

4. Arrange capacity contracts for low wind and solar power production periods.

Throughout the research we have also found that to ensure reliable delivery of power throughout the year in a renewable future, contracts need to be in place to supply sufficient power to the grid when the power generation from wind and solar are low for prolonged periods and energy storage capacity is not sufficient to support the grid for the length of these periods. An example of which in our simulations would be five days in December with a limited output of renewable power from both wind and solar.

5. Improve efficiency of buildings and appliances.
We also need to make sure that even with smart technology available to reduce our power consumption bills, we aim to improve the efficiency of our buildings and appliances. We need to make sure that as more heat pumps go on the market, our houses are better insulated to sustain heat throughout the day. This helps with both, reduced energy demand and improvements in optimized heating schedules as better insulated homes can turn their heating off for longer periods allowing the higher utilization of renewable sources.

6.2 Model improvements

Throughout the thesis, we have discussed potential future improvements for our modelling. We believe the improvements outlined below would provide the highest benefit in terms of simulation accuracy.

As discussed in Chapter 3, due to insufficient publicly available data, we had to estimate the number of power plant parameters in our simulations. We believe this could be investigated further by engaging with the industry and experts at the NG as they might be able to provide true parameters of the power plants to achieve more accurate representation of power plant behaviour.

Due to time constraints, we were unable to model in-home batteries and instead modelled all storage as grid-connected. Modelling individual domestic energy storage could help improve the accuracy of our simulations as in many cases, houses with in house

storage would try to use the energy produced locally to avoid network charges similarly to that discussed in [129]. In [129], authors discuss the importance of including distributed energy storage and bi-directional charging of electric vehicles in the house when these are exposed to ToU tariffs and power generation from on-site renewable energy generation. Presently, the study looked at taking grid prices as an exogenous variable, but using our wholesale price modelling this price could become endogenous in the model.

Building modelling could also be improved by using higher-order building model for building behaviour, as discussed in Chapter 4. We believe this could have a significant impact on the results, especially if we move towards a future of low-temperature heating systems and better-insulated homes as these systems take longer to raise the temperature of buildings these time lags need to be accounted for.

In modelling the demand, we have also made a simple assumption of the relationship of I&C DSR. We believe that further analysis of I&C DSR is needed for accurate modelling of the electricity prices in the future grid. As we have seen from Chapter 5 the cost of I&C DSR is one of the main determinants of the peak electricity prices. One approach future research could consider is using BM unit import rates as defined in [130] and derive price/demand curves from the values recorded.

Simulation results in Chapter 5 have been provided for a winter month (specifically January) as our research focused on the importance of space heating (specifically the increased uptake of HPs). Further extension of research could use the same modelling tools to simulate the grid behaviour over the whole year. Entire year simulation could provide additional insights on grid emissions and the utilisation of renewable energy sources over the year where during summer months the demand for electricity could

be lower (due to reduced space heating requirements) whilst more power would be produced from solar.

6.3 Future research

Some areas of research have been outside of the scope of this thesis, although they could be of interest in shaping the grid of the future. We have outlined some of these below.

Whilst modelling energy storage facilities we found that if they were exposed to the same price signals, they would be switching at similar times, in effect causing large changes in the electricity demand and supply on the network. We have used relaxation methods to smooth this effect in our modelling due to the instability it was causing in the market search mechanism, but further analysis should be conducted into whether this could potentially cause problems in the future electricity market and we need to find ways of smoother grid scale battery charging and discharging.

In Chapter 1, we have briefly discussed a concept of TE where the grid is continuously adapting to the real-time grid conditions. We believe in this kind of future, shorter settlement periods would be required to achieve grid balance through market price signals. We have briefly looked into the reduced settlement period effect on wholesale electricity prices and initial results look promising. Some of the optimization models have been written to cater to shorter settlement periods allowing future researchers, to extend our modelling to include these shorter settlement periods.

Further, in our modelling, we have assumed that DUoS charging across GB would be uniform and based on the average demand of the system over the simulation in particular half-hours. Once some clarity is provided into the future of DUoS charging structure, future research could attempt to estimate area-specific DUoS charges. We have attempted to research this using our simplified modelling of DUoS but due to the limited amount of agents available in our model have been unable to devise the area-specific DUoS charges. Ability to model area-specific electricity markets could also help us better understand the benefits of peer-to-peer trading. Peer-to-peer trading has been shown to improve the efficiency of the grid use, reduce the need for network reinforcement and customer bills as well as reduce the carbon emissions. In [42], authors have shown the possible reduction in electricity bills of market participants by 28.94% whilst also reducing the reliance on grid electricity by 42.13% through sharing the excess electricity locally [42].

Bibliography

[1] Parliament of the United Kingdom. *Climate Change Act 2008*. 2008.
URL: `https://www.legislation.gov.uk/ukpga/2008/27/contents` (visited on 09/28/2020).

[2] Modassar Chaudry et al. "Uncertainties in decarbonising heat in the UK". In: *Energy Policy* 87 (2015), pp. 623–640.

[3] National Grid. *Future Energy Scenarios, 2018*. Technical Report. National Grid, 2017.

[4] Ofgem. *Domestic RHI*. 2019.
URL: `https://www.ofgem.gov.uk/environmental-programmes/domestic-rhi/about-domestic-rhi` (visited on 05/08/2019).

[5] DBEIS. *Quality assurance at heart of new £2 billion green homes grants*. 2020.
URL: `https://www.gov.uk/government/news/quality-assurance-at-heart-of-new-2-billion-green-homes-grants` (visited on 08/04/2020).

[6] E4tech et al. *Realising the potential of demand-side response to 2025*. Tech. rep.
London: Department for Business, Energy and Industrial Strategy, 2017.

[7] Matt Thompson, Matt Davison, and Henning Rasmussen. "Valuation and optimal operation of electric power plants in competitive markets". In: *Operations Research* 52.4 (2004), pp. 546–562.

[8] Sydney D Howell, Paul V Johnson, and Peter W Duck. "A rapid PDE-based optimization methodology for temperature control and other mixed stochastic and deterministic systems". In: *Energy and buildings* 43.7 (2011), pp. 1523–1530.

[9] Federal Energy Regulatory Commision. *Definition of Demand Response*. 2018. URL: `https://www.ferc.gov/industries/electric/indus-act/demand-response/dr-potential.asp` (visited on 04/20/2018).

[10] Kitty Stacpoole, Hongjian Sun, and Jing Jiang. "Smart Scheduling of Household Appliances to Decarbonise Domestic Energy Consumption". In: *2019 IEEE/CIC International Conference on Communications Workshops in China (ICCC Workshops)*. IEEE. 2019, pp. 216–221.

[11] Farrokh A Rahimi and Ali Ipakchi. "Transactive energy techniques: closing the gap between wholesale and retail markets". In: *The Electricity Journal* 25.8 (2012), pp. 29–35.

[12] Sijie Chen and Chen-Ching Liu. "From demand response to transactive energy: state of the art". In: *Journal of Modern Power Systems and Clean Energy* 5.1 (2017), pp. 10–19.

[13] Nikolaos G Paterakis, Ozan Erdinç, and João PS Catalão. "An overview of Demand Response: Key-elements and international experience". In: *Renewable and Sustainable Energy Reviews* 69 (2017), pp. 871–891.

[14] Sen Li et al. "Market-based coordination of thermostatically controlled loads—Part I: A mechanism design formulation". In: *IEEE Transactions on Power Systems* 31.2 (2015), pp. 1170–1178.

[15] Duncan S Callaway and Ian A Hiskens.
"Achieving controllability of electric loads".
In: *Proceedings of the IEEE* 99.1 (2010), pp. 184–199.

[16] Mohamed H Albadi and Ehab F El-Saadany.
"A summary of demand response in electricity markets".
In: *Electric power systems research* 78.11 (2008), pp. 1989–1996.

[17] Qi Wang et al. "Review of real-time electricity markets for integrating distributed energy resources and demand response".
In: *Applied Energy* 138 (2015), pp. 695–706.

[18] IRENA. *Time-Of-Use Tariffs Innovation Landscape Bried*. 2019. URL: https://www.irena.org/-/media/Files/IRENA/Agency/Publication/2019/Feb/IRENA_Landscape_ToU_tariffs_2019.pdf?la=en&hash=E565514088C268EE9BFE542A6E1E5DB10E508620 (visited on 01/27/2020).

[19] Ana Soares, Alvaro Gomes, and Carlos Henggeler Antunes.
"An agent-based modelling approach for domestic load simulation".
In: *ECEEE SUMMER STUDY PROCEEDINGS*.

[20] Carbon Co-op. *Energy Community Aggregator Services*. Feasibility Study. Carbon Co-op, 2018.
URL: https://cc-site-media.s3.amazonaws.com/uploads/2019/01/ECAS-Local-Flexibility-Markets.pdf (visited on 05/20/2019).

[21] nedo. *Smart Community Demonstration Project in Manchester, U.K.* Trial finding report. GMCA, 2016. URL: https://www.nedo.go.jp/content/100788809.pdf (visited on 05/20/2019).

[22] Haider Tarish Haider, Ong Hang See, and Wilfried Elmenreich.
"A review of residential demand response of smart grid".
In: *Renewable and Sustainable Energy Reviews* 59 (2016), pp. 166–178.

[23] Pedram Samadi et al. "Advanced demand side management for the future smart grid using mechanism design".
In: *IEEE Transactions on Smart Grid* 3.3 (2012), pp. 1170–1180.

[24] European Commision. *Energy Efficiency Directive*. 2019.
URL: `https://ec.europa.eu/energy/en/topics/energy-efficiency/energy-efficiency-directive` (visited on 05/01/2019).

[25] Liyan Jia and Lang Tong. "Optimal pricing for residential demand response: A stochastic optimization approach". In: *2012 50th Annual Allerton Conference on Communication, Control, and Computing (Allerton)*.
IEEE. 2012, pp. 1879–1884.

[26] Nicholas Good et al.
"Optimization under uncertainty of thermal storage-based flexible demand response with quantification of residential users' discomfort".
In: *IEEE Transactions on Smart Grid* 6.5 (2015), pp. 2333–2342.

[27] Sijie Chen, Qixin Chen, and Yin Xu. "Strategic bidding and compensation mechanism for a load aggregator with direct thermostat control capabilities".
In: *IEEE Transactions on Smart Grid* 9.3 (2016), pp. 2327–2336.

[28] ofgem. *Breakdown of an electricity bill*. 2019. URL:
`https://www.ofgem.gov.uk/data-portal/breakdown-electricity-bill` (visited on 08/20/2020).

[29] Ofgem. *Map: who operates the electricity distribution network?* 2018.
URL: `https://www.ofgem.gov.uk/key-term-explained/map-who-operates-electricity-distribution-network` (visited on 04/15/2019).

[30] Electricity North West. *Use of System Charging Statement*. 2018. URL:
`https://www.enwl.co.uk/about-us/regulatory-information/use-of-system-charges/current-charging-information/` (visited on 07/13/2019).

[31] Imbalance Pricing Guidance.
"A guide to electricity imbalance pricing in Great Britain".
In: *Elexon [online]* (2014).

[32] neta - The New Electricity Trading Arrangements.
Balancing Mechanism Reporting Service (BMRS). 2018.
URL: `https://www.bmreports.com`.

[33] National Grid ESO. *Data finder and explorer*. 2019.
URL: `https://www.nationalgrideso.com/balancing-data/data-finder-and-explorer` (visited on 04/25/2019).

[34] Octopus Energy. *Agile Tariff*. 2019.
URL: `https://octopus.energy/agile/#what-does-it-cost` (visited on 05/29/2019).

[35] Leigh Tesfatsion. "Electric power markets in transition: Agent-based modeling tools for transactive energy support".
In: *Handbook of computational economics*. Vol. 4. Elsevier, 2018, pp. 715–766.

[36] Philipp Ringler, Dogan Keles, and Wolf Fichtner. "Agent-based modelling and simulation of smart electricity grids and markets–a literature review".
In: *Renewable and Sustainable Energy Reviews* 57 (2016), pp. 205–215.

[37] Patrick Joyce. "The Walrasian tatonnement mechanism and information".
In: *The RAND Journal of Economics* (1984), pp. 416–425.

[38] Javier Hernández Avalos. *Optimal Stockpiles Under Stochastic Uncertainty*.
The University of Manchester (United Kingdom), 2015.

[39] Paul Johnson, Sydney Howell, and Peter Duck.
"Partial differential equation methods for stochastic dynamic optimization: an application to wind power generation with energy storage".

In: *Philosophical Transactions of the Royal Society A: Mathematical, Physical and Engineering Sciences* 375.2100 (2017), p. 20160301.

[40] Duy Thanh Nguyen, Michael Negnevitsky, and Martin de Groot. "Walrasian market clearing for demand response exchange". In: *IEEE Transactions on Power Systems* 27.1 (2011), pp. 535–544.

[41] Erik Miehling and Demosthenis Teneketzis. "A decentralized mechanism for computing competitive equilibria in deregulated electricity markets". In: *2016 American Control Conference (ACC)*. IEEE. 2016, pp. 4107–4113.

[42] Robin-Joshua Meinke, SUN Hongiian, and Jing Jiang. "Optimising Demand and Bid Matching in a Peer-to-Peer Energy Trading Model". In: *ICC 2020-2020 IEEE International Conference on Communications (ICC)*. IEEE. 2020, pp. 1–6.

[43] Octopus Energy. *Introducing Outgoing Octopus*. 2020. URL: `https://octopus.energy/outgoing/` (visited on 09/28/2020).

[44] Anke Weidlich and Daniel Veit. "A critical survey of agent-based wholesale electricity market models". In: *Energy Economics* 30.4 (2008), pp. 1728–1759.

[45] Poyry. *BID3*. 2015. URL: `https://www.netzentwicklungsplan.de/sites/default/files/paragraphs-files/150623_nep2015-modellingapproach-detailonbid3v100.pdf` (visited on 04/29/2019).

[46] Poyry. *BID3 Power Market Model*. 2015. URL: `http://www.poyry.com/sites/default/files/media/related_material/bid3_brochure_v100.pdf` (visited on 09/10/2019).

[47] Ziqing Jiang and Qian Ai. "Agent-based simulation for symmetric electricity market considering price-based demand response". In: *Journal of Modern Power Systems and Clean Energy* 5.5 (2017), pp. 810–819.

[48] Hamid Reza Arasteh et al.
"Integrating commercial demand response resources with unit commitment".
In: *International Journal of Electrical Power & Energy Systems* 51 (2013), pp. 153–161.

[49] Zhi Zhou, Fei Zhao, and Jianhui Wang. "Agent-based electricity market simulation with demand response from commercial buildings".
In: *IEEE Transactions on Smart Grid* 2.4 (2011), pp. 580–588.

[50] Fanlin Meng et al.
"An integrated optimization+ learning approach to optimal dynamic pricing for the retailer with multi-type customers in smart grids".
In: *Information Sciences* 448 (2018), pp. 215–232.

[51] Dimitrios Papadaskalopoulos and Goran Strbac. "Decentralized participation of flexible demand in electricity markets—Part I: Market mechanism".
In: *IEEE Transactions on Power Systems* 28.4 (2013), pp. 3658–3666.

[52] Joseph-Frédéric Bonnans et al.
Numerical optimization: theoretical and practical aspects.
Springer Science & Business Media, 2006.

[53] Zixu Liu, Xiaojun Zeng, and Fanlin Meng. "An Integration Mechanism between Demand and Supply Side Management of Electricity Markets".
In: *Energies* 11.12 (2018), p. 3314.

[54] John Q Cheng and Michael P Wellman. "The WALRAS algorithm: A convergent distributed implementation of general equilibrium outcomes".
In: *Computational Economics* 12.1 (1998), pp. 1–24.

[55] Chung-Hsiao Wang and K Jo Min.
"Electric power plant valuation: A real options approach".
In: *IIE Annual Conference. Proceedings*.
Institute of Industrial and Systems Engineers (IISE). 2006, p. 1.

[56] Chen Chen and George M Bollas. "Dynamic optimization of a subcritical steam power plant under time-varying power load".
In: *Processes* 6.8 (2018), p. 114.

[57] G Scarabello et al. "Optimization of thermal power plants operation in the German de-regulated electricity market using dynamic programming".
In: *ASME International Mechanical Engineering Congress and Exposition*.
Vol. 45226. American Society of Mechanical Engineers. 2012, pp. 147–160.

[58] Brinckerhoff Parsons.
"Technical Assessment of the Operation of Coal & Gas Fired Plants".
In: *Deparment of Energy and Climate Change (DECC): London, UK* (2014).

[59] Elexon. *Term glossary*. 2018.
URL: `https://www.elexon.co.uk/glossary/` (visited on 04/04/2019).

[60] Wartsila.
Combustion Engine vs. Gas Turbine: Part Load Efficiency and Flexibility.
2018. URL: `https://www.wartsila.com/energy/learning-center/technical-comparisons/combustion-engine-vs-gas-turbine-part-load-efficiency-and-flexibility` (visited on 11/11/2019).

[61] Kenneth Van den Bergh and Erik Delarue.
"Cycling of conventional power plants: technical limits and actual costs".
In: *Energy Conversion and Management* 97 (2015), pp. 70–77.

[62] Donald E Kirk. *Optimal control theory: an introduction*.
Courier Corporation, 2004.

[63] Michael S Branicky, Vivek S Borkar, and Sanjoy K Mitter.
"A unified framework for hybrid control: Model and optimal control theory".
In: *IEEE transactions on automatic control* 43.1 (1998), pp. 31–45.

[64] Zhuliang Chen and Peter A Forsyth. "A semi-Lagrangian approach for natural gas storage valuation and optimal operation".
In: *SIAM Journal on Scientific Computing* 30.1 (2008), pp. 339–368.

[65] Elexon. *API User Guide*. 2018. URL:
`https://www.elexon.co.uk/wp-content/uploads/2016/10/Application-Programming-Interfaces-API-and-Data-Push-user-guide.pdf` (visited on 04/12/2019).

[66] Elexon. *Generators and their Fuel Types*. 2018.
URL: `https://www.bmreports.com/bmrs/%20cloud_doc/BMUFuelType.xls` (visited on 10/28/2018).

[67] Variable Pitch. *Generators and their Fuel Types*. 2018.
URL: `https://www.variablepitch.co.uk/grid/` (visited on 11/20/2018).

[68] Ricardo Chacartegui et al.
"Real time simulation of medium size gas turbines".
In: *Energy Conversion and Management* 52.1 (2011), pp. 713–724.

[69] DECC. *Prices of Fuels Purchased by Majority Power Producers*. 2018.
URL: `https://www.gov.uk/government/statistical-data-sets/prices-of-fuels-purchased-by-major-power-producers` (visited on 11/06/2018).

[70] LSE. *What does the October 2018 Budget mean for UK carbon pricing in a no-deal Brexit?* 2018.
URL: `http://www.lse.ac.uk/GranthamInstitute/news/what-does-the-october-2018-budget-mean-for-uk-carbon-pricing-in-a-no-deal-brexit/` (visited on 03/20/2019).

[71] Ember. *EU trading carbon price*. 2018. URL: `https://sandbag.org.uk/carbon-price-viewer/` (visited on 02/12/2020).

[72] Daily FX. *EUR/GBP exchange rate*. 2019. URL: `https://www.dailyfx.com/eur-gbp` (visited on 03/05/2019).

[73] GOV.UK. *Greenhouse gas reporting: conversion factors 2018*. 2018. URL: `https://www.gov.uk/government/publications/greenhouse-gas-reporting-conversion-factors-2018` (visited on 07/20/2019).

[74] Michael JD Powell. "On search directions for minimization algorithms". In: *Mathematical programming* 4.1 (1973), pp. 193–201.

[75] Eurelectric. *Efficiency in Electricity Generation*. 2003.

[76] Muhammad Akmal and Brendan Fox. "Modelling and simulation of underfloor heating system supplied from heat pump". In: *2016 UKSim-AMSS 18th International Conference on Computer Modelling and Simulation (UKSim)*. IEEE. 2016, pp. 246–251.

[77] He Hao et al. "A generalized battery model of a collection of thermostatically controlled loads for providing ancillary service". In: *2013 51st Annual Allerton Conference on Communication, Control, and Computing (Allerton)*. IEEE. 2013, pp. 551–558.

[78] Department of Energy and Climate Change. *Energy Follow-Up Survey (EFUS): 2011*. 2011. URL: `https://www.gov.uk/government/statistics/energy-follow-up-survey-efus-2011` (visited on 01/29/2020).

[79] ofgem. *Understanding trends in energy prices*. 2019. URL: `https://www.ofgem.gov.uk/gas/retail-market/retail-market-monitoring/understanding-trends-energy-prices` (visited on 05/07/2019).

[80] nest. *Nest Learning Thermostat*. 2018. URL: `https://nest.com/uk/thermostats/nest-learning-thermostat/overview/`.

[81] Tado. *Smart Thermostat*. 2018. URL: `https://www.tado.com/gb/` (visited on 09/12/2019).

[82] Hive. *Smart Thermostat*. 2018. URL: `https://www.hivehome.com/` (visited on 09/12/2019).

[83] EDF. *Smart Thermostat*. 2018. URL: `https://www.edfenergy.com/smart-home/smart-thermostat` (visited on 11/20/2019).

[84] Alper Alan et al. "A field study of human-agent interaction for electricity tariff switching". In: (2014).

[85] Rayoung Yang and Mark W Newman. "Learning from a learning thermostat: lessons for intelligent systems for the home". In: *Proceedings of the 2013 ACM international joint conference on Pervasive and ubiquitous computing*. 2013, pp. 93–102.

[86] Mike Shann et al. "Save Money or Feel Cozy?: A field experiment evaluation of a smart thermostat that learns heating preferences". In: *Proceedings of the 16th Conference on Autonomous Agents and MultiAgent Systems*. Vol. 16. International Foundation for Autonomous Agents and Multiagent Systems (IFAAMAS). 2017.

[87] Wei Zhang et al. "Aggregate model for heterogeneous thermostatically controlled loads with demand response". In: *2012 IEEE Power and Energy Society General Meeting*. IEEE. 2012, pp. 1–8.

[88] Daniele Menniti et al. “Purchase-bidding strategies of an energy coalition with demand-response capabilities”.
In: *IEEE Transactions on Power Systems* 24.3 (2009), pp. 1241–1255.

[89] Raimo P Hämäläinen et al. “Cooperative consumers in a deregulated electricity market—dynamic consumption strategies and price coordination”.
In: *Energy* 25.9 (2000), pp. 857–875.

[90] D Menniti et al. “Coalition of consumers in a deregulated electricity market: Analyses of consumption dynamics of air conditioning users”.
In: *2006 IEEE PES Power Systems Conference and Exposition*. IEEE. 2006, pp. 1174–1181.

[91] Alex Rogers et al. “Adaptive home heating control through Gaussian process prediction and mathematical programming”. In: (2011).

[92] Mike Shann and Sven Seuken. “Adaptive home heating under weather and price uncertainty using GPs and MDPs”. In: *Proceedings of the 2014 international conference on Autonomous agents and multi-agent systems*. 2014, pp. 821–828.

[93] Liyan Jia et al.
“Multi-scale stochastic optimization for home energy management”.
In: *2011 4th IEEE International Workshop on Computational Advances in Multi-Sensor Adaptive Processing (CAMSAP)*. IEEE. 2011, pp. 113–116.

[94] Liyan Jia and Lang Tong.
“Dynamic pricing and distributed energy management for demand response”.
In: *IEEE Transactions on Smart Grid* 7.2 (2016), pp. 1128–1136.

[95] Riccardo Maria Vignali et al.
“Energy management of a building cooling system with thermal storage: An

approximate dynamic programming solution". In: *IEEE Transactions on Automation Science and Engineering* 14.2 (2017), pp. 619–633.

[96] Michael Shann and Sven Seuken.
"An active learning approach to home heating in the smart grid". In:
IJCAI. 2013.

[97] Pervez Hameed Shaikh et al. "A review on optimized control systems for building energy and comfort management of smart sustainable buildings".
In: *Renewable and Sustainable Energy Reviews* 34 (2014), pp. 409–429.

[98] Tom Søndergaard Pedersen et al.
"Using heat pump energy storages in the power grid".
In: *2011 IEEE International Conference on Control Applications (CCA)*.
IEEE. 2011, pp. 1106–1111.

[99] Raimo P Hämäläinen and Juha Mäntysaari.
"Dynamic multi-objective heating optimization".
In: *European Journal of Operational Research* 142.1 (2002), pp. 1–15.

[100] Tahar Nabil et al.
"Maximum likelihood estimation of a low-order building model".
In: *2016 24th European Signal Processing Conference (EUSIPCO)*.
IEEE. 2016, pp. 702–707.

[101] Alessandro Fonti et al. "Low order grey-box models for short-term thermal behavior prediction in buildings".
In: *Energy Procedia* 105 (2017), pp. 2107–2112.

[102] Saeid Bashash and Hosam K Fathy.
"Modeling and control insights into demand-side energy management through setpoint control of thermostatic loads".

In: *Proceedings of the 2011 American Control Conference*. IEEE. 2011, pp. 4546–4553.

[103] BRE. *BRE Domestic Energy Model*. 2012.
URL: `https://www.bre.co.uk/page.jsp?id=3176` (visited on 05/06/2019).

[104] DECC. *National Household Model*. 2019.
URL: `https://www.deccnhm.org.uk/` (visited on 04/05/2019).

[105] All Out A/C & Heating.
Guidelines for Optimal Thermostat Placement in Your Katy Home. 2016.
URL: `https://alloutacandheating.com/2016/06/28/guidelines-for-optimal-thermostat-placement-in-your-katy-home/` (visited on 05/23/2019).

[106] Fuchang Gao and Lixing Han. "Implementing the Nelder-Mead simplex algorithm with adaptive parameters".
In: *Computational Optimization and Applications* 51.1 (2012), pp. 259–277.

[107] Prepared by BRE on behalf of the Department of Energy and Climate Change. *Energy Follow-Up Survey 2011, Methodology*.
Technical Report. DECC, 2013.
URL: `https://assets.publishing.service.gov.uk/government/uploads/system/uploads/attachment_data/file/274780/11_Methodology.pdf` (visited on 02/14/2019).

[108] Greenmatch. *Measuring Heating Capacity*. 2018.
URL: `https://www.greenmatch.co.uk/green-energy/central-heating-capacity` (visited on 12/09/2018).

[109] Department for Communities and Local Government.
English Housing Survey. 2015. URL:

https://www.gov.uk/government/collections/english-housing-survey (visited on 07/20/2018).

[110] Dark Sky. *Weather Forecasting and Visualization*. 2018. URL: https://darksky.net/.

[111] LMFIT. *Non-Linear Least-Squares Minimization and Curve-Fitting for Python*. 2019. URL: https://lmfit.github.io/lmfit-py/fitting.html (visited on 06/05/2019).

[112] Department of Energy and Climate Change. *Domestic Energy Prices*. 2017. URL: https://www.gov.uk/government/collections/domestic-energy-prices (visited on 09/24/2020).

[113] Homely Energy Ltd. *Homely Energy Ltd*. 2019. URL: www.homelyenergy.com (visited on 01/19/2020).

[114] BRE group. *The Government's Standard Assessment Procedure for Energy Rating of Dwellings*. 2019. URL: https://www.bregroup.com/wp-content/uploads/2019/11/SAP-10.1-08-11-2019_1.pdf (visited on 09/29/2019).

[115] Marek Miara et al. "Efficiency of Heat Pumps in Real Operating Conditions". In: *10th IEA Heat Pump conference, Tokyo*. 2011.

[116] OVO energy. *How much heating energy do you use?* 2019. URL: https://www.ovoenergy.com/guides/energy-guides/how-much-heating-energy-do-you-use.html (visited on 10/12/2019).

[117] Jenny Love et al. "The addition of heat pump electricity load profiles to GB electricity demand: Evidence from a heat pump field trial". In: *Applied Energy* 204 (2017), pp. 332–342.

[118] Delta. *IEA HPT Programme Annex 42: Heat Pumps in Smart Grids*. 2018. URL: https://assets.publishing.service.gov.uk/government/uploads/system/uploads/attachment_data/file/680514/heat-pumps-smart-grids-executive-summary.pdf (visited on 01/30/2018).

[119] Energy Networks Association. *Distribution Charges Overview*. 2020. URL: https://www.energynetworks.org/electricity/regulation/distribution-charging/distribution-charges-overview.html#:~:text=The%20DUoS%20tariffs%20are%20calculated,HV%20levels%20of%20the%20network. (visited on 06/13/2020).

[120] Office for National Statistics. *Total number of households by region and country of the UK, 1996 to 2017*. 2016. URL: https://www.ons.gov.uk/peoplepopulationandcommunity/%20birthsdeathsandmarriages/families/adhocs/%20005374totalnumberofhouseholdsbyregionandcountryoftheuk1996to2015 (visited on 01/25/2018).

[121] National Grid ESO. *Carbon Intensity API*. 2020. URL: https://www.carbonintensity.org.uk/ (visited on 09/01/2020).

[122] GridCarbon. *GridCarbon: A smartphone app to calculate the carbon intensity of the UK electricity grid*. 2017. URL: www.gridcarbon.uk (visited on 09/01/2020).

[123] Iain Staffell. "Measuring the progress and impacts of decarbonising British electricity". In: *Energy Policy* 102 (2017), pp. 463–475.

[124] Carbon Footprint. *2019 Grid Electricity Emissions Factors v1.0*. 2019. URL: https://www.carbonfootprint.com/docs/2019_06_emissions_factors_sources_for_2019_electricity.pdf (visited on 09/26/2020).

[125] Elexon. *Elexon Insights: Interconnector flows in and out of Great Britain*. 2019. URL: https://www.elexon.co.uk/about/interconnectors/elexon-insights-interconnector-flows-in-and-out-of-great-britain/ (visited on 09/01/2020).

[126] Government of Canada. *Understanding the tables*. 2020. URL: https://www.nrcan.gc.ca/energy-efficiency/energy-efficiency-transportation/personal-vehicles/choosing-right-vehicle/buying-electric-vehicle/understanding-tables/21383 (visited on 09/26/2020).

[127] T. W. Davies. *Calculation of CO2 emissions*. 2020. URL: https://people.exeter.ac.uk/TWDavies/energy_conversion/Calculation%20of%20CO2%20emissions%20from%20fuels.htm (visited on 09/26/2020).

[128] Ofgem. *Electricity Settlement Reform*. 2020. URL: https://www.ofgem.gov.uk/electricity/retail-market/market-review-and-reform/smarter-markets-programme/electricity-settlement-reform (visited on 03/20/2020).

[129] Daniel Gosselin, Jing Jiang, and Hongjian Sun. "Household level distributed energy management system integrating renewable energy sources and electric vehicles". In: *2017 IEEE 85th Vehicular Technology Conference (VTC Spring)*. IEEE. 2017, pp. 1–6.

[130] Elexon. *Balancing Mechanism Glossary*. 2018. URL: https://www.elexon.co.uk/glossary (visited on 05/29/2019).